THREE-DIMENSIONAL ECHOCARDIOGRAPHY IN CORONARY ARTERY DISEASE

ISBN 90-73235-17-0

Printed by Optima Grafische Communicatie, Rotterdam.

THREE-DIMENSIONAL ECHOCARDIOGRAPHY IN CORONARY ARTERY DISEASE

Drie-Dimensionale Echocardiografie Technieken Van Coronaire Hartziekten

PROEFSCHRIFT

ter verkrijging van de graad van doctor
aan de Erasmus Universiteit Rotterdam
op gezag van de rector magnificus
Prof. Dr. P.W.C. Akkermans M.A.
en volgens besluit van het college voor promoties

De openbare verdediging zal plaatsvinden op
Woensdag, 22 september 1999 om 15:45 uur

Door

Jiefen Yao
geboren te Shandong, P. R. China

Promotiecommissie

Promotores:	Prof. dr. J.R.T.C. Roelandt
Overige leden:	Prof. dr. Ir N. Bom
	Prof. dr. N.G. Pandian
	Prof. dr. P.J. Koudstaal

Financial support by the Netherlands Heart foundation (NHS) for the publication of this thesis is gratefully acknowledged.

To my mom
For our dreams
And the memories we share

CONTENTS

CHAPTER 1

INTRODUCTION AND OUTLINE OF THESIS

Introduction and Outline of Thesis

Two-dimensional echocardiography has proven to be a very useful tool in the evaluation of global and regional left ventricular function in patients with coronary artery disease. It has also been used in recognizing viable versus non-viable myocardium, combined with exercise or pharmacological stress. Recent development in transpulmonary ultrasound contrast agents inspired new interest in the cardiologists in myocardial perfusion imaging. Though most agents have proven helpful in (a few agents, including Optison™ and Leovist™, have been approved for clinical application in several continents) left ventricular border delineation, their roles in myocardial perfusion imaging has not been studied extensively. The ability of two-dimensional methods in accurate assessment of the site and extent of wall motion and perfusion abnormalities is limited to the use of a few selected cross-sectional views of the left ventricle and employment of geometric assumptions of the ventricular cavity and walls. This leads to source of errors in quantitative studies of non-symmetric ventricles such as those undergone myocardial infarction and geometric remodeling. Two-dimensional echocardiography is also limited in the evaluation of the mechanism of and in quantifying the severity of mitral regurgitation in patients with ischemic heart disease. Other complications of ischemic heart disease such as intracardiac thrombus can be diagnosed by two-dimensional echocardiography, but a more reproducible technique, such as three-dimensional echocardiography, may provide more reliable data on the therapeutic results in serial follow-up studies. Imaging of the blood vessels including coronary and carotid arteries has been relied mainly on invasive techniques. Two-dimensional ultrasound has shown limited promises in vascular imaging.

Both the heart and the blood vessels are three-dimensional structures. An ideal approach in accurate and comprehensive examination of the heart and blood vessels is one that can collect volumetric information of the heart or vessels and is able to display them in three dimensions. Three-dimensional echocardiography has demonstrated its superiority over two-dimensional methods in quantification of chamber volumes and function and in display of congenital or valvular abnormalities. Its role in the evaluation of coronary artery disease has not been fully explored.

The purpose of this thesis was to examine the potential of three-dimensional echocardiography in qualitative and quantitative evaluation of coronary artery disease and related abnormalities.

Chapter 2 is an overview of three-dimensional echocardiography and its application in coronary artery disease. It alludes to many new directions of three-dimensional echocardiography and a need of integrating various techniques to form a muti-dimension, multi-modality and multi-media technique in the future.

Chapter 3 examines the accuracy and reproducibility of volume measurement in normal and asymmetric left ventricles using three-dimensional data acquired in various intervals. It has important clinical implications in facilitates its daily application and in serial follow-up studies by shortening data acquisition time.

Chapter 4 introduced, for the first time,

a method of quantitating infarct myocardial mass, based on the dysfunctional myocardial mass by three-dimensional echocardiography, in a setting of experimental acute coronary artery occlusion.

Chapter 5 further validated the method used in Chapter 4 by quantifying the dysfunctional myocardial mass in patients with single episode of myocardial infarction. Good correlation was obtained between three-dimensional echocardiography and magnetic resonance imaging methods.

Chapter 6 explored the potential of three-dimensional myocardial contrast echocardiographic perfusion imaging in the assessment of the efficacy of reperfusion, using an intravenous contrast agent (NC100100), by quantifying the myocardial mass at risk of infarction during coronary occlusion and the residual infarct mass following reperfusion therapy.

Chapter 7 presents the feasibility of three-dimensional echocardiography in coronary artery imaging and its quantitative accuracy in the assessment of the severity of stenotic lesions, in comparison with coronary angiography.

Chapter 8 demonstrates the ability of three-dimensional ultrasound of carotid arteries in quantitative analysis of the plaque volumes and the severity of carotid stenoses. It depicts the impact of endarcterectomy on the local vessel geometry.

Chapter 9 displays the qualitative as well as quantitative ability of three-dimensional echocardiography in studying various mass lesions, including intracardiac thrombi and intravascular atheroma.

Chapter 10 presents a quantitative study of mitral valve regurgitation using three-dimensional echocardiography. It demonstrates the advantage of three-dimensional reconstruction and display of the regurgitant jets and points out possible problems and future directions.

CHAPTER 2

THREE-DIMENSIONAL ECHOCARDIOGRAPHY AND CORONARY ARTERY DISEASE

This chapter is based on the following review papers:

1. Jiefen Yao, Jos R.T.C. Roelandt. Three-dimensional echocardiography: a new era of cardiac imaging. ***Current Med Literature: Cardiac Imaging*** **1997;Pilot Issue:2-10**
2. Jos R.T.C. Roelandt, Jiefen Yao, Jaroslaw D. Kasprzak. Three-dimensional echocardiography. ***Current Opinion in Cardiology*** **1998,13:386-396**
3. Jiefen Yao, Qi-Ling Cao, Geral Marx, Natesa G. Pandian. Three-dimensional echocardiography: Current development and future directions. ***J Med Ultrasound*** **1996;4(1): 11-19**
4. Stefano De Castro, Jiefen Yao, Francisco Fedele, Natesa G. Pandian. Three-dimensional echocardiography in ischemic heart disease. ***Coronary Artery Disease*** **1998;9(7):427-434**

Three-Dimensional Echocardiography and Coronary Artery Disease

Jiefen Yao, MD; Stefano De Castro, MD; Natesa G. Pandian, MD; Jos R.T.C. Roelandt, MD.

The development of echocardiography has been a major advance in diagnostic cardiology. While M-mode echocardiography provides limited information on cardiac anatomy and pathologies, cross-sectional echocardiography has brought a revolution of cardiac imaging due to its ability of tomographic viewing of the cardiac structures. Combined with spectral Doppler and color Doppler recording of intracardiac blood flow signals, cross-sectional echocardiography is able to provide us with plentiful information on cardiac structure, function and hemodynamics both qualitatively and quantitatively in most cardiovascular disorders.[1-6] Nevertheless, every facet of the heart including morphology, function and blood flows are three-dimensional in nature. Accurate evaluation of cardiac performance and cardiac diseases from a limited number of cross-sectional images of the heart remains a difficult process of mental conceptualization that requires considerable experience. This process becomes further complicated when the dimension of time is added for structural and functional assessment of a dynamic heart. The ability to objectively view the heart and its structures in three dimensions as it is could complement current modalities for echocardiographic imaging and facilitate the diagnosis of various cardiac abnormalities.

The attempt to develop three-dimensional echocardiographic reconstruction and display of cardiac structures was started in early 1970s and great progress has been achieved since then. [7-14] In its early stage, three-dimensional echocardiography was applied mainly in volume measurement of the ventricles using multiple cross-sectional images that employ laborious manual tracing of the cardiac borders.[10, 11] Reconstruction of those tracings into static wire-frame pictures may demonstrate the shape of the ventricular cavity, but does not provide tissue-depicting information of the heart.[15] Recently, along with the rapid evolution in computer technology, three-dimensional echocardiography has grown into a well-developed technique, such as volume-rendered three-dimensional reconstruction, able to display dynamic images of the heart that also depict depth of the cardiac structures in their realistic forms.[16-17] Many clinical and experimental studies have demonstrated that it is now ready for clinical employment.[18-23]

PRINCIPLES AND TECHNIQUES OF THREE-DIMENSIONAL ECHOCARDIOGRAPHY

Real-Time Three-Dimensional Echocardiography.

The ideal but most challenging direction for echocardiography is real-time three-dimensional imaging when the ultrasound examination is performed. A real-time volumetric ultrasound imaging system has been developed. The system is based on a novel matrix, phased array transducer allowing rapid steering of a two-dimensional beam over a three-dimensional space in a pyramidal format.[24-25] The heart can be imaged from various optimal acoustic windows. This mode of three-dimensional echocardiography has great potential in improving anatomical visualization and fast diagnosis of morphological cardiac disor-

ders, left ventricular function assessment and regional or global wall motion analysis in various situations including stress or exercise tests. Because of a short image acquisition time, this method would be optimal for myocardial perfusion study, if modalities necessitate for contrast echocardiography such as harmonic imaging, transient imaging and power Doppler imaging could be implemented into the system. So far, this method has been applied in surface examination only. For transesophageal use, the size of the probe needs to be minimized. Although initial results with real-time, three-dimensional echocardiography are promising, further improvement in image quality is needed for its clinical application.

Three-Dimensional Echocardiographic Image Reconstruction.

The commonly used term "three-dimensional echocardiography" usually means off-line computer assisted reconstruction of three-dimensional images from a series of cross-sectional echocardiographic images collected using conventional two-dimensional transthoracic or transesophageal transducers. Though various methods have been employed, the essential steps of three-dimensional reconstruction are as follows: 1) data acquisition; 2) data processing and; 3) three-dimensional image rendering and display.

All commercially available ultrasound instrument incorporated with either transthoracic or transesophageal transducers can be used for three-dimensional echocardiographic image collection. Frequently, a dedicated computer is coupled with the ultrasound unit for random and sequential acquisition of images and for reconstruction and analysis of three-dimensional data. Some commercially available two-dimensional echocardiographic systems are now also equipped with three-dimensional data acquisition and storage software. The acquired data usually need an off-line workstation for three-dimensional image reconstruction or quantitative analysis. Devices for intravascular, intracardiac and peripheral vascular three-dimensional imaging have been developed as well, but are not discussed in detail here.[26-28]

Data acquisition. Three-dimensional reconstruction requires accurate information on spatial position of each image plane relative to its location in the heart. Temporal information has to be considered for correct registration of the images in sequential cardiac phases. Various approaches for data acquisition have been developed that can be divided into two major categories - random imaging and sequential imaging.

Random data acquisition. Also known as free-hand imaging, random mode data acquisition requires a spatial sensoring device (magnetic sensors or acoustic sensors) to detect and registrate the location of the transducer (or the imaging plane). The heart can be scanned at one acoustic window by tilting the probe or at different acoustic windows.[29] Therefore, limitation by restricted or sub-optimal acoustic windows is minimized. However, care must be taken to avoid big gaps between imaging planes for accurate three-dimensional reconstruction. The volumetric data set can be used to extract static wire-frame objects or surfaces of selected structures, which are converted to geometric rather than anatomic representations for projection onto a two-dimensional screen. The three-dimensional images are usually generated from manually derived contours of the two-dimensional images, from a tedious and time-consuming process.

While this approach has resulted in improved measurements of chamber volumes and evaluation of surface shapes, it has not allowed tissue-depicting three-dimensional images.

Sequential data acquisition. Three modes of sequential data acquisition are currently available using predetermined steps

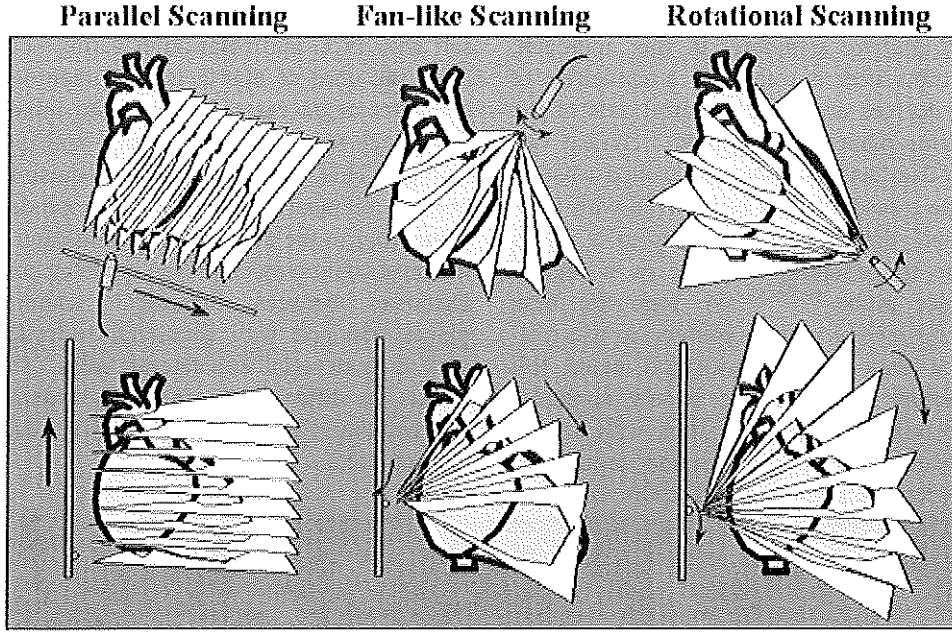

Figure 1. Schematics showing various modes of three-dimensional echocardiographic data acquisition with precordial (upper drawings) and transesophageal (lower drawings) approaches.

for sequential image collection with ECG and respiration gating for temporal image registration (figure 1).

Linear scanning. Parallel equidistantly spaced images can be collected by computer controlled movement of the ultrasound probe or transducer in a liner direction. A surface probe can be moved in predefined steps by a computer controlled sliding device adapted externally to it. A special transesophageal probe was developed for this mode of data acquisition, the distal part of which consists of multiple semicircular plastic segments that can be mechanically straightened after the probe is advanced into the esophagus. A sliding carriage, on which the transducer is mounted, is housed in the distal part of the probe and can be moved in equal steps under the control of computer considering cardiac and respiratory cycles.[30-32] But this probe did not succeed in routine clinical use because of difficult intraesophagus introduction and poor patient acceptance for its size. The three-dimensional data set resulted from parallel acquisition is prism shaped and the "stepping resolution" at each depth depends on the distance between the parallel images, with better resolution in data acquired with smaller acquisition steps.

Fan-like scanning. A pyramidal data set can be obtained by moving the ultrasound transducer in a fan-like arc at prescribed angles. This is accomplished by computer controlled motors adapted to the transducer or probe in surface or transesophageal ap-

proaches.[33-35] Distances between imaging planes vary with depth with the largest gaps in the far field, thus, this region contains less structural information and has less resolution.

Rotational scanning. In this approach, the transducer is rotated in a semicircle of 180 degrees around the central axis of the imaging plane that results in a conical volume data set. Computer-controlled rotation of the transducer can be realized with a rotational device adapted either to a multiplane transesophageal probe or a regular surface probe.[16, 36-38] We were the first, among several pioneer centers, to use rotational data acquisition which made this technique practical and widely applied.[39] This mode of data acquisition with a commercially available ultrasound unit alone (Hewlett Packard, SONOS 2500, Andover, MA, USA) has been brought to clinical use with both transthoracic and transesophageal multiplane transducers.[40] Rotation of the transducer and collection of images at every step is controlled by the ultrasound unit itself with ECG and respiration gating obviating the need of interfacing an additional computer or an externally mounted motoring device for transducer rotation and data storage. This fashion of data acquisition needs a relatively smaller acoustic window comparing to the above two methods and is the most commonly employed mode by now. Distances between individual scanning planes obtained with rotational technique vary in both axial and lateral fields. This results in different structural information and resolution in any given point for each cutting plane.

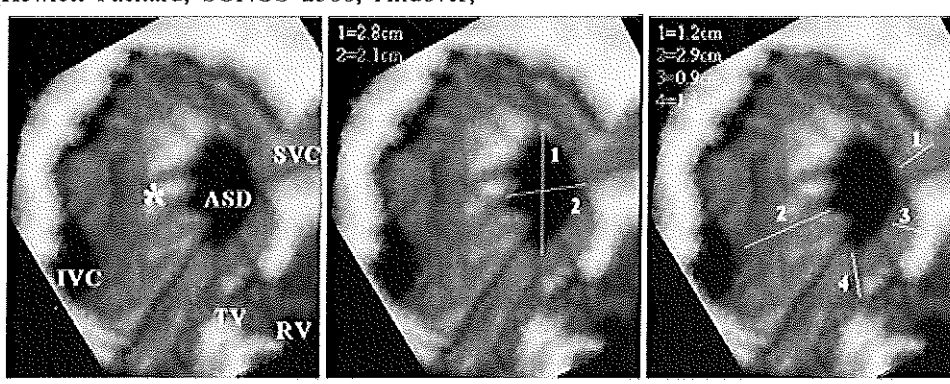

Figure 2. Three-dimensional image of a atrial septal defect viewed en face from the right atrium. Size, shape and location of the irregular shaped defect (ASD) and the atrial septal aneurysm (*) is shown crisply. Direct measurements of the maximal and minimal diameters of the defect on three-dimensional image (middle panel) are very close to surgical measurements. Measurement of the surrounding tissue from the defect to superior and inferior vena cava, anterior aortic wall and tricuspid valve annulus (right panel) provides useful information for selection of interventional defect closing method. SVC = superior vena cava; IVC = inferior ven cava ; ASD = atrial septal defect; TV = tricuspid valve; RV = right ventricle.

Data processing, rendering and display. The two-dimensional images collected in the above mentioned fashions are digitized and realigned according to their spatial and temporal sequences. Geometric transformation is necessary for images acquired in rotational or fan-like scanning manners to convert the data points into an isotropic cubic data set. Gaps between individual images are filled by the computer with different interpolation algorithms for different acquisition modes, such as "trilinear cylindrical

interpolation" for data from rotational scanning. Then the pixels in two-dimensional images are transformed into voxels in a volumetric three-dimensional data set. Small motion artifacts resulted from movement of the patient, respiration-related movement of the heart or movement of the probe as well as artifacts caused by ultrasound noises can be minimized using various image processing filters. At this stage, the volumetric data set can be sliced to derive cross-sectional images in any desired cutting planes or be rendered into various forms of three-dimensional images.[17, 41]

With voxel-based volumetric three-dimensional data set, cross-sectional cutting planes can be derived arbitrarily using various algorithms. *Anyplane* method is the basic algorithm in generating cross-sectional images. Three perpendicular axes in the three-dimensional data set referred to the Cartesian coordinate system are used for guiding cutting plane manipulation. Innumerable cross-sectional views of the heart which is difficult or physically impossible to obtain from conventional precordial or transesophageal acoustic windows can be computed from three-dimensional data set and displayed dynamically in cine-loop format. *Paraplane* method is used to derive multiple parallel equidistant cross-sectional views through a region of the heart at selected intervals based on definition of one anyplane image. *Long-axis* and *short-axis* methods are used to produce multiple long or short axis images of a ventricle or an object in the heart with equally distributed intervals (distances or angles). *Mainplane* method creates three orthogonal cutting planes perpendicular to each other through an interested region of the heart by defining first one anyplane. These secondary derived cross-sectional images form three-dimensional data set aids in systematic review of the cardiac structures, selection of optimal cutting planes and quantification of regional volumes of a selected territory.

To view the heart in three-dimensions, reconstruction and display of three-dimensional images from the processed three-dimensional data set is essential. Several rendering techniques have been developed for this purpose. *Wire-frame formation* is used to generate three-dimensional images of the heart in a cage-like picture. This algorithm is mainly used in randomly collected data (though it can also be used for sequentially collected images) and for chamber volume quantification.[15] Manual tracing of the acquired cardiac images is required and the reconstructed image is often displayed in static mode. Although a surface calculated by the computer can be applied to the wire-frame image, this form of reconstruction can not provide details of the cardiac structure or texture of the cardiac tissue. *Surface rendering technique* extracts the contour of the structure from three-dimensional data set and displays in a solid appearance the surface of the object that faces the observer. Shadowing algorithms can be used to create a three-dimensional perspective. Information of the tissue beneath the surface is missing.[17] *Volume rendering technique* engages all the information of the cardiac structures within the volumetric data set to create three-dimensional images that closely resemble the true anatomy of the heart. Depending on the level of opacification, shading and lighting of a volume-rendered image, the structure may either appear solid (similar to the effect of surface-rendered images) or transparent, the later allowing one to see through the "surface". Three kinds of shading techniques (distance shading, gray level gradient coding, and texture shading) are

usually used and mixed with different weighting factors to generate a three-dimensional display of the depths and textures of the cardiac structures.[42] The three-dimensional effect can be further enhanced by creating rotational sequences of the image upon display.

Volume-rendered three-dimensional data

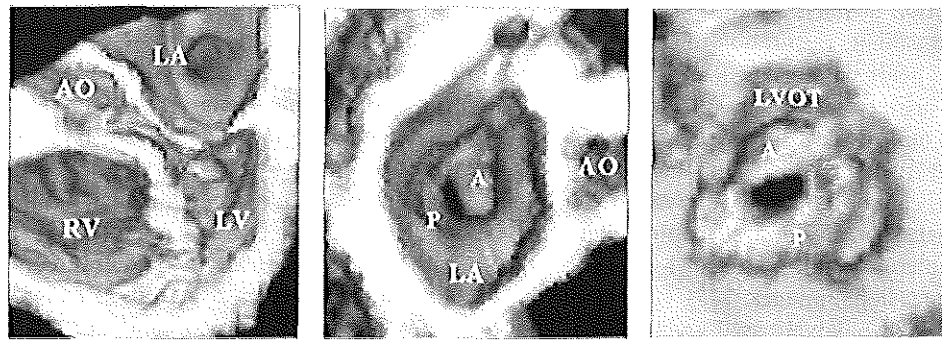

Figure 3. Volume-rendered three-dimensional images of a stenotic mitral valve in a longitudinal (left) and in transverse formats viewed from above (upper right) and below (lower right) in diastole. The restricted opening and doming of the leaflets are observed in all these projections. LA = left atrium; AO = aorta; RV = right ventricle; LV = left ventricle; LVOT = left ventricular outflow tract; A = anterior mitral leaflet; P = posterior mitral leaflet.

set can be electronically segmented and sectioned. To display intracardiac structures, the heart can be opened by choosing a cutting plane and reconstruct the image beyond this plane as if the heart is cut open in surgery. Three-dimensional projections of the heart in conventional orientations employed in two-dimensional echocardiography are easily perceived and enthusiasm is evoked by projections of unconventional views and those similar to surgeon's views of the heart not accessible with any other techniques.[43] These can be achieved by manipulation of the cutting planes and rotation of the three-dimensional image to obtain ideal projections. Mitral and tricuspid valve can be viewed either from above (simulating atriotomy) or from below (as with ventriculotomy). Likewise, the aortic valve can be visualized from above with electronic aortotomy and from below looking through the left ventricular outflow tract. In dynamic mode display, the opening and closing of the cardiac valves can be observed readily. Atrial and ventricular septa can be examined *en face* with better perception of their spatial relationship with adjacent structures. Longitudinal views are useful to display chamber size and ventricular function, as well as valvular movements and intracardiac flow jets. Special structures can be revealed by various display projections including unconventional views, especially in patients with complex congenital heart diseases. The strength of offering unlimited number of cross-sectional views and three-dimensional projections could also be too intimidating. Guidelines to identify clinically useful cutting planes are being formulated for application in various categories of disease.[17]

CURRENT EXPERIENCE WITH AND CLINICAL APPLICATIONS OF THREE-DIMENSIONAL ECHOCARDIOGRAPHY

Three-dimensional echocardiography has produced promising results from both experimental and clinical studies in the past two and half decades. It has been applied in various clinical scenarios with different set-

tings including echocardiographic laboratory, various in-patient care units, operating room and emergency room. Favorable experience has been gained in its clinical applications with both transthoracic and transesophageal image data acquisition. A volumetric data set of the heart can be achieved in a few minutes, from which multiple two-dimensional and three-dimensional images can be reconstructed and displayed off-line. This might probably shorten the examination time of imaging plane manipulation for morphologic study and decrease the discomfort of the patient.

Unrestricted Cutting Planes

Limitations of acoustic access to discretionary cutting planes and spatial registration of individual images with conventional two-dimensional echocardiography can potentially be overcome by three-dimensional echocardiography.[41] It is possible to select any desired cutting planes of the heart from a volumetric three-dimensional data set and to display the corresponding cross-sectional images. Slicing of a given region with parallel equidistant cutting planes can be performed accurately in a fashion similar to computed tomography or magnetic resonance imaging. A structure or a cavity can be cut in true longitudinal or transverse planes referred to a common "long-axis", independent to the transducer position during image collection. Optimal cross-sectional planes of the heart can be obtained for accurate measurement of various dimensions (of cavity or defect) and areas (of stenotic valve or regurgitant orifice) and for better evaluation of morphology and function of a given structure with more objectivity and less operator dependency.

Three-Dimensional Display Projections

A major advantage of three-dimensional echocardiography over any two-dimensional approaches is that it can reproduce numerous novel cross-sectional cutting planes and three-dimensional display projections of the cardiac structures. Dynamic volume-rendered three-dimensional reconstructions provide accurate spatial and temporal information valuable for comprehensive evaluation of cardiac function and morphologic abnormalities. The reconstructed images can be displayed in dynamic (cine-loop), static or frame-by-frame fashion.

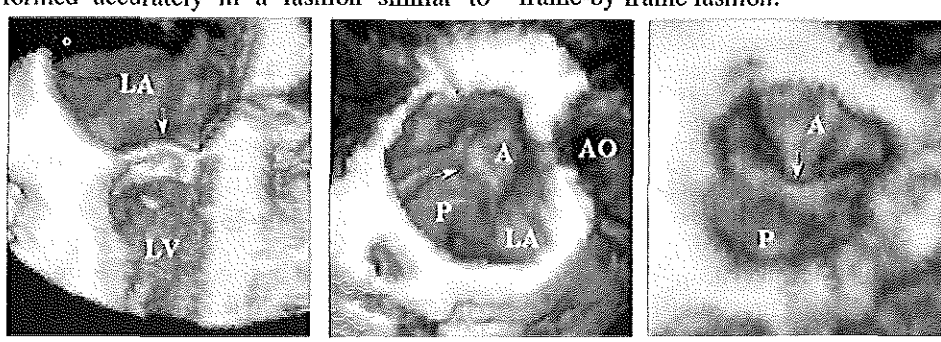

Figure 4. Three-dimensional images from a patient with mitral valve prolapse (arrow) in longitudinal (left) and transverse views observed from above (middle) and from below (right) in systole. The abbreviations are the same as in figure 3.

Three-dimensional echocardiography has been proven valuable in congenital heart diseases for better evaluation of morphologic abnormalities and understanding of complex spatial relationships.[20, 21, 30, 35, 44-46] Three-dimensional en face views of atrial or ven-

tricular septal defect, from right or left side, not only provide surgeon's view of the defect before the heart is open but also enable accurate measurement of the dimensions of the defect directly on three-dimensional images and, most importantly, measurement of the tissues surrounding the defect, the later being crucial for planning interventional procedures especially for close-chest closure of the defect using transcatheter closing device (Figure 2). Various three-dimensional projections help in discern congenital malformations of the heart such as bicuspid aortic valve and subaortic membrane and in differentiating mitral valve from tricuspid valve in patients with transposition of great arteries. Other congenital anomalies such as cleft or parachute mitral valve and tricuspid valve atresia can be demonstrated by three-dimensional reconstruction and direct measurement such as extent of mitral valve cleft derived.

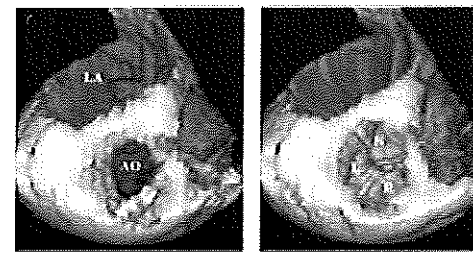

Figure 5. Three-dimensional images of a normal aortic valve viewed from above in systole (left) and diastole (right). The three cusps and their coaptation lines are clearly defined. N = non-coronary cusp: R = right-coronary cusp; L = left coronary cusp. The other abbreviations are the same as in figure 3.

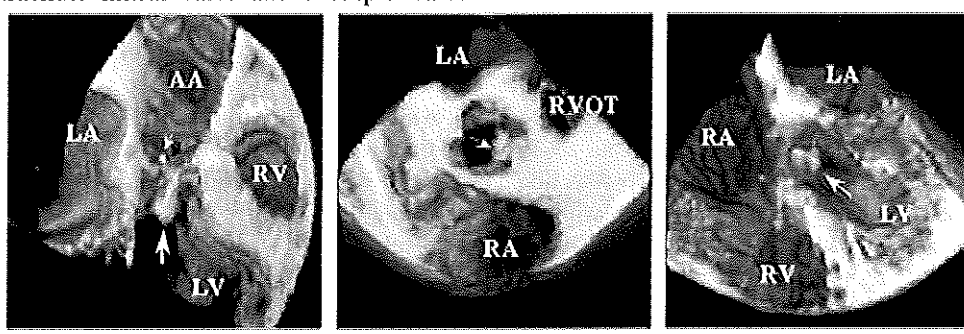

Figure 6. Various projections from three-dimensional reconstruction of multiple aortic valve vegetations of a patient with infective endocarditis. The left image is in a longitudinal format. Two vegetations (small and big arrows) are seen on non-coronary (the smaller one) and right-coronary (the bigger one) cusps separately. In dynamic display, the mobility of the vegetations along with the movement of the aortic valve are better appreciated. The bigger vegetation is seen in short axis view from aorta during systole (middle image) and prolapse into left ventricular outflow tract during diastole (right image) as observed in a foreshortened four-chamber format. AA = ascending aorta; RA = right atrium; RVOT = right ventricular outflow tract. The other abbreviations are same as in figure 3.

Evaluation of valvular heart diseases can also be improved by three-dimensional echocardiography.[19, 47-52] Diastolic doming and restricted motion of stenotic mitral valve, thickness of the mitral valve leaflets and involvement of the subvalvular structures can be displayed with longitudinal and transverse views from different directions (Figure 3). Mitral or tricuspid valve prolapse is shown on three-dimensional images as a bulging or protrusion on the atrial side of the mitral valve and a depression on the ventricular side. The exact location and extension of prolapse can be visualized and it can be important information for the surgeons for planning surgical procedures (Figure 4).

Similarly, aortic and pulmonary valve abnormalities can be observed in multiple projections as well (Figure 5 and 6). Prosthetic valves can be reconstructed and their sitting and function be evaluated. When combined with color Doppler flow imaging, intracardiac flow jets with relatively high velocities, such as regurgitant jets or blood

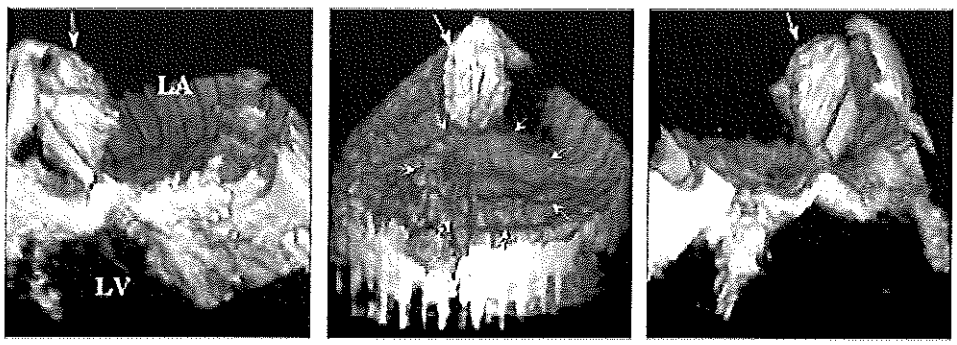

Figure 7. Multiple projections of three-dimensional reconstructions of color Doppler flow imaging from a patient with a perivalvular leakage (big arrow) after mitral valve replacement with a single-disc mechanical prosthesis. The origin, size and direction of the jet is well defined. The mechanical prosthesis in mitral valve position is observed and closes well (small arrows). The abbreviations are the same as in figure 3.

flow through a stenotic valve, can be reconstructed and displayed in three dimensions.[53-54] The site of origin, direction of trajectory, geometric distribution and morphology of the jet is better appreciated (Figure 7). Multiple jets, unusual path of jet traveling and interaction between compound jets can be better understood with dynamic volumetric display. Three-dimensional echocardiography might also provide a better access for quantitative evaluation of valvular abnormalities using proximal flow convergence or vena contracta of the flows.

Three-dimensional echocardiography has been used in almost all kinds of cardiac disorders and various benefits have been achieved. Evaluation of intracardiac or intravascular masses including vegetations, tumors, thrombi or plagues is facilitated both qualitatively (by three-dimensional display of their site, size, attachment and mobility) and quantitatively (by accurate measurement of their dimensions and volumes) (Figure 8).[55] We have also examined aortic diseases such as dilatation, aneurysm, dissection or coarctation with three-dimensional echocardiography and incremental information was obtained.

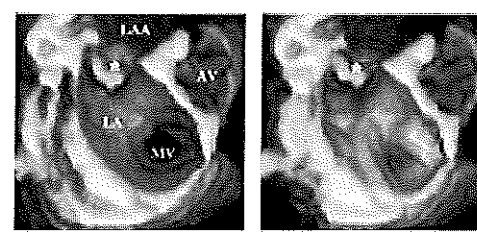

Figure 8. Diastolic (left) and systolic (right) three-dimensional images of a thrombus originated from left atrial appendage extended to left atrium in a patient with mitral valve stenosis. LAA = left atrial appendage; The other abbreviations are the same as in figure 3.

Volume Quantification

Application of three-dimensional reconstruction for quantitative volume measurements of the left and right ventricles provided good correlations with angiography, magnetic resonance imaging or established

two-dimensional methods (in vivo) and anatomical measurements (in vitro) (Table).[18, 29, 56-65] At present, ventricular volumes are calculated by manual endocardial tracing of sequential short axis views derived by parallel slicing through three-dimensional data set at prescribed thickness intervals at either end-systole or end-diastole. Volume quantification is achieved by summation of the voxels included in the.

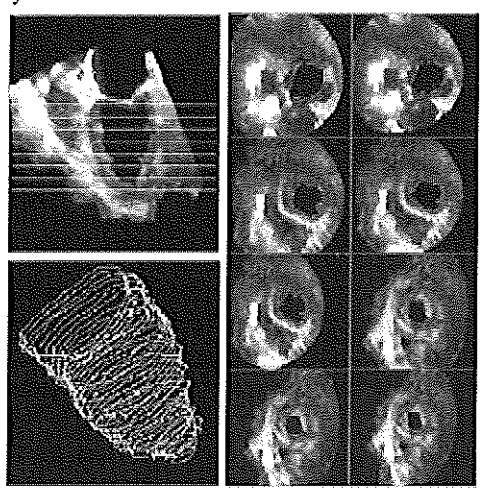

Figure 9. Principle of left ventricular volume calculation using a three-dimensional data set. An end-diastolic longitudinal view is selected as a reference image (left panel) and the left ventricle is sectioned into parallel short-axis slices with equal thickness (middle panels). The contour of the left ventricular cavity is traced and the volume of each slice is calculated. Summation of the volumes of all slices provides the total volume of the left ventricle (right panel). If volumes are measured for both end-diastole and end-systole, stroke volume of the left ventricle can be calculated by subtraction of systolic from diastolic volume.

traced area with subsequent summing of the subvolumes of each slice with known slice thickness (Figure 9). Stroke volume and ejection fraction of a given chamber can be derived from its end-systolic and end-diastolic volumes. The rationale behind the accuracy and reproducibility of volume measurement with three-dimensional echocardiography in comparison with any two-dimensional method is that the three-dimensional approach obviates any geometric assumptions of the shape of the measured chamber. Therefore, three-dimensional volume measurement can be applied to any objects such as intracardiac masses or abnormal blood flow jets

Limitations

The currently used volume-rendered three-dimensional echocardiography, though well-accepted for clinical application, has the following limitations: 1) The prescribed data acquisition require minutes (2-10min), with ECG and respiratory gating. This might prevent it from being used for stress or contrast echocardiography in which the time window for data acquisition is very much limited. The longer the acquisition time, the greater the potential is in producing motion artifacts from movements of the patient or the probe; 2) the acquired data requires processing before three-dimensional reconstruction can be performed. Effort is being made to make this process faster. 3) There is a non-negligible learning curve in three-dimensional reconstruction, which takes minutes to hours, depending on the experience and expertise of the operator in three-dimensional echocardiography.

POTENTIAL APPLICATIONS OF THREE-DIMENSIONAL ECHOCARDIOGRAPHY IN CORONARY ARTERY DISEASE

Coronary heart disease is one of the most commonly encountered diseases for the cardiologists. Two-dimensional echocardiography is often limited in accurate evaluation of regional wall motion abnormalities and the myocardial mass at risk of injury or infarct mass in patients with ischemic heart disease, due to geometric remodeling of the left ventricle. Three-dimensional echocardiography

has shown its potential in accurate evaluation of volumes and function of both normal and deformed ventricles and in analysis and quantitative measurements of regional wall motion abnormalities and myocardial perfusion territories.[65-67]

Evaluation of regional wall motion abnormalities

The extent of myocardial damage during acute myocardial infarction is an important determinant of long and short term prognosis.[68,69] While two-dimensional echocardiography can detect the location and severity of regional wall motion abnormalities, its ability in quantifying the real myocardial mass involved in dysfunction is limited by using just a few cross-sectional views of the left ventricle. The inability of conventional two-dimensional echocardiography in obtaining true short-axis views and unforshortened apical views of the left ventricle could lead to errors in the evaluation of the true extent of regional wall motion abnormalities by employing geometric assumptions. In addition, because of the movement of the heart, the imaging plane on two-dimensional echocardiogram is constantly changing. Three-dimensional echocardiography, by obtaining a volumetric data set of the left ventricle, can produce multiple parallel short axis views of the left ventricle, which can be used in accurate assessment of global or regional left ventricular function without the need of any geometric assumption. The three-dimensional data can be displayed in dynamic mode and analyzed in static frames. It has been demonstrated that the infarcted myocardial mass resulted from coronary occlusion can be quantified based upon the dysfunctional mass of the left ventricle from three-dimensional echocardiography.[66] The three-dimensional echocardiographic method in quantifying dysfunctional myocardial mass is explained in detail in chapters 4 and 5.

Evaluation of regional myocardial perfusion abnormalities

After acute coronary occlusion, the dysfunctional myocardial region represents the region at risk of infarction and indicates the extent of infarction only if no revascularization procedure is performed. In patients with chronic coronary artery disease, especially previous myocardial infarction, or after reperfusion therapy, the dysfunctional mass can not be used to quantify the infarcted myocardial mass. In these patients, dysfunction of the myocardium could result from multiple causes including myocardial stunning and hibernation, eventhough blood flow has been restored in these regions. Contrast echocardiography is potentially useful in differentiating viable from nonviable myocardium by using microbubbles to indicate the presence or absence of blood flow. Two-dimensional contrast echocardiography has shown to be useful in the detection of myocardial perfusion abnormalities. It suffers from the same limitations of two-dimensional methods in quantitative analysis of regional myocardial dysfunction. The potential of three-dimensional contrast echocardiography in myocardial perfusion imaging has raised great interest.[70,71] The development of transpulmonary ultrasound contrast agents has greatly facilitated the procedure of contrast echocardiography by using intravenous, instead of transcatheter, administration of contrast agent. It is still challenging to obtain a good three-dimensional data set following a bolus peripheral administration of contrast agent. We have reported accurate quantitation of infarct myocardial mass from perfusion defect myocardium by three-dimensional contrast echocardiography following prolonged

coronary artery occlusion, as well as following reperfusion therapy, using peripheral contrast administration.[72,73] Chapter 6 is a report of our recent study in the feasibility and accuracy of three-dimensional contrast echocardiography in quantifying myocardial mass at risk during acute ischemia and the infarcted myocardial mass following reperfusion therapy, and thus the salvaged myocardium and the efficacy of reperfusion.

Evaluation of coronary artery lesions

Two-dimensional echocardiography has been attempted in the visualization of the proximal coronary arteries, which is often limited, by the orientation of the cutting plane, in obtaining optimal views of the coronary arteries. Three-dimensional echocardiography can overcome this limitation with ability of anyplane reconstruction. Besides, most of the proximal segments of the coronary arteries can be obtained within one data set with the probe in a fixed position, using rotational imaging method.[74] This may minimize the discomfort to the patient due to the manipulation of the transducer in searching for optimal views of the coronary arteries, often happens in two-dimensional studies. Stenotic lesions in various segments of the coronary can be displayed in both two-dimensional (anyplane) views and three-dimensional images. Spatial relationship between the stenotic lesions and the cardiac structures can be demonstrated by three-dimensional data, which may provide useful information for interventional procedures such as coronary bypass surgery or intracoronary stent placement.

Evaluation of other coronary artery disease related abnormalities

Three-dimensional reconstruction has also proved useful in providing incremental information in other coronary artery related abnormalities.

In patients with ischemic mitral regurgitation, not only the regional myocardial dysfunction can be localized and quantified, the mechanism of mitral regurgitation can be better understand by comprehensive analysis of the regional wall motion, regional shape changes of the left ventricular cavity and the function of the papillary muscles. The regurgitant jet can be displayed in three dimensions and its origin, distribution and size are better appreciated.[75]

Mural thrombus is not an infrequent echocardiographic findings in patients with ischemic heart disease, especially ischemic cardiomyopathy and left ventricular aneurysm due to myocardial infarction. It can be a source of systemic embolization. A reproducible documentation with three-dimensional echocardiography of the location, mobility and size of the thrombus can be useful (figure 10).

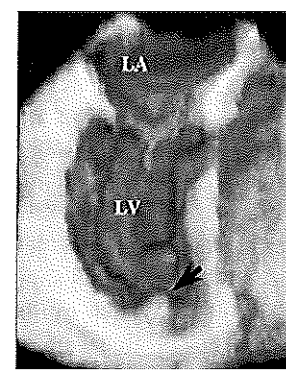

Figure 10. Three-dimensional image of the left atrium (LA) and left ventricle (LV) from a patient with anterior myocardial infarction. An apical thrombus (black arrow) is clearly seen from a data set was obtained with a trans- eso-phageal approach.

FUTURE DIRECTIONS

Three-dimensional echocardiography is likely to become a standard echocardiographic examination in the future. It provides clinicians with more confidence in the diagnosis of cardiac disease and adds insights to the understanding of complex pathologies. Further development and improvement for its use in clinical practice include faster or on-line data acquisition,

processing and reconstruction and easier and more versatile approaches to quantitative analysis including surface area measurement. A number of new technologies have emerged and showed promising results in multidimensional study of the heart and vessels. Progress is made in improving the image quality and incorporating various modalities such as second harmonic imaging in real-time three-dimensional echocardiography. Three-dimensional data acquisition is no longer a time consuming process with the newly developed ultrafast or real-time data acquisition technique. Color coded display of intracardiac blood flows and digitized local velocity information may allow better evaluation of many valvular or congenital cardiac disorders. Three-dimensional physiologic imaging such as tissue Doppler imaging and myocardial perfusion imaging may provide additional in depth understanding of the disease process. Analysis of the global and regional shape and wall stress may aid in clinical prognosis of ischemic heart disease and cardiac function. New display methods such as holography allows for multi-projection display of the three-dimensional structure of the heart on a two-dimensional surface.[76,77] Virtual reality technique may aid in better understanding of complex spatial relationships of normal and pathological cardiac structures and its interactive ability may be used in better and real-time guidance in interventional procedures.[78] Stereolithography or modeling of the cardiac structures may present the clinicians with solid cardiac specimen of the live patients before cardiac surgery or non-surgical interventions.[79]

1. Feigenbaum H: *Echocardiography*: The echocardiographic examination. 5th ed. 1994, P: 68-133, Lea & Febiger, Philadelphia, USA.
2. Tajik AJ, Seward JB, Hagler DJ, Mair DD, Lie JT: Two-dimensional real-time ultrasonic imaging of the heart and great vessels: technique, image orientation, structure identification, and validation. *Mayo Clin Proc* 1978;53:271-303.
3. Pandian NG, Hsu TL, Schwartz SL, Weintraub A, Cao QL, Schneider AT, Gordon G, England M, Simonetti J: Multiplane transesophageal echocardiography. *Echocardiography* 1992;9:649-
4. Hatle L, Angelsen B: *Doppler ultra-sound in cardiology*: Physical principles and clinical application. 2nd ed. 1985, Lea & Febiger, Philadelphia, USA.
5. Roelandt JRTC, Sutherland GR, Iliceto S, Linker DT: *Cardiac Ultrasound*. 1993, churchill Livingstone, UK.
6. Shiota T, Jones M, Valdes-Cruz LM, Shandas R, Yamada I, Sahn DJ: Color flow Doppler determination of transmitral flow and orifice area in mitral stenosis: experimental evaluation of the proximal flow-convergence method. *Am Heart J* 1995;129:114-123
7. Dekker DL, Piziali RL, Dong E Jr: A system for ultrasonically imaging the human heart in three dimensions. *Comput Biomed Res* 1974;7:544-553
8. Moritz WE, Shreve PL: A microprocessor based spatial locating system for use with diagnostic ultrasound. *Proc IEEE* 1976;64:066-974
9. Matsumoto M, Matsuo H, Kitabatake A, Inoue M, Hamanaka Y: Three-dimensional echocardiograms and two-dimensional echocardiographic images at desired planes by a computerized system. *Ultrasound Med Biol* 1977;3:163-178
10. Ariet M, Geiser EA, Lupkiewicz SM, Conetta DA, Conti CR: Evaluation of a three-dimensional reconstruction to compute left ventricular volume and mass. *Am J Cardiol* 1984;54:415-420
11. Linker DT, Mortiz WE, Pearlman AS: A new three-dimensional echocardiographic method of right ventricular volume measurement: in vitro validation. *J Am Coll Cardiol* 1986;8:101-106
12. Levine RA, Handschumacher MD, Sanfilippo AJ, Hagege AA, Harrigan P, Marshall JE, Weyman AE: Three-dimensional echocardiographic reconstruction of the mitral valve, with implications for the diagnosis of mitral valve prolapse. *Circulation* 1989;80:589-598
13. King DL, Harrison MR, King Jr DL, Gopal AS, Martin RP, DeMaria AN: Improved reproducibility of left atrial and left ventricular measurements by guided three-dimensional echocardiography. *J Am Coll Cardiol* 1992;20:1238-1245
14. Belohlavek M, Foley DA, Gerber TC, Kinter TM, Greenleaf JF, Seward JB: Three- and four-dimensional cardiovascular ultrasound imaging: A new era for echocardiography. *Mayo Clin Proc* 1993;68:221-240
15. Levine RA, Weyman AE, Handschumacher MD:

Three-dimensional echocardiography: techniques and applications. *Am J Cardiol* 1992;69:121H-131H

16. Roelandt JRTC, Ten Cate FJ, Vletter WB, Taams MA: Ultrasonic dynamic three-dimensional visualization of the heart with a multiplane transesophageal imaging transducer. *J Am Soc Echocadiogr* 1994;7:217-229
17. Pandian NG, Roelandt J, Nanda NC, Sugeng L, Cao QL, Azevedo J, Schwartz SL, Vannan MA, Ludomirski A, Marx G, Vogel M: Dynamic three-dimensional echocardiography: Methods and clinical potential. *Echocardiography* 1994:11:237-259
18. Jiang L, Siu SC, Handschumacher MD, Guererro JL, Vazquez de Prada JA, King ME, Picard MH, Weyman AE, Levine RA: Three-dimensional echocardiography: in vivo validation for right ventricular volume and function. *Circulation* 1994;89:2342-2350
19. Nanda NC, Roychoudhury D, Chung SM, Kim KS, Ostlund V, Klas B: Quantitative assessment of normal and stenotic aortic valve using transesophageal three-dimensional echocardiography. *Echocardiography* 1994;11:617-625
20. Rivera JM, Siu SC, Handschumacher MD, Lether JP, Guerrero JL, Vlahakes GJ, Mitchell JD, Weyman AE, King MEE, Levine RA: Three-dimensional reconstruction of ventricular septal defects: validation studies and in vivo feasibility. *J Am Coll Cardiol* 1994;23:201-208
21. Vogel M, Losch S: Dynamic three-dimensional echocardiography with a computed tomography imaging probe: initial clinical experience with transthoracic application in infants and children with congenital heart defects. *Br Heart J* 1994;71:462-467
22. Pai RG, Tanimoto M, Jintapakorn W, Azevedo J, Pandian NG, Shah PM: Volume-rendered three-dimensional dynamic anatomy of the mitral annulus using a transesophageal echocardiographic technique. *J Heart Valve Dis* 1995;4:623-627
23. Wang XF, Li ZA, Cheng TO, Xie MX, Hu G, Deng YB, Liu L, Lu Q: Four-dimensional echocardiography: methods and clinical application. *Am Heart J* 1996;132:672-684
24. von Ramm OT, Smith SW. Real time volumetric ultrasound imaging system. *J Digit Imaging* 1990;3:261-266
25. Sheikh KH, Smith SW, Von Ramm OT, Kisslo J: Real-time, three-dimensional echocardiography: feasibility and initial use. *Echocardiography* 1991;8:119-125
26. Roelandt JRTC, Mario C, Pandian NG, Li WG, Keane D, Slager CJ, Feyter PJ, Serruys PW: Three-dimensional reconstruction of intracoronary ultrasound images: rationale, approaches, problems, and directions. *Circulation* 1994;90:1044-1055
27. Chandrasekaran K, Sehgal CM, Hsu TL, Young NA, D'Adamo AJ, Robb RA, Pandian NG: Three-dimensional volumetric ultrasound imaging of arterial pathology from two-dimensional intravascular ultrasound: an in vitro study. *Angiology* 1994;45:253
28. von Birgelen C, Di Mario C, Li W, Schuurbiers JC, Slager CJ, de Feyter PJ, Roelandt JR, Serruys PW. Morphologic analysis in three-dimensional intracoronary ultrasound: an in vitro and in vivo study performed with a novel system for the contour detection of lumen and plaque. *Am Heart J* 1996;132:516-527
29. Gopal AS, Shen Z, Sapin PM, Keller AM, Schnellbaecher MJ, Leibowitz DW, Akinboboye OO, Rodney RA, Blood DK, King DL: Assessment of cardiac function by three-dimensional echocardiography compared with conventional noninvasive methods. *Circulation* 1995;92:842-853
30. Fulton DR, Marx GR, Pandian NG, Romero BA, Mumm B, Krauss M, Wollschlager H, Ludomirsky A, Cao QL: Dynamic three-dimensional echocardiographic imaging of congenital heart defects in infants and children by computer-controlled tomographic parallel slicing using a single integrated ultrasound instrument. *Echocardiography* 1994;11: 155-164
31. Ross JJ Jr, D'Adamo AJ, Karalis DG, Chandrasekaran K: Three-dimensional transesophageal echo imaging of the descending thoracic aorta. *Am J Cardiol* 1993;71:1000-1002
32. Pandian NG, Nanda NC, Schwartz SL, Fan P, Cao QL: Three-dimensional and four-dimensional transesophageal echocardiographic imaging of the heart and aorta in humans using a computed tomographic imaging probe. *Echocardiography* 1992;9:677-687
33. Delabays A, Pandian NG, Cao QL, Sugeng L, Marx G, Ludomirski A, Schwartz S: Transthoracic real-time three-dimensional echocardiography using a fan-like scanning approach for data acquisition: methods, strength, problems, and initial clinical experience. *Echocardiography* 1995;12:49-59
34. Martin RW, Bashein G, Zimmer R, Sutherland J: An endoscopic micromanipulator for multiplanar transesophageal imaging. *Ultrasound Med Biol* 1986;12:965-97
35. Belohlavek M, Foley DA, Gerber TC, Greenleaf JF, Seward JB: Three-dimensional ultrasound imaging of the atrial septum: normal and pathologic anatomy. *J Am Coll Cardiol* 1993;22:1673-1678
36. Roelandt J, Salustri A, Bruining N: Precordial and transesophageal dynamic three-dimensional echocardiography with rotatable (multiplane) transducer systems. *Ultrasound Med Biol* 1994;20:532
37. Binder T, Globits S, Zangeneh M, Gabriel H, Rothy W, Koller J, Glogar D: Three-dimensional echocardiography using a transesophageal imaging probe.

Potentials and technical considerations. *Eur Heart J* 1996;17:619-628
38. Fyfe DA, Ludomirsky A, Sandhu S, Dhar PK, Silberbach M, Sahn DJ: Left ventricular outflow tract obstruction de-fined by active three-dimensional echo-cardiography using rotational trans-thoracic acquisition. *Echocardiography* 1994;11:607-615
39. Ludomirsky A, Vermilion R, Nesser J, Marx G, Vogel M, Derman R, Pandian N: Transthoracic real-time three-dimensional echocardiography using the rotational scanning approach for data acquisition. *Echocardiography* 1994;11:599-606
40. Yao J, Cao QL, Pandian NG, Sugeng L, Marx G, Masani N, Yeung H. Multiplane transthoracic echocardiography: Image orientation, anatomic correlation, and clinical experience with a prototype phased array multilane surface probe. *Echocardiography* 1997;14(6):559-88
41. Roelandt J, Salustri A, Vletter W, Nosir Y, Bruining N: Precordial multiplane echocardiography for dynamic anyplane, paraplane and three-dimensional imaging of the heart. *The Thoraxcentre Journal* 1994;6(5):4-13
42. Cao QL, Pandian NG, Azevedo J, Schwartz SL, Vogel M, Fulton D, Marx G: Enhanced comprehension of dynamic cardiovascular anatomy by three-dimensional echocardiography with the use of mixed shading techniques. *Echocardiography* 1994;11:627-633
43. Schwartz SL, Cao QL, Azevedo J, Pandian NG: Simulation of intraoperative visualization of cardiac structures and study of dynamic surgical anatomy with real-time three-dimensional echocardio-graphy. *Am J Cardiol* 1994;73:501-507
44. Marx G, Fulton DR, Pandian NG, Vogel M, Cao QL, Ludomirski A, Delabays A, Sugeng L, Klas B: Delineation of site, relative size and dynamic geometry of atrial septal defects by real-time three-dimensional echocardiography. *J Am Coll Cardiol* 1995;25:482-490
45. Salustri A, Spitaels S, McGhie J, Vletter W, Roelandt JRTC: Transthoracic three-dimensional echocardiography in adult patients with congenital heart disease. *J Am Coll Cardiol* 1995;26:759-767
46. Vogel M, Ho SY, Lincoln C, Yacoub MH, Anderson RH: Three-dimensional echocardiography can simulate intra-operative visualization of congenitally malformed hearts. *Annals of Thoracic Surgery.* 1995;60:1282-1288
47. Levine RA, Handschumacher MD, Sanfilippo AJ, Hagege AA, Harrigan P, Marshall JE, Weyman AE: Three-dimensional echocardiographic reconstruction of the mitral valve, with implications for the diagnosis of mitral valve prolapse. *Circulation* 1989;80:589-598
48. Cheng TO, Wang XF, Zheng LH, Li ZA, Lu P: Three-dimensional transesophageal echocardiography in the diagnosis of mitral valve prolapse. *Am Heart J* 1994; 128:1218-1224
49. Trocino G, Salustri A, Roelandt JR, Ansink T, van Herwerden L: Three-dimensional echocardiography of a flail tricuspid valve. *J Am Soc Echocardiogr* 1996;9:91-93
50. Salustri A, Becker AE, Van Herwerden L, Vletter WB, Ten Cate FJ, Roelandt JRTC: Three-dimensional echocardiography of normal and pathologic mitral valve: A comparison with two-dimensional transesophageal echocardiography. *J Am Coll Cardiol* 1996;27:1502-1510
51. Kasprzak JD, Salustri A, Roelandt JR, Cornel JH: Comprehensive analysis of aortic valve vegetation with anyplane, paraplane, and three-dimensional echocardiography [letter] *European Heart J* 1996;17:318-320
52. Hozumi T, Yoshikawa J, Yoshida K, Akasaka T, Takagi T, Yamamuro A. Assessment of flail mitral leaflets by dynamic three-dimensional echocardiographic imaging. *J Am Cardiol* 1996;79:223-225
53. Yao J, Cao QL, Marx G, Pandian NG: Three-dimensional echocardiography: Current development and future directions. *J Med Ultrasound* 1996;4(1): 11-19
54. Delabays A, Sugeng L, Pandian NG, Tsu TL, Ho SL, Chen CH, Marx GR, Schwartz SL, Cao QL: Dynamic three-dimensional echocardiographic assessment of intracardiac blood flow jets. *Am J Cardiol* 1995;76:1053-1058
55. Borges AC, Witt C, Bartel T, Muller S, Konertz W, Baumann: Preoperative two- and three-dimensional transesophageal echocardiographic assessment of heart tumors. *Annals of Thoracic Surgery* 1996;61:1163-1167
56. Nixon JV, Saffer SI, Lipscomb K, Blomqvist CG: Three-dimensional echoventriculography. *Am Heart J* 1983;106:435-442
57. Fazzalari NL, Goldblatt E, Adams APS: A composite three-dimensional echocardiographic technique for left ventricular volume estimation in children: comparison with angiography and established echocardiographic method. *J Clin Ultrasound* 1986;14:663-674
58. Martin RW, Bashein G: Measurement of stroke volume with three-dimensional transesophageal ultrasonic scanning: comparison with thermodilution measurement. *Anesthesiology* 1989;70:470-476
59. Zoghbi WA, Buckey JC, Massey MA, Blomqvist CG: Determination of left ventricular volumes with use of a new nongeometric echocardiographic method: Clinical validation and potential application. *J Am Coll Cardiol* 1990;15:610-617
60. Gopal AS, Keller AM, Rigling R, King Jr DL, King DL: Left ventricular volume and endocardial surface

area by three-dimensional echocardiography: comparison with two-dimensional echocardiography and nuclear magnetic imaging in normal subjects. *J Am Coll Cardiol* 1993;22:258-270

61. Handschumacher MD, Lethor JP, Siu SC, Mele D, Rivera M, Picard MH, Weyman AE, Levine RA: A new integrated system for three-dimensional echocardiographic reconstruction: development and validation for ventricular volume with application in human subjects. *J Am Coll Cardiol* 1993;21;743-753
62. Siu SC, Rivera JM, Guerrero JL, Handschumacher MD, Lethor JP, Weyman AE, Levine RA, Picard MH: Three-dimensional echocardiography: in vivo validation for left ventricular volume and function. *Circulation* 1993;88 [part 1]:1715-1723
63. King DL, Gopal AS, Keller AM, Sapin PM, Schröder KM: Three-dimensional echocardiography. Advances for measurement of ventricular volume and mass. *Hypertension* (suppl I) 1994;23:I-172-I-179
64. Sapin PM, Schroder KM, Gopal AS, Smith MD, DeMaria AN, King DL: Comparison of two- and three-dimensional echocardiography with cineventriculography for measurement of left ventricular volume in patients. *J Am Coll Cardiol* 1994;24:1054-1063
65. Nosir YFM, Fioretti PM, Vletter WB, Boersma E, Salustri A, Postma JT, Reijs AEM, Ten Cate FJ, Roelandt JRTC: Accurate measurement of left ventricular ejection fraction by three-dimensional echocardiography. A comparison with radionuclide angiography. *Circulation* 1996;94:460-466
66. Yao J, Cao QL, Masani N, Delabays A, Magni G, Acar P, Laskari C, Pandian NG. Three-dimensional echocardiographic estimation of infarct mass based on quantification of dysfunctional left ventricular mass. *Circulation* 1997;96(5):1660-6
67. Delabays A, Cao QL, Yao J, Magni G, Kanojia A, Acar P, Laskari C, Masani N, Schwartz S, Pandian N: Contrast three-dimensional echocardiography in acute myocardial infarction: 3-D reconstruction of perfusion defects yields accurate estimate of infarct mass and extent. (abstract 718-4) *J Am Coll Cardiol* 1996;27(2) [suppl A]:63A
68. Multicenter Postinfarction Reasearch Group. Risk stratification and survival aftre nmyocardial infarction. *N Engl J Med* 1983;309:331-338.
69. Sanz G, Castaner A, Betriu , Magrina J, Roig E, Coll S, Pare JC, Navarrolopez F. Determinants of prognosis in survivors of acute myocardial infarction. *N Engl J Med* 1982;306:1065-1070.
70. Linka AZ, Ates G, Wei K, Firoozan S, Skyba DM, Kaul S. Three-dimensional myocardial contrast echocardiography: validation of in vivo risk and infarct volumes. *J Am Coll Cardiol* 1997;30(7):1892-1899.
71. Kasprzak JD, Vletter WB, Roelandt JRTC, van Meegen JR, Johnson R, Ten Cate FJ. Visualization and quantification of myocardial mass at risk using three-dimensional contrast echocardiography. *Cardiovasc res.* 1998;40:314-21.
72. Masani ND, Yao J, Cao QL, Avelar E, Vannan M, Pandian N. Identification of myocardial infarction by contrast echocardiography using a new transpulmonary agent-NC100100: comparison of anterior vs. posterior, and patchy vs. solid necrosis. (abstract) *J Am Coll Cardiol* 1998; 31(suppl A):438A
73. Yao J, Takeuchi M, Teupe C, Avelar E, Abadi C, Ogunyankin K, Pandian N. 3-dimensional contrast echocardiography can delineate and quantify residual infarct mass and salvaged myocardial mass in reperfused myocardium following acute ischemia: experimental studies using a new contrast agent - SHU 563A. (abstract 1008) *Circulation* 1998;17:I-194
74. Yao J, Taams MA, Kasprzak JD, de Feijter PJ, ten Cate FJ, van Herwerden LA, Roelandt JRTC. Usefulness of three-dimensional transesophageal echocardiographic imaging for evaluating narrowing in the coronary arteries. *Am J Cardiol*
75. Yao J, Masani N, Cao QL, Nikuta P, Pandian NG. Clinical application of transthoracic Volume-rendered three-dimensional echocardiography in the assessment of mitral regurgitation. *Am J Cardiol* 1998;82:189-196
76. Vannan MA, Cao QL, Pandian NG, Sugeng L, Schwartz SL, Dalton MN. Volumetric multiplexed transmission holography of the heart with echocardiographic data. *J Am Soc Echocardiogr* 1995;8:567-575.
77. Hunziker PR, Smith S, Scherrer-Crosbie M, Liel-Cohen N, Levine RA, Nesbitt R, Benton SA, Picard MH. Dynamic holographic imaging of the beating human heart. *Circulation* 1999;99: e3
78. Bruining N, Roelandt JRTC, Janssen M, grinst G, Berlage T, Waldinger J, Mumm B. Virtual reality : a teaching and training tool or just a computer game? *Thoraxcenter J* 1998;(10):7-10
79. Gilon D, Cape EG, Handschumacher MD, Jiang L, Sears C, Solheim J, Morris E, Strobel JT, Miller-Jones SM, Weyman AE, Levine RA. Insights from three-dimensional echocardiographic laser stereolithography. Effect of leaflet funnel geometry on the coefficient of orifice contraction, pressure loss, and the Gorlin formula in mitral stenosis. *Circulation* 1996;94: 452-459.

CHAPTER 3

APPROPRIATE THREE-DIMENSIONAL ECHOCARDIOGRAPHIC DATA ACQUISITION INTERVAL FOR LEFT VENTRICULAR VOLUME QUANTIFICATION: IMPLICATIONS FOR CLINICAL APPLICATION

Jiefen Yao, MD; Jaroslaw D. Kasprzak, MD; Youssef F.M. Nosir, MD; René Frowijn, MSc; Wim B. Vletter, MSc; Jos R.T.C. Roelandt, MD, PhD

Submitted

Appropriate Three-Dimensional Echocardiographic Data Acquisition Interval for Left Ventricular Volume Quantification: Implications for Clinical Application

Jiefen Yao, MD; Jaroslaw D. Kasprzak, MD; Youssef F.M. Nosir, MD; René Frowijn, MSc; Wim B. Vletter, MSc; Jos R.T.C. Roelandt, MD, PhD

Background: Volume-rendered three-dimensional echocardiography (3DE) acquired with small imaging intervals has been validated for accurate left ventricular (LV) volume measurement. However, its clinical application is often impeded by the lengthy acquisition time. The aim of this study was to examine the accuracy of LV volume measurement from 3DE data acquired at different intervals. **Methods:** Transthoracic 3DE data sets of LV were acquired at intervals of 2°, 6°, 9°, 12°, 15°, 18° and 20° in 10 human subjects with various cardiac shapes and function. The LV end-diastolic volume (EDV) and end-systolic volume (ESV) were measured from each 3DE data set using the "summation of discs" method. Inter- & intra-observer variabilities were also examined. Measurements obtained from data acquired at 2° intervals were used as references of comparison. **Results:** From 10 subjects, a total of 70 3DE data sets were obtained. Data acquisition time decreased from 189±143 minutes at intervals of 2° to 19±6 minutes at 20°. LV EDV and ESV slightly decreased from data obtained at larger intervals, but no statistical significance was found among the measurements derived from data obtained at various intervals. Excellent agreement was obtained between intra-observer measurements (r=0.97, SEE=6.8 ml and mean difference = 0.7±5.6ml for LVEDV; and r=0.96, SEE=6.0ml and mean difference=-1.2±6.6ml for LVESV). **Conclusion:** Data acquired at 12° and 15° remained accurate for LV volume measurement and saved over 80% of time in comparison with data acquired at 2° intervals. Further increase in imaging intervals tended to underestimate LV volumes without significant acceleration of the procedure.

Key Words: Three-dimensional echocardiography, left ventricular function

Volume-rendered three-dimensional echocardiography (3DE) acquired with small imaging intervals between scan planes has been validated for accurate left ventricular (LV) volume measurement.[1,2] 3DE data acquisition with small intervals usually takes minutes or even longer, depending on the heart rate and rhythm of the patient. The lengthy acquisition time is one of the major limitations of 3DE in its clinical application. The smaller the intervals, the longer it takes for data acquisition, the more the chances are to result in motion artifacts. This comprehended the employment of 3DE in its daily clinical application, as well as in many emergency settings, despite its superiority over two-dimensional echocardiography (2DE) in the accuracy of LV volume and function measurement. The aim of this study was to examine the accuracy of LV volume measurement from 3DE data sets acquired at different imaging intervals and the time spent for data acquisition.

Methods

3DE data acquisition was performed in 10 subjects (9 males, age 49±19 years old, ranged from 25-74 years). They included 3 normal volunteers with normal LV shape and function, 2 patients with regional wall motion abnormalities due to coronary artery disease and 5 patients with hypertrophic cardiomyopathy. From each subject, 7 data sets were obtained at the apical window using rotational scanning format gated to electrocardiogram and expiration, with imaging intervals of 2°, 6°, 9°, 12°, 15°, 18° and 20°, respectively, after an informed consent was obtained. A commercially available 3DE processing system (TomTec, EchoScan 3.1, TomTec Imaging System GmbH, Munich, Germany) was used in controlling

imaging plane rotation, storing and processing of the acquired images and quantitative measurement of LV volumes from the 3DE data sets. From each data set, the LV was sectioned into 8 parallel, equidistant slices. By manually tracing the endocardial borders on all slices, LV end-diastolic volume (LVEDV) and end-systolic volume (LVESV) were measured using "summation of discs" method. All measurements were repeated by the same observer two weeks later and also by another observer to test inter- and intra-observer agreements and variabilities.

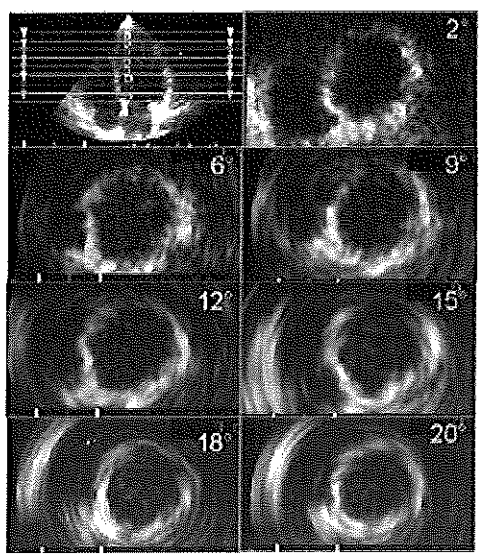

Figure 1. Examples of mid-LV short-axis views reconstructed from 3DE data sets acquired at rotational scanning intervals of 2°, 6°, 9°, 12°, 15°, 18° and 20°, respectvely, as annotated in each panel. The upper left panel is a LV 4-chamber view used as a reference image to confirm reconstruction of true short-axis views and to decide the thickness of the LV short-axis slices so that the whole LV chamber is included for measurement.

All values were expressed as mean ± SD or mean ± SEE. Results from data acquired at 2° intervals were used as reference. Comparison between data obtained with various intervals were examined using linear regression method, paired student t test and Bland-Altman analysis. A p value of < 0.05 was defined statistically significant.

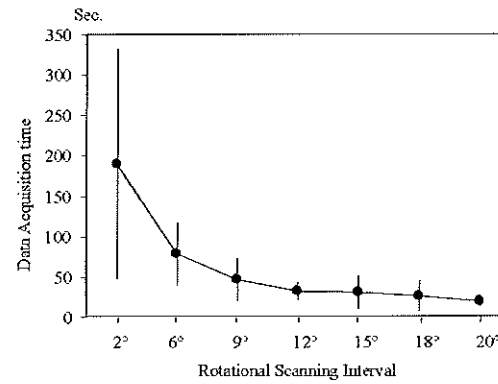

Figure 2. Time used for 3DE data acquisition (y axis, mean ± SD) at rotational scanning intervals of various degrees (x axis).

Results

A total of 70 3DE data sets at rotational scanning intervals of 2°, 6°, 9°, 12°, 15°, 18° and 20° were obtained from 10 subjects. Figure 1 are examples of mid-LV short-axis views reconstructed from 3DE data sets obtained at intervals of 2°, 6°, 9°, 12°, 15°, 18° and 20° from a patient. The data acquisition time was 189±143 (88 to 570) seconds at 2° intervals. Data acquisition time decreased with increase of intervals. At intervals of 20°, the 3DE data acquisition time was 19±6 (15 to 36) seconds (figure 2). Both LVEDV and LVESV from data obtained at different acquisition intervals correlated well with that from 2° intervals. However, there was a tendency of decrease in measured LV volumes with the increase in data acquisition intervals, eventhough no significant difference was observed between values of LV volumes from data acquired at various intervals and in comparison with data from 2° intervals. Good correlation was obtained between both inter-observer and intra-observer measurements, with less variabil-

ities at smaller intervals. No significant difference was observed even at data obtained at intervals as big as 20° (Table 1). Good agreement was also obtained from intra- and- interobserver measurements with increased, but nonsignificant, variabilities at larger intervals.

Table 1. Comparison of time and LV volume measurements between data acquired at various intervals as compared to that at 2° intervals.

Int.	Time	LVEDV	LVESV	r	SEE	P	Diff.	P
2°	189±143	119±23	74±21	-	-	-	-	-
6°	78±39	115±23	73±21	0.99	4.0	<.0001	-2.5±4.0	NS
9°	47±27	112±28	73±20	0.98	7.1	<.0001	-4.1±6.8	NS
12°	33±11	111±30	70±20	0.97	8.2	<.0001	-6.0±7.8	NS
15°	30±21	111±28	70±20	0.97	8.5	<.0001	-6.3±8.1	NS
18°	25±20	108±31	68±19	0.94	11.7	<.0001	-8.3±11.1	NS
20°	19±6	103±27	69±18	0.95	9.5	<.0001	-10.5±9.9	NS

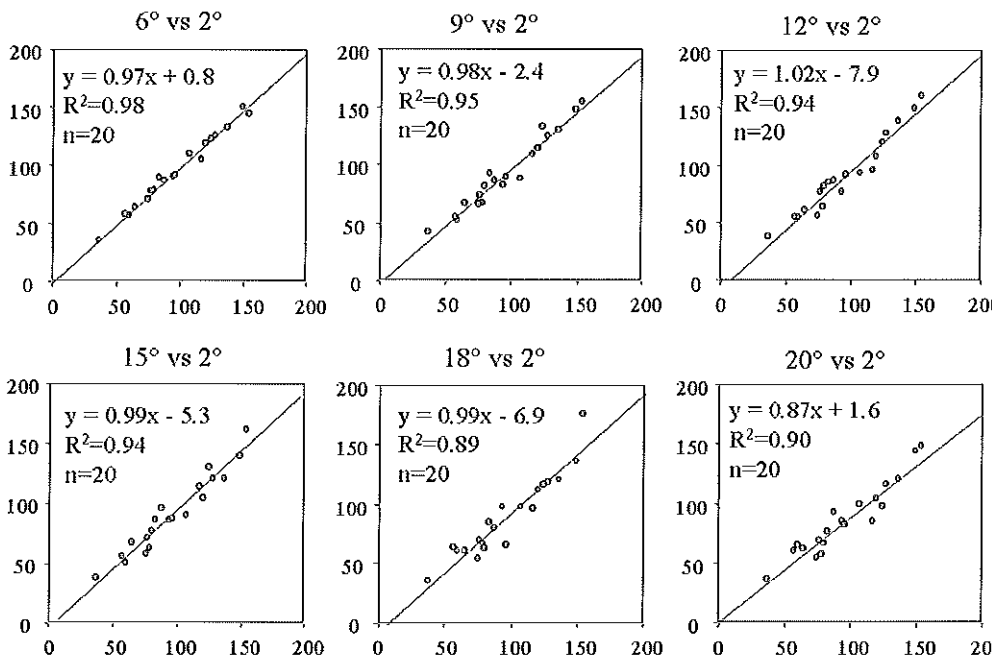

Figure 3. Comparison of the measurements of LVEDV and LVESV from 3DE data sets obtained at various rotational sacnning intervals with that obtained at 2°, using linear regression method.

Discussion

The significance of accurate assessment of LV volume and function has been widely recognized by clinicians in the management of patients with primary or secondary cardiac abnormalities. Various geometric assumptions of the LV have been used when measuring the LV volume or ejection fraction by 2DE.[3-7] These geometric models work well with normal LV, but less so with abnormal LVs. At times when the function and/or the shape of the LV changes, often are times when the estimation of the LV

volume and/or function important in clinical patient management. The limitation of 2DE in the accuracy of LV volume measurement is mainly due to the use of limited number of cutting planes and off-axis views in extrapolating the whole LV cavity. 3DE, on the other hand, uses the volumetric data of the LV in calculating its volume, obviating the need of geometric assumptions. It is, therefore, more accurate than 2DE methods, even in abnormal LV. However, the clinical application of 3DE in daily clinical practice for LV volume and function assessment is hampered by its lengthy data acquisition time and processing time. The later has been improved by shortening the image processing time and by facilitating and simplifying data analysis and quantitative measurement methods. In our study, subjects with various shapes and functional status of LV were chosen to test the accuracy of 3DE acquired at different intervals. The results showed that, by saving over 80% of time, 3DE data sets acquired at 12° intervals yielded accurate and reproducible measurements of LV volumes in comparison with data acquired at 2° intervals. Further increase in acquisition intervals (15° or more) did not accelerate data acquisition significantly, but tended to underestimate LV volumes and increase measurement variabilities (Table 2).

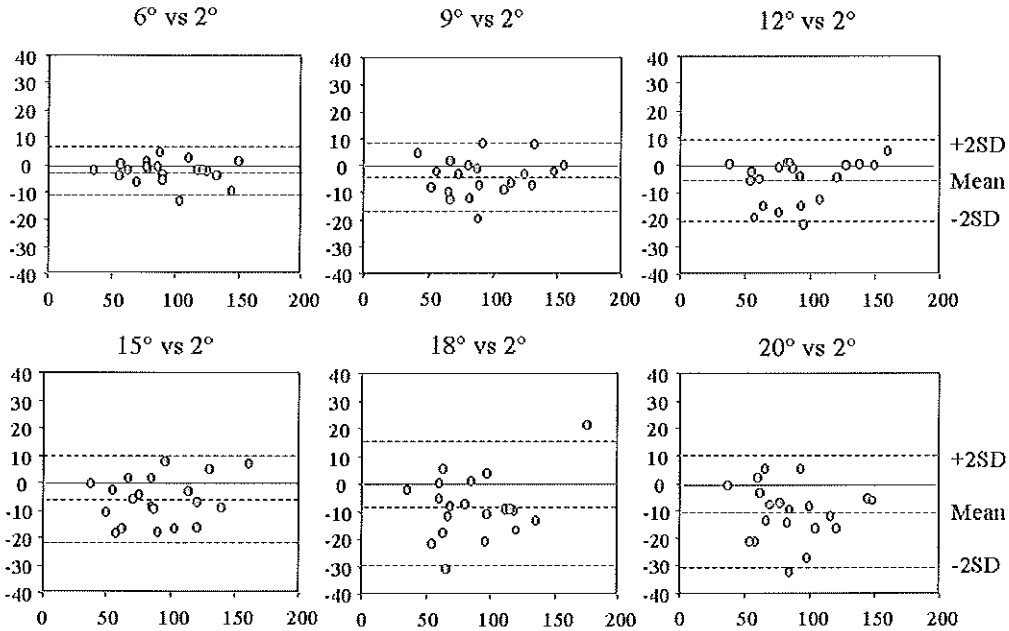

Figure 4. Bland-Altman analysis showing the discrepancies between measurements of LVEDV and LVESV from data acquired at various intervals in comparison with that obtained at 2°.

Table 2. intra-observer and inter-observer variabilities in the measurement of LV volumes from 3DE data sets acquired at various rotational intervals.

	Intra-observer			Inter-observer		
Int	R^2	SEE	Diff.	R^2	SEE	Diff.
2°	.96	6.3	1.0±6.4	.98	4.3	0.3±4.1
6°	.96	6.3	0.1±3.2	.95	6.8	-0.7±3.8
9°	.98	4.6	0.2±4.7	.92	8.9	2.8±9.1
12°	.96	6.5	0.0±7.0	.91	9.9	0.7±10.1
15°	.97	6.4	1.3±6.1	.84	12.8	-1.5±12.9
18°	.97	6.0	-0.7±6.7	.79	15.4	0.7±15.9
20°	.94	7.5	0.2±7.2	.78	16.0	5.4±15.2

Int. = interval, Diff. = mean difference.

This study had the following limitations. The number of subjects was too small to be divided into subgroups of different categories of diseases. However, the preliminary results were obtained from subjects of whom the majority had abnormal LVs. A future study in a larger group of patients with various abnormalities and shape changes of LV may further define the appropriate 3DE data acquisition interval in different subgroups. We did not compare the 3DE measurement of LV volume from data acquired at various intervals with an independent technique since the accuracy of LV volume measurement from data obtained at 2° rotational scanning intervals has been previously proven.

1. Nosir YFM, Fioretti PM, Vletter WB, Boersma E, Salustri A, Postma JT, Reijs AEM, Ten Cate FJ, Roelandt JRTC. Accurate measurement of left ventricular ejection fraction by three-dimensional echocardiography. A comparison with radionuclide angiography. *Circulation* 1996;94:460-466.
2. Nosir YF, Lequin MH, Kasprzak JD, van Domburg RT, Vletter WB, Yao J, Stoker J, Ten Cate FJ, Roelandt JR. Measurements and day-to-day variabilities of left ventricular volumes and ejection fraction by three-dimensional echocardiography and comparison with magnetic resonance imaging. *Am J Cardiol* 1998;82:209-214
3. Parisi AF, Moynihan PF, Feldman CL, Folland ED. Approaches to determination of left ventricular volume and ejection fraction by real-time two-dimensional echocardiography. Clin Cardiol 1979;2:257-263.
4. Schiller NB, Acquatella H, Ports TA, Drew D, Goerke J, Ringertz H, Silverman NH, Brundage B, Botvinick EH, Boswell R, Carlsson E, Parmley WW. Left ventricular volume from paired biplane two-dimensional echocardiography. Circulation 1979;60:547-555.
5. Gehrke J, Leeman S, Raphael M, Pridie RB. Non-invasive left ventricular volume determination by two-dimensional echocardiography. Br Heart J 1975;37:911-916.
6. Folland ED, Parisi AF, Moynihan PF, Jones DR, Feldman CL, Tow DE. Assessment of left ventricular ejection fraction and volumes by real-time, two-dimensional echocardiography: a comparison of cineangiographic and radionuclide techniques. Circulation 1979;60:760-766.
7. Wyatt HL, Meerbaum S, Gueret P, Corday E. Cross-sectional echocardiography. III. Analysis of mathematical models for quantifying volumes of symmetric and asymmetric left ventricles. Am Heart J 1980;100:821-828.

CHAPTER 4

THREE-DIMENSIONAL ECHOCARDIOGRAPHIC ESTIMATION OF INFARCT MASS BASED ON QUANTIFICATION OF DYSFUNCTIONAL LEFT VENTRICULAR MASS

Jiefen Yao, MD; Qi-Ling Cao, MD; Navroz Masani, MBBS; Alain Delabays, MD; Giuseppina Magni, MD; Philippe Acar, MD; Cleo Laskari, MD; Natesa G. Pandian, MD

Circulation **1997;96(5):1660-1666**

Three-Dimensional Echocardiographic Estimation of Infarct Mass Based on Quantification of Dysfunctional Left Ventricular Mass

Jiefen Yao, MD; Qi-Ling Cao, MD; Navroz Masani, MBBS; Alain Delabays, MD; Giuseppina Magni, MD; Philippe Acar, MD; Cleo Laskari, MD; Natesa G. Pandian, MD

Background. Two-dimensional echocardiography is useful for estimating the extent of infarct-related wall motion abnormalities. Such estimation however is based on a few selected, non-parallel views and extrapolated for the whole left ventricle (LV). This approach does not provide us with the actual amount of dysfunctional myocardium. Volume-rendered 3-dimensional echocardiography (3DE) might be able to overcome these limitations. In this study we explored: 1) how well volume-rendered 3DE delineates regional dysfunction of the infarcted LV; and 2) how well dysfunctional myocardial mass quantified by 3DE reflects the actual anatomic infarct mass.

Methods and results. 3DE was performed before and 3 hours after coronary occlusion in 16 dogs. Viewing the LV in parallel equidistant short axis slices, the region of dysfunction on each slice was demarcated, from which the dysfunctional myocardial mass was derived. Using triphenyl tetrazolium chloride staining, anatomic infarct regions were delineated, dissected and weighed to obtain anatomic infarct mass. we also examined the accuracy of three-dimensional echocardiographic quantification of left ventricular infarction when data were acquired in steps of 1, 2, 3 and, 5 degree increments in 8 dogs. The anatomic infarct mass was 16.3 ± 7.7 gm (mean±SD) (range: 6.4 to 31.4 gm); the dysfunctional mass estimated by 3DE was 17.4 ± 9.1 gm (range: 5.2 to 39.0 gm). The mean difference was 1.0 gm. The correlation between dysfunctional mass (y) and infarct mass (x) was: $y = 1.1x - 0.6$, $r = 0.93$ ($P < 0.0001$). The percent of LV involved in infarction was 18.2 ± 5.8% (range: 9.1 to 26.1%); the percent of LV involved in regional dysfunction was 18.3 ± 6.9 % (range 7.9 to 31.2%) .The mean difference was 0.1%. The correlation between percent of LV involved in infarction (x) and percent of LV involved in dysfunction (y) was $y = 1.0x - 1.1$, $r = 0.92$ ($P < 0.0001$). No significant difference was found between three-dimensional measurements from data acquired with 1, 2, 3, or 5 degrees.

Conclusions. Volume-rendered 3DE crisply displays regional dysfunction of infarcted LV. 3DE measured dysfunctional mass accurately reflects the anatomically infarcted mass.

Key Words. echocardiography, myocardial infarction, cardiovascular diseases, myocardium, infarction

Accurate estimation of myocardial infarct size is known to have prognostic and therapeutic implications.[1,2] Two-dimensional echocardiography has become the most commonly used technique to identify regional myocardial dysfunction caused by infarction and to estimate the extent of dysfunctional left ventricular myocardium. Two-dimensional echocardiographic assessment of dysfunctional myocardium has been shown to correlate with infarct size both in experimental and clinical studies.[3-7] However, most such studies employed a few selected two-dimensional views in short-axis or apical orientations, from which the extent of the wall motion abnormality was computed. A percentage of dysfunctional myocardium was often derived either for a given two-dimensional slice or extrapolated for the whole ventricle.[8-11] Effort has not been directed to evaluate how well the extent of regional dysfunctional myocardium reflects the actual anatomic mass of the infarcted myocardium. One of the major reasons for this is the inability of two-dimensional echocardiography, hampered by the limited number of imaging planes available to examine a three-dimensional organ, to accurately measure left ventricular mass and in particular the mass of a given myocardial region. This difficulty is compounded when the infarcted region undergoes expansion which leads to regional geometric distortion of the left ventricle. Such distortion could lead to errors when one attempts to extrapolate functional infarct size from limited two-dimensional views. If the whole ventricle could be interrogated with more imaging

samples, the resulting three-dimensional data could aid in more accurate quantitation of dysfunctional myocardium. Although attempts have been made to employ three-dimensional reconstruction techniques to examine ischemic myocardial dysfunction, they have not been applied widely because they were rather laborious and did not allow visualization of the left ventricular myocardium. Volume-rendered three-dimensional echocardiography has recently proven to be clinically feasible.[12-14] This technique is capable of reproducing dynamic cardiac anatomy in all its dimensions and also yielding quantitative data. Preliminary studies have suggested that it might be possible to measure myocardial mass.[15] However, the utility of three-dimensional echocardiography in qualitative depiction of wall motion abnormalities and in quantitative estimation of the extent of dysfunctional myocardium is not known. This study was designed to address the following questions: (1) how well volume-rendered three-dimensional echocardiography demonstrates regional myocardial dysfunction in three-dimensional display projections; and (2) how well three-dimensional echocardiographic quantification of dysfunctional left ventricular mass reflects actual anatomic infarct mass.

Methods

We employed three-dimensional echocardiography in an open-chest canine model of acute myocardial infarction. Using a rotational mode of data acquisition, three-dimensional data sets were collected, three-dimensional reconstructions were performed and display projections derived from various orientations to identify regional dysfunction. The mass of the whole left ventricle and that of the dysfunctional region were quantified from the three-dimensional data set. Triphenyl tetrazolium chloride (TTC) staining was utilized to delineate and quantify infarcted regions in the autopsied hearts. The mass of the whole left ventricle and that of the infarcted region were determined. The echocardiographic data were compared to the actual anatomic data.

Animal preparation

Sixteen mongrel dogs (22 ± 4 kg in weight) were sedated with intramuscular acepromazine (20-30 mg), anesthetized with intravenous sodium pentobarbital (25 mg/kg of body weight), intubated, and ventilated with room air using a volume cycle respirator. Lead II of the electrocardiogram was monitored throughout the experiment. A femoral artery and vein were instrumented with fluid-filled catheters for the purpose of monitoring arterial pressure and fluid and drug administration. The chest was opened by mid-line sternotomy. A pericardial cradle was created and the heart exposed. One of the main coronary arterial branches or its major secondary branches (left anterior descending coronary artery in 10 dogs and posterior descending coronary artery in 6 dogs) was isolated and occluded with a silk snare. Lidocaine (1 mg/kg bolus before coronary occlusion and 0.5 mg/min continuous infusion thereafter) was given intravenously to prevent ventricular fibrillation. Three hours after coronary occlusion, a water-bath was arranged above the pericardial cradle for ultrasound transmission without affecting the hemodynamics of the heart. Data acquisition for three-dimensional echocardiography was then performed. At the end of the experiment, the dog was euthanized with an intravenous injection of 10 ml potassium chloride (10%) and TTC staining performed for measurement of the anatomical mass of infarcted myocardium.

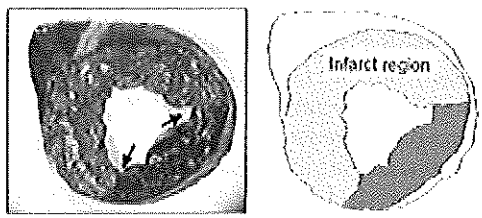

Figure 1. Anatomical specimen from a canine heart showing infarct demarcation by triphenyl tetrazolium chloride (TTC) staining. The infarct zone is seen as a pale region. Whereas the non-infarct region is stained red (dark) by TTC. There is a clear delineation between infarct and non-infarct regions (arrows).

Measurement of total left ventricular mass and infarct mass

A solution of 1% TTC was prepared at a temperature of approximately 37 °C and 250 ml was perfused into the root of the aorta at a pressure of 120 mmHg immediately after the dog was sacrificed while the ascending aorta was clamped. The heart was explanted, the left ventricle isolated, weighed and cut into 6 to 8 parallel transverse slices; each slice was ≈ 1 cm thick. The infarct region was defined visually based on its pale appearance in contrast to the non-infarct area stained red by TTC (Figure 1). After delineating the infarct region by examining both sides of each slice, the infarct zones were carefully dissected out in each slice and weighed. From the total left ventricular mass and the infarct mass data, the percentage of left ventricle involved in infarction was calculated.

Data acquisition for three-dimensional echocardiography

A commercially available ultrasound unit (Sonos 2500, Hewlett-Packard, Andover, Massachusetts) was employed for two-dimensional image acquisition. This instrument was interfaced with a commercially available three-dimensional image processing system (EchoScan, version 3.0, TomTec Imaging Systems, Boulder, Colorado) for on-line data acquisition and storage, and off-line data processing, three-dimensional reconstruction, display and quantification. A carriage device with a rotational motor was mounted onto a 2.5/5 MHz imaging transducer which was then positioned to image the heart through the water-bath from an anterior epicardial orientation. The rotation of the transducer and thus the imaging plane was controlled by the three-dimensional system in a predefined manner. Two-dimensional imaging of the left ventricle was initiated in a long-axis orientation and images were obtained at every three degrees from 0 through 180 degrees. In 8 dogs, additional data acquisitions were performed with intervals of 1, 2 and 5 degrees, respec-

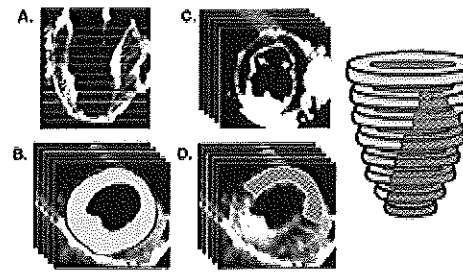

Figure 2. Method for quantitation of dysfunctional myocardial mass by volume-rendered three-dimensional echocardiography. The three-dimensional data set of the left ventricle was electronically cut into 12 to 15 equidistant slices (A). For determining total left ventricular mass, the myocardium of the left ventricle on each transverse slice was contoured and labeled (B). By integrating the slice thickness with the slice area, the volume of each slice and the total volume of all myocardial slices were computed in an automated manner. Myocardial volume (ml) multiplied by assumed specific gravity (1.04 gm/ml) provided myocardial mass (gm). For measurement of the mass of dysfunctional myocardium, each parallel short-axis two-dimensional left ventricular slice extracted from the three-dimensional data set was viewed in a dynamic mode. The segments that exhibited discrete akinesis or dyskinesis were demarcated (C). These segments were contoured and labeled (D). The volume of the dysfunctional myocardial segments (the labeled regions) was derived, and multiplied by the specific gravity of the myocardium, the mass of the dysfunctional myocardium was generated.

tively. Electrocardiographic and respiratory gating were used for spatial and temporal registration of the images. The acquired data were calibrated, reformatted and stored in the computer and transferred onto optical laser disks for off-line processing and analysis

Echocardiographic data processing, three-dimensional reconstruction, display and quantification

The acquired ultrasound data were post-processed and interpolated into a voxel-rendered three-dimensional data set. Three-dimensional images of the left ventricle before and after coronary occlusion were reconstructed using different cutting planes and projections. The feasibility and ease of displaying and identifying regional left ventricular dysfunction from longitudinal, sagittal and coronary sections were assessed.

Three-dimensional echocardiographic quantification of dysfunctional mass was performed by a blinded observer. The three-dimensional data set of the left ventricle was electronically segmented into 12 to 15 equidistant slices (5.6 - 5.8 mm thick) in short axis orientation for computation of total left ventricular mass and for calculation of dysfunctional myocardial mass (Figure 2A). For determination of total left ventricular mass each short axis slice was reviewed in real time and frame by frame. The left ventricular epicardial and endocardial borders were traced at end diastole using a trackball and digitizing system integrated in to the three-dimensional processing computer. The cross sectional area of the left ventricular myocardium obtained between the epicardial and endocardial contours was given a computer derived "label". (Figure 2B). By integrating the slice thickness with the slice area, the volume of each slice and the total volume of all myocardial slices were computed in an automated manner by the following quantification algorithm: volume (ml) = $\sum$(area of each slice [mm^2] x slice thickness [mm]). Myocardial volume multiplied by assumed specific gravity (1.04 gm/ml) provided myocardial mass (gm). For measurement of the mass of the dysfunctional myocardium, each paraplane short axis slice was viewed in dynamic mode. Discrete akinetic or dyskinetic segments were identified, a contour drawn around them from endocardium to epicardium (Figure 2C) and a label derived (Figure 2D). The volume and mass of the dysfunctional segments (the labeled regions) were calculated as described above. From these data, the percentage of the total left ventricular myocardium involved in regional myocardial dysfunction was calculated. The three-dimensional data set was processed and quantitative data derived weeks apart in a blinded manner for evaluating intra-observer variability. Another investigator analyzed the data for obtaining inter-observer variability.

Segmental analysis

To identify the site of infarction, the transverse cut in which the papillary muscles were largest was examined in both anatomical specimens and in short axis images from the three-dimensional data set by 2 blinded observers. A transparent overlay with 16 equally spaced radii was used to divide the specimens and images into 16 segments. The zero point was located at the anterior ventriculo-septal junction and the center of the grid placed at the center of the left ventricular cavity. Segments with evidence of infarction by TTC staining and akinesis or dyskinesis by echocardiography were identified and compared. 112 segments in 7 dogs were analyzed for this purpose.

Statistical analysis

Echocardiographic and anatomic data are expressed as mean ± standard deviation. To detect differences between three-dimensional echocardiographic measurements with anatomic data, we used Student's

paired t test. Data was compared using simple linear regression and the mean differences and limits of agreements were analyzed by Bland and Altman's method. Inter- and intra-observer variability are expressed as the coefficient of variance. For the above analyses, a p value of <0.05 was considered significant. To detect differences between three-dimensional echocardiographic acquired using different degree increments, analysis of variance (ANOVA) was used with a Bonferroni-Dunn correction for which a p value of <0.005 was considered significant.

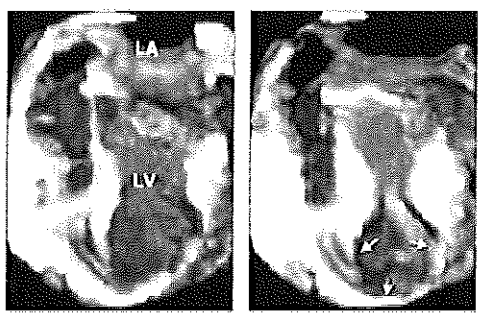

Figure 3. Diastolic (left) and systolic (right) three-dimensional echocardiographic projectionsin a four chamber format after occlusion of the left anterior descending coronary artery. The heart was cut in such a way as if the observer views the heart in an anterior lateral position. Regional cavity dilation in the apical portion and dyskinesis are evident (arrows).

Results

Three-dimensional echocardiographic display of ischemic myocardial dysfunction

This study yielded good quality three-dimensional reconstructions in all experiments. Myocardial regions that exhibited regional dysfunction could be well identified in dynamic three-dimensional projections. The left ventricle before coronary occlusion showed normal contraction and wall thickening in all regions during systole in all 16 dogs. Regions of dysfunctional myocardium following coronary occlusion displayed various regional wall motion abnormalities in volume-rendered dynamic three-dimensional images (Figure 3,4). Dynamic displays also demonstrated regional cavity dilation in all dogs following coronary occlusion. In addition to dynamic displays, extraction of the whole myocardium and dysfunctional regions could be performed in all dogs (Figure 5). Such displays allowed a direct three-dimensional perception of the location and extent of dysfunctional myocardium. The dysfunctional territories exhibited various sizes, shapes and locations in different dogs depending upon the site of coronary occlusion.

Comparison of three-dimensional echocardiographic quantification of dysfunctional myocardium to measurements from anatomic heart specimens

TTC staining demonstrated evidence of infarction in all canine hearts. Total left ventricular mass was 87 ± 21 gm (range: 54 to 123 gm). The mass of infarcted myocardium was 16.3 ± 7.7 gm (range: 6.4 to 31.4 gm) and the mass of dysfunctional myocardium determined by three-dimensional echocardiography was 17.4 ± 9.1 gm (range: 5.2 to 39.0 gm) (p = NS) (Figure 6A). The percentage of the left ventricular mass involved in infarction based on TTC staining was 18.2 ± 5.8% (range: 9.1 to 26.1%) and was not significantly different from the percentage of dysfunctional myocardium derived from three-dimensional echocardiography (18.3 ± 6.9 %, range 7.9 to 31.2%) (p = NS) (Figure 6B).

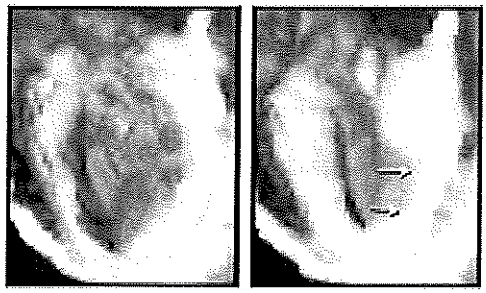

Figure 4. Diastolic (left) and systolic (right) three-dimensional echocardiographic projections after occlusion of the posterior descending coronary artery. Dyskinesis of the lateral posterior wall is displayed (arrows).

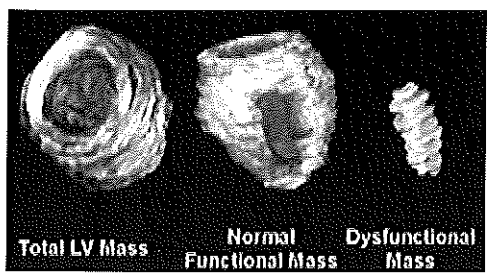

Figure 5. Volume-rendered three-dimensional images extracted from the three-dimensional data set of the contoured left ventricle displaying the whole left ventricular myocardium, normally functioning myocardium, and dysfunctional myocardium.

The correlation between three-dimensional echocardiography (y) and anatomic measurements (x) in the determination of total left ventricular mass was: $y = 0.8x + 7.3$, $r = 0.96$, $P < 0.0001$. The mean difference between these two methods was 1.2 gm. (p = NS). The correlation between dysfunctional mass determined by three-dimensional echocardiography (y) and infarct mass derived from TTC staining (x) was: $y = 1.1x - 0.6$, $r = 0.93$, $P < 0.0001$. The difference between these two methods was 1.0 ± 3.3 gm. (p = NS) (Figure 7). The correlation between the percentage of left ventricle involved in dysfunction as determined by three-dimensional echocardiography (y) and in anatomic infarction determined by TTC staining (x) was: $y = 1.0x - 1.1$, $r = 0.92$, $P < 0.0001$. Difference between these two methods was 0.1 ± 3.2 %, p = NS (Figure 8).

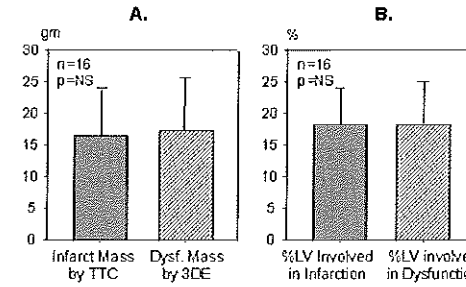

Figure 6. Bar graphs showing: A. infarct mass and dysfunctional mass; and B. Percent of left ventricular myocardium infarcted and percent of myocardium that was dysfunctional. TTC = TTC staining, Dysf. = dysfunctional, 3DE = three-dimensional echocardiography, %LV = percent of left ventricle.

When we analyzed the measurements of dysfunctional mass, left ventricular myocardial mass and percent of dysfunctional myocardium obtained with different imaging intervals (1, 2, 3 and 5 degrees), we observed that there was no difference in the correlations with anatomic infarct mass. Mean differences were not significant (table 1). No significant difference was found between three-dimensional measurements of data collected with different degree increments.

In 7 dogs, 112 left ventricular segments (from 7 slices, one slice in each dog) were analyzed by both three-dimensional and anatomical method. Among these segments, 29 showed evidence of infarction by TTC staining. 28 segments on two-dimensional images of the three-dimensional data set showed regional dysfunction (Table 2). The predictive accuracy for infarct location by 3DE was 90%. The discordance between echocardiographic and anatomic identification of the infarct segments was limited to one adjacent segment in each study which

may have been due to the difference in definition of the zero point.

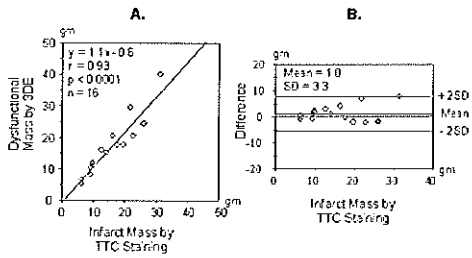

Figure 7. A: Regression plot showing the correlation between dysfunctional mass measured by three-dimensional echocardiography and infarct mass by TTC staining; B: Bland-Altman scattergram depicting the difference (y axis) between dysfunctional mass measured by three-dimensional echocardiography and infarct mass. The solid line shows the mean value and dotted lines ±2 standard deviations. 3DE = three-dimensional echocardiography, Difference = difference between dysfunctional mass by three-dimensional echocardiography and infarct mass by TTC staining.

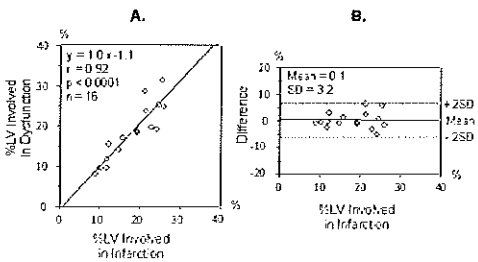

Figure 8. A: Regression plot showing the correlation between percent of left ventricular myocardium involved in dysfunction and percent of left ventricle involved in infarction. B: Bland-Altman scattergram showing the difference (y axis) between percent of left ventricle involved in dysfunction and the percent involved in infarction. %LV = percent of left ventricle, Difference = difference between percent of left ventricle involved in dysfunction and percent of left ventricle involved in infarction.

Intra- and inter-observer variability of quantitative analysis of three-dimensional data

In determining dysfunctional myocardial mass with three-dimensional echocardiography, the intra-observer variability was 2%, the difference between two measurements was 0.3±0.7 gm. The intraobserver variability for determining the percentage of dysfunctional left ventricular myocardium was 2%. The difference between these measurements was 0.3±0.9% with no statistical significance. The inter-observer variability for determining dysfunctional mass was 7.9%. The difference between measurements by two observers was 1.8±1.9 gm (p=NS). For quantifying the percent of left ventricular myocardial mass involved in dysfunction, the inter-observer variability was 11%. The difference between two observations was 1.6±3.1% (p=NS).

Discussion

Our animal study demonstrates that the actual mass of infarcted myocardium can be determined based on in vivo volume-rendered three-dimensional echocardiographic quantitation of the mass of dysfunctional myocardium in the setting of acute coronary occlusion. There was an excellent correlation between the mass of dysfunctional myocardium and pathologic infarct mass without systematic over- or underestimation. Furthermore, this three-dimensional echocardiographic method yielded an accurate measure of the percent of left ventricular myocardium that was dysfunctional and thus the percent of infarcted myocardium. In contrast to previous echocardiographic studies that derived the percent of infarcted myocardium by extrapolation from a few two-dimensional slices, three-dimensional echocardiography allowed analysis of multiple parallel and equidistant slices and thus more reliable quantification of the mass of dysfunctional myocardium. In addition to quantitative information, this technique also yielded dynamic three-dimensional projections of the left ventricle in numerous cutting planes and aided in visual appraisal of the wall motion abnormalities and infarct-induced alterations in regional shape.

Table 1. Quantification of Dysfunctional Myocardial Mass, Percent Dysfunctional Mass and LV Mass from 3D Data Set Acquired With Different Steps Compared With Anatomic Measurements.

Comparison with Anatomic Data and Acquisition Interval	Mean±SD	p	Regression Equation	r	Difference, Mean±SD	p
Dysfunctional mass, g						
1°	18.9±10.4	<0.001	y=1.0x-0.1	0.96	0.9±2.9	NS
2°	20.1±12.7	<0.001	y=1.3x-3.0	0.96	2.1±4.3	NS
3°	19.6±11.9	<0.001	y=1.2x-1.6	0.95	1.7±4.2	NS
5°	19.3±12.0	<0.001	y=1.2x-1.9	0.94	1.3±4.4	NS
Dysfunctional mass, %						
1°	19.3±7.2	<0.001	y=1.0x+0.7	0.94	1.2±2.5	NS
2°	20±9.4	<0.001	y=1.3x-3.7	0.93	1.8±4.1	NS
3°	19.2±8.5	<0.001	y=1.1x-1.6	0.90	1.0±3.9	NS
5°	20.1±9.4	<0.01	y=1.2x-2.0	0.86	1.9±5.0	NS
LV mass by 3DE, g						
1°	94.5±25.1	<0.0001	y=1.0x+0.7	0.98	0.3±4.7	NS
2°	93.3±23.6	<0.0001	y=0.9x+5.3	0.98	1.5±5.1	NS
3°	95.8±26.2	<0.0001	y=1.0x-0.9	0.97	1.0±6.4	NS
5°	91.5±22.3	<0.0001	y=0.9x+8.6	0.98	3.4±5.8	NS

Two-dimensional echocardiography in the evaluation of the extent of myocardial infarction

If accurately measured, the extent of regional myocardial dysfunction could be used to assess the size of myocardial infarction. Among several imaging techniques employed to assess the effects of infarct on regional left ventricular function, two-dimensional echocardiography has been used extensively for quantitative assessment of regional wall motion abnormalities and various methods have been utilized to obtain a quantitative estimate of regional dysfunction.[1-11] In many studies, the left ventricle was imaged in a few two-dimensional echocardiographic views (usually 3 to 4 short axis views and 1 or 3 apical views) and the circumferential extent of dysfunctional myocardium was determined based on a quantitative or semiquantitative method. From such measurements the fraction of left ventricle that was dysfunctional was extrapolated. Such data were then correlated to infarct size determined pathologically. Pandian et al showed that the fraction of the left ventricle that was dyskinetic correlated well with anatomically determined infarct fraction of left ventricle (r=0.92 and 0.94 at 20 minutes and 2 days after coronary occlusion).[5] Weiss et al demonstrated a correlation coefficient of 0.90 between the circumferential extent of myocardial akinesis and dyskinesis and the circumferential extent of transmural infarction.[9] Guyer et al compared the percentage of endocardium with abnormal wall motion with that of the endocardial surface overlying histochemically determined infarction; a correlation of r=0.86 was obtained.[11] While a good correlation between the proportion of dysfunctional left ventricular myocardium and the percentage infarct size was shown in these studies, it has not been possible previously to estimate the actual infarct mass in grams. The disadvantages of these conventional approaches include: (1) Only a few two-dimensional echocardiographic views were used to extrapolate for the whole left ventricle. (2) Internal anatomical landmarks were used for obtaining the short-axis images and slice distances were impossible to determine. Furthermore, the short-axis images were usually recorded from one acoustic window by tilting the

probe, therefore the acquired images were not truly parallel. (3) During the cardiac cycle, the heart rotates and moves transversely and longitudinally in the thoracic cavity, complicated by movements caused by respiration leading to errors in analysis of two-dimensional slices.

Table 2. Segmental comparison of dysfunctional and infarct myocardium.

	Anatomy	
3DE	+	-
+	23	5
-	6	78

Anatomy = segments of infarction on TTC stained specimen; 3DE = segments of dysfunction on three-dimensional echocardiography.

The advantages of volume-rendered three-dimensional echocardiography in myocardial infarction

Three-dimensional echocardiography overcomes the drawbacks of two-dimensional echocardiography in quantitation of infarct-related dysfunctional myocardium in the following aspects. Systematic step-wise data acquisition permits imaging of the whole ventricle. The interpolated three-dimensional data set can then be electronically segmented into equidistant parallel slices which enables automatic volume computation with a computer algorithm. The extrinsic movement of the heart caused by respiration can be minimized with the application of respiratory gating using thoracic impedance. Geometric assumptions employed often in two-dimensional echocardiographic methods are made unnecessary.

The volume-rendered three-dimensional echocardiographic approach we employed has particular strengths. Studies that employed two-dimensional data acquisition guided by position-locator devices did not yield dynamic three-dimensional projections and required extensive border tracing for derivation of quantitative data.[16] In an in vitro study in which pins were placed on the myocardium to simulate "infarct areas", good correspondence was shown between the three-dimensional surface area and the simulated "infarct area".[17] However, this algorithm has not been validated in vivo for quantitation of infarct-related myocardial dysfunction. Furthermore this study did not provide tissue-depiction in three-dimensional projections.

With volume-rendered three-dimensional echocardiography, gaps between two-dimensional image slices can be interpolated and pixels turned into voxels while retaining the characteristic appearance of cardiac tissue in gray scale. Dynamic three-dimensional images can be reconstructed without any tracing of the cardiac silhouettes on two-dimensional images. Manual labeling is required only for quantitative data. With the application of various shading techniques such as distance, texture and gradient of the examined object, the reconstructed three-dimensional echocardiographic images portray cardiac structures in a more realistic appearance.[18] Furthermore, volume-rendered three-dimensional echocardiography has the ability of displaying cardiac images in a dynamic mode. This allows visual appraisal of global and regional left ventricular function, detection of wall motion abnormalities and aneurysmal deformations. Another important strength of our approach is the ability to quantify the mass of the whole ventricle and that of the dysfunctional region.

An interesting observation in our three-dimensional echocardiographic study is the lack of overestimation of infarct size based on the quantification of dysfunctional mass; this is in contrast to previous two-dimensional echocardiographic observations. This is intriguing to us. While there is no clear answer to why it is so, we feel that this could be explained by the following: (1) In quantifying regional dysfunction, only discretely akinetic or dyskinetic segments were

included. Previous two-dimensional echocardiographic investigations often included hypokinetic segments in their analysis; (2) The actual mass of dysfunctional region was determined in our study while two-dimensional echocardiographic studies employed extrapolation of percent dysfunction per slice or for the whole ventricle; (3) We employed a multitude of equidistant parallel slices for determining the mass of regional dysfunction. In previous studies, only a few short or long-axis slices were analyzed and often they were not truly tomographic, parallel or equidistant since images were often derived by tilting or rotating the transducer relying on internal landmarks; (4) The infarct was transmural in all our dogs while many past studies included nontransmural infarcts as well; and (5) In determining anatomic infarct after TTC staining, we dissected the infarct regions and weighed them; in most previous studies, the infarct regions were traced, the areas measured and infarct size indirectly extrapolated. We feel that these methodological differences between our study and previous investigations could explain the lack of overestimation of infarct size by our three-dimensional echocardiographic approach.

One may consider that, for accurate three-dimensional echocardiographic quantification, data acquisition at smallest interval (such as at 1 degree) with more samples, would provide more accurate measurement than those collected with larger intervals. Our data in the last 8 dogs demonstrated that 3-degree interval for data acquisition is as good as 1 and 2 degrees for accurate measurement of dysfunctional myocardial mass, even in the setting of small infarcts. Acquisition with 5-degree intervals also yielded good correlation with anatomical measurements, especially in quantifying left ventricular mass.

Limitations of our study

There are some limitations in this study. 1) In our open-chest dog experiments, we employed an anterior epicardial window for image acquisition. How well three-dimensional echocardiographic data collection from the parasternal and apical acoustic windows provides reliable quantitative information can not be determined from this study. 2) While an excellent relationship between dysfunctional mass and infarct mass was shown in this study, the effect of reperfusion on such a relationship cannot be derived from this study. This, however, could be addressed separately using a reperfusion model. 3) In our series of dogs, all infarcts were transmural. Our observations on the estimation of infarct mass can not be directly applied to nontransmural infarcts. This important aspect requires further investigation. 4) While computation of the mass of labeled dysfunctional regions was done automatically by the image processing unit, the demarcation of regional dysfunction on paraplane two-dimensional slices was performed manually since automated edge detection software for three-dimensional data analysis was not available. Such software is being developed and could, in the future, make the analysis easier. Despite visual delineation of dysfunctional areas, the method has provided excellent estimates of dysfunctional and infarct masses. 5) This study was not designed to provide a segment-by-segment echocardiographic versus anatomic comparison. To verify that our identification of dysfunctional myocardium was correct, we performed such an analysis in a single slice in which anatomical landmarks were identified most reliably. This could have biased our segmental data to a certain degree.

Conclusion

Demonstration that three-dimensional echocardiography can yield quantitative measures of the mass of whole left ventricular myocardium, dysfunctional region

and thus infarct size has important investigative and clinical implications. This method could be used to study the effects of physiologic, pharmacologic and therapeutic interventions on infarcted myocardium in a more versatile manner than hitherto feasible. Dynamic volume-rendered three-dimensional display and accurate quantitation of global and regional left ventricular function could be of value in patients with myocardial infarction and a variety of other pathophysiologic scenarios; this requires clinical investigation.

1. Nishimura RA, Tajik AJ, Shub C, Miller FA, Ilstrup DM, Harrison CE. Role of two-dimensional echocardiography in the prediction of in-hospital complications after acute myocardial infarction. J Am Coll Cardiol 1984;4:1080-1087
2. Kan G, Visser CA, Koolen JJ, Dunning AJ. Short and long term predictive value of admission wall motion score in acute myocardial infarction: A cross-sectional echocardiographic study of 345 patients. Br Heart J 1986;56:422
3. Gallagher KP, Kumada T, Koziol JA, McKown MD, Kemper WS, Ross J, Jr. Significance of regional wall thickening abnormalities relative to transmural myocardial perfusion in anesthetized dogs. Circulation 1980; 62:1266-1274
4. Lieberman AN, Weiss JL, Jugdutt BI, Becker LC, Bulkley BH, Garrison JG, Hutchins GM, Kallman CA, Weisfeldt ML. Two-dimensional echocardiography and infarct size: relationship of regional wall motion and thickening to the extent of myocardial infarction in the dog. Circulation 1981; 63;739-746
5. Pandian NG, Koyanagi S, Skorton DJ, Collins SM, Eastham CL, Kieso RA, Marcus ML, Kerber RE. Relations between 2-dimensional echocardiographic wall thickening abnormalities, myocardial infarct size and coronary risk area in normal and hypertrophied myocardium in dogs. Am J Cardiol 1983;52:1318-1325
6. Pandian NG, Skorton DJ, Collins SM, Koyanagi S, Kieso R, Marcus ML, Kerber RE. Myocardial infarct size threshold for two-dimensional echocardiographic detection: Sensitivity of systolic wall thickening and endocardial motion abnormalities in small versus large infarcts. Am J Cardiol 1985;55:551-555
7. Otto CM, Stratton JR, Maynard C, Althouse R, Johannessen KA, Kennedy JW. Echocardiographic evaluation of segmental wall motion early and late after thrombolytic therapy in acute myocardial infarction: The western Washington tissue plasminogen activator emergency room trial. Am J Cardiol 1990;65:132-138
8. Parisi AF, Moynihan PF, Folland ED, Feldman CL. Quantitative detection of regional left ventricular contraction abnormalities by two-dimensional echocardiography. II. Accuracy in coronary artery disease. Circulation 1981;63:761-767
9. Weiss JL, Bulkley BH, Hutchins GM, Mason SJ. Two-dimensional echocardiographic recognition of myocardial injury in man: Comparison with postmortem studies. Circulation 1981; 63:401-408
10. Force T, Kemper A, Perkins L, Gilfoil M, Cohen C, Parisi AF. Overestimation of infarct size by quantitative two-dimensional echocardiography: The rule of tethering and of analytic procedures. Circulation 1986;73:1360-1368
11. Guyer DE, Foale RA, Gillam LD, Wilkins GT, Guerrero JL, Weyman AE. An echocardiographic technique for quantifying and displaying the extent of regional left ventricular dyssynergy. J Am Cardiol 1986;8:830-835
12. Pandian NG, Nanda NC, Schwartz SL, Fan P, Cao QL, Sanyal R, Hsu TL, Mumm B, Wollschlager H, Weitrayb A. Three-dimensional and four-dimensional transesophageal echocardiographic imaging of the heart and aorta in humans using a computed tomographic imaging probe. Echocardiography 1992;9:677-687
13. Delabays A, Pandian NG, Cao QL, Sugeng L, Marx G, Ludomirski A, Schwartz SL. Transthoracic real-time three-dimensional echocardiography using a fan-like scanning approach for data acquisition: methods, strength, problems, and initial clinical experience. Echocardiography 1995;12:49-59
14. Schwartz SL, Cao QL, Azevedo J, Pandian NG. Simulation of intraoperative visualization of cardiac structures and study of dynamic surgical anatomy with real-time three-dimensional echocardiography. Am J Cardiol 1994;73:501-507
15. Delabays A, Cao QL, Sugeng L, Magni G, Yao J, Vannan M, Schwartz S, Pandian N. Is there a critical amount of ischemic myocardium required to produce a detectable wall motion abnormality? A quantitative 3-dimensional echocardiographic contrast study. (abstract) Circulation 1995;92:I-261
16. Jiang L, Siu SC, Handschumacher MD, Guererro JL, Vazquez de Prada JA, King ME, Picard MH, Weyman AE, Levine RA. Three-dimensional echocardiography: in vivo validation for right

ventricular volume and function. Circulation 1994;89:2342-2350

17. King DL, Gopal AS, King DL Jr, Shao MYC. Three-dimensional echocardiography: In vitro validation for quantitative measurement of total and "infarct" surface area. J Am Soc Echocardiogr 1993;6:69-76

18. Cao QL, Pandian NG, Azevedo J, Schwartz SL, Vogel M, Fulton D, Marx G. Enhanced comprehension of dynamic cardiovascular anatomy by three-dimensional echocardiography with the use of mixed shading techniques. Echocardiography 1994;11:627-633

CHAPTER 5

THREE-DIMENSIONAL ECHOCARDIOGRAPHIC ASSESSMENT OF THE EXTENSION OF DYSFUNCTIONAL MASS IN PATIENTS WITH CORONARY HEART DISEASE

Stefano de Castro, MD; Jiefen Yao, MD; Giuseppina Magni, MD; Luca Cacciotti, MD; Paolo Trambaiolo, MD; Marcello de Sanctis, MD; Francesco Fedele, MD

Am J Cardiol. **1998;81(12A):103G-106G**

Three-Dimensional Echocardiographic Assessment of the Extension of Dysfunctional Mass in Patients with Coronary Heart Disease

Stefano de Castro, MD; Jiefen Yao, MD; Giuseppina Magni, MD; Luca Cacciotti, MD; Paolo Trambaiolo, MD; Marcello de Sanctis, MD; Francesco Fedele, MD

Two-dimensional (2D) echocardiographic estimation of infarcted mass is limited by having only a few selected nonparallel views for data analysis. Volume-rendered three-dimensional (3D) echocardiography may be able to overcome the above limitations, because it uses multiple, parallel 2D images to derive quantitative data. Previous experimental studies demonstrated that 3D echocardiography is an accurate and reproducible method to assess dysfunctional mass. To estimate the accuracy of 3D echocardiography in humans, we evaluated 10 patients who had a single myocardial infarction. All patients underwent 2D and 3D echocardiography using the transesophageal approach, and contrast (gadolinium) magnetic resonance imaging (MRI), considered a reference standard for infarcted tissue detection. The mean extent of dysfunctional mass by MRI was 28±13 g and by 3D echocardiography was 30±12 g; the mean difference was1.9±2.3 g (p = not significant). Linear regression between the 2 measurements was y = 0.97x – 1.12, r = 0.98. Dysfunctional mass derive from 3D echocardiography reflects the real site and extension of damaged myocardium.

Echocardiography has evolved over the last 3 decades from single beam imaging to sophisticated two-dimensional (2D) and Doppler techniques, which allow the study of cardiac structure, function and hemodynamics in detail. However, an inherent limitation of conventional echocardiography is that it uses only 2 dimensions in depicting complex three-dimensional (3D) structures, such as the heart and great vessels. This may imply an incomplete appreciation of the spatial relationship between cardiac structures and geometric assumptions may be needed to extrapolate quantitative data, particularly when the shape of the cardiac chambers are deformed.

The extent of myocardial damage during acute myocardial infraction is the most important determinant of prognosis.[1,2] The 2D echocardiographic estimation of infarcted mass is limited by the use of a few selected nonparallel views extrapolated from the whole left ventricle. Dynamic volume-rendered 3D echocardiography has become a practical reality, able to overcome the above mentioned limitations, since it utilizes multiple, parallel 2D images to produce quantitative data.[3,4] Previous studies demonstrated that 3D echocardiography is an accurate and reproducible method to assess left ventricular mass and dysfunctional mass in experimentally created infarcted ventricles.[5-7] In this study, we report the preliminary results of a comparative analysis between 3D echocardiography and magnetic resonance imaging (MRI) in the assessment of regional dysfunctional mass in patients with ischemic heart disease.

Methods

The study group consisted of 10 selected patients (all men; mean age 56±7 years) who had a previous and single episode of myocardial infarction. All patients were asymptomatic, without complex cardiac arrhythmias. After a diagnostic examination and MRI with a gadolinium contrast agent for infarcted tissue detection. MRI and 3D echocardiographic studies were performed within 1 week. Informed consent was obtained from each patient.

Instrumentation and 3D echocardiographic data acquisition: A 64 element phased-array echocardiographic system

(Sonos 2500; Hewlett-Packard, Andover, MA, USA), with integrated software able to rotate the ultrasound beam in a predetermined manner, was used. The multiplane transesophageal probe was introduced into the esophagus with the patient in the left decubitus position after local anesthetic spray (lidocaine 2%) to the hypopharynx, and general sedation (intravenous diazepam 2.5 – 10 mg). The probe was positioned at the mid-esophageal window for image acquisition and was kept stationary during the study. The transducer was rotated every 3° in a 0 -180° arc, with the reference position corresponding to the 4-chamber view. Electrocardiographic and respiratory gating, automatically provided by the integrated software, were used for spatial and temporal registration of acquired images. A total of 60 sequential cross-sections during a complete cardiac cycle were acquired and transferred onto a laser disk for subsequent postprocessing and data analysis. For measurement of the total left ventricular mass and for calculation of dysfunctional mass, multiple short-axis cross-sectional views were electronically segmented into 12 – 15 equidistant slices (5 mm in slice distance) form the apex to the mitral annular level (Figure 1). For determining left ventricular mass, the myocardium of left ventricle on each transverse slice was contoured and labeled. By integrating the slice thickness with the slice area, the volume of each slice and the total volume of all myocardial slices were computed in an automated manner by a new quantification algorithm. Myocardial mass volume multiplied by assumed specific gravity (1.05 g/ml) provided myocardial mass (weight in grams). For measurement of dysfunctional myocardial mass, the following steps were performed: each short-axis 2D slice extracted from the 3D data set was viewed in a dynamic fashion In these images, regional wall motion abnormalities were clearly evident. The segments that exhibited discrete hypokinesis, akinesis, or dyskinesis were demarcated. These segments were contoured and labeled. The volume of the dysfunctional myocardial segments (the labeled regions) was provided automatically by the computer as mentioned above. Using the specific gravity of the myocardium, the mass of the dysfunctional myocardium was generated. From theses data, the percentage of the total left ventricular myocardium involved in regional myocardial dysfunction was calculated as well (Figure 2).

Figure 1. Three-dimensional reconstruction of the left ventricle in a 5-chamber projection in a patient with akinesis of the interventricular septum. The endocardium at the level of the lateral wall and apex is well delineated.

Instrumentation and MRI acquisition: Images were obtained from a commercially available 1-Telsa superconducting magnet (magnetom Impact; Simens, Erlangen, Germany) with body-array coil. Then, 10 – 20 minutes after intravenous injection of paramagnetic contrast agent (Gd-DTPA Magnevist; Schering: 0.2 mg/kg), a double oblique orientation fast GRE (FLASH) single-slice-multiphase technique (TR 5 msec, TE 2.2 msec, flip angel 25°, 128 x, FOV 350 mm, 10-mm slice thickness) was em-

ployed, encompassing the entire left ventricle along its long axis with repeated breath-hold acquisitions (18 sec) of 5 electrocardiographically gated short-axis images for each slice level without interslice gap.

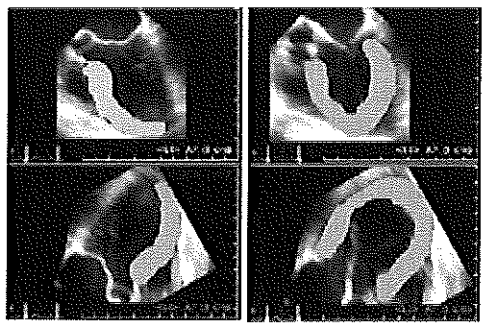

Figure 2. Quantitation of total left ventricular mass and regional dysfunctinal mass by 3Dechocardiography. Delineation and computation of regional dysfunctional mass (left) and total left ventricular mass (right) by 3D echocardiography. In this example, the total extent of interventricular septum was akinetic.

Visual assessment of infarct location was based on the (10 presence of areas with significantly increased signal intensity (intensity ratio > 1.4),[8,9] and (2) evidence of wall motion abnormalities on the cineloop view of single-phase, multi-slice, short-axis images. In the presence of apical left ventricle involvement, additional multi-phase long-axis acquisitions were employed to obtain a better definition of apical left ventricle dysfunction. All sets of images were then subjected to quantitative functional analysis by means of a dedicated software package for short-axis MRI (ARGUS; Simens, Erlangen, Germany). After manual boundary delineation on end-diastolic and end-systolic short axis magnified images of each level, leaving out the papillary muscles, a center of mass (epicardial centroid floating) was determined by the image processing software, and the left ventricular myocardium was divided clockwise into 12 equally spaced segments by radii generated from the center of the mass, with computerized assessment of segmental end-diastolic wall thickness and absolute systolic wall thickening. To assess interobserver variability with respect to manual boundary tracing, MRI images were independently evaluated by 2 experienced observers without knowledge of previous echocardiographic results; measurements were repeated by 1 observer, 1 month after the first evaluation to assess intraobserver variability.

The results of quantitative functional analysis were transferred to the baseline images, summing at each slice level the segmental areas (cm^2) with significant dysfunction (absolute systolic wall thickening <2),[10] then multiplying the obtained value by slice thickness (1 cm) and standard myocardial density (1.05 g/cm^3), thus obtaining the dysfunctional left ventricular mass (grams).

Statistical analysis: 3D measurements were compared with MRI data using simple linear regression analysis and Student's paired *t* test. Difference between 3D echocardiographic and MRI measurements was evaluated with Bland-Altman analysis.[11] Inter- and intra-observer variability was calculated as the difference between 2 observations divided by the mean values.

Results

Good quality 3D reconstructions were obtained in all patients. The extent of dysfunctional mass by MRI was 10-54g (mean 28 ± 13 g), and by 3D echocardiography was 11 –60 g (mean 30 ± 12 g); the mean difference was 1.9 ± 2.3 g (p = not significant). Linear regression analysis between the 2 measurements was $y = 0.97x - 1.12$; ($r = 0.98$; $p<0.0001$). Mean left ventricular mass by MRI was 147 ± 17 g (range 122-

170 g), and by 3D echocardiography, 149 ± 17 g (range 127-175 g); the mean difference between the 2 techniques was 2.2 ± 1.1 g (p = not significant). Linear regression analysis was y = 0.81x + 25.3 (r = 0.80, p<0.001). The mean percent dysfunctional mass by MRI was 19 ± 10% and by 3D echocardiography was 20 ± 9% (p = not significant). Interobserver variability for dysfunctional mass by 3D echocardiography was 5 ± 2%.

Discussion

According to our preliminary results, we can affirm that 3D echocardiography is a feasible and a reproducible method for quantitation of dysfunctional mass in patients with ischemic heart disease. In fact, we found an excellent correlation between the extent of dysfunctional mass obtained by 3D echocardiography and MRI without significant under- or overestimation. In addition, a good correlation was found between the percentage of left ventricular dysfunctional myocardium calculated by MRI and by 3D echocardiography.

Conventional 2D echocardiography is an established method for noninvasive evaluation of regional myocardial dyssynergy. Clinical and experimental studies have demonstrated a clear relation between the site and extent of echocardiographically defined regional dysfunction and the pathologic evidence of infarction.[12,13] Unfortunately, quantitative analysis of regional dysfunction is affected by translation and rotation of the heart, respiratory movements and a relatively poor precordial resolution of he left ventricle. Using various echocardiographic techniques,[14,15] semiquantitative analysis is usually extrapolated from a few nonequidistant or nonparallel 2D images (3 short-axis and 1 or 2 apical views) using internal anatomic landmarks as a reference position.

Previous experimental animal studies demonstrated that 3D echocardiography is able to overcome the above limitations, since the extent of dysfunctional mass is calculated from multiple parallel views precisely realigned according to a predefined respiratory and electrocardiographic gating.[5,7] Our results also confirm that 3D echocardiography is an accurate technique for the definition and quantitation of dysfunctional myocardial regions in a clinical setting.

Table 1. Assessment of dysfunctional versus total ventricular mass.

Patient No.	MRI DM, g	3DE DM, g	MRI LVM, g	3DE LVM, g	DM 3DE, %	DM MRI, %
1	12	15	160	145	10	8
2	41	40	170	165	24	25
3	15	18	150	155	12	10
4	28	31	155	175	18	16
5	22	25	155	147	17	15
6	10	11	130	127	9	8
7	37	40	139	137	29	27
8	43	40	122	129	31	33
9	54	60	164	170	35	32
10	21	22	123	140	16	15
Mean	28	30	147	149	20	19
SD	13	12	16	17	9	10

3DE DM = extent of dysfunctional mass by 3D echocardiography; 3DE LVM = left ventricular mass by 3D echocardiography; MRI DM = extent of dysfunctional mass by MRI; MRI LVM = left ventricular mass by MRI; %DM = percentage of dysfunctional mass determined by the ration between dysfunctional mass and left ventricular mass.

Limitations

We acknowledge that our results are preliminary and therefore the real feasibility of 3D echocardiography in the clinical scenario needs to be established. Moreover, the assessment of dysfunctional mass was based on visual assessment using both MI and 3D echocardiography techniques. The 3D examination were obtained through a transesophageal approach and therefore is a semi-invasive technique, which cannot be, at the moment, widely applied to all patients with ischemic heart disease.

Conclusion

Our results demonstrated that 3D echocardiography is able to clearly display and quantify wall motion abnormalities in patients with previous myocardial infarction. The percentage of dysfunctional myocardium can also be assessed, giving important physiologic and clinical information for the treatment of patients with ischemic heart disease.

1. Multicenter Postinfarction Reasearch Group. Risk stratification and survival aftre mmyocardial infarction. *N Engl J Med* 1983;309:331-338.
2. Sanz G, Castaner A, Betriu , Magrina J, Roig E, Coll S, Pare JC, Navarrolopez F. Determinants of prognosis in survivors of acute myocardial infarction. *N Engl J Med* 1982;306:1065-1070.
3. Dekker DL, Piziali RL, Dong E Jr. A system for ultrasounically imaging the human heart in three dimensions. *Comput Biomed Res* 1974;7:544-553.
4. Matsumoto M, Matsuo H, kitabatake A, Inoue M, Hamanaka Y, Tamura S, Tanaka K, Abe H. three-dimensional echocardiograms and two-dimensional echocardiographic images at desired planes by a omputerized system. *Ultrasound Med biol* 1977;3:163-178.
5. Delabays A, Sugeng L, Cao QL, Magni G, Schwartz S, Pandian N: Quantitative three-dimensional echocardiographic estimation of ischemic and nonischemic myocardial mass and its relation to the mass of dysfunctional LV myocardium during coronary occlusion. (abstract) *J Am Coll Cardiol* 1995;25(suppl)163A.
6. Laskari C, Delabays A, Yao J, Cao QL, Magni G, De Castro S, Acar P, Vannan M, Schwartz SL, Pandian NG. Accurate estimation of left Ventricular mass in vivo by voxel-based three-dimensional echocardiography (abstract) *J Am Coll Cardiol* 1996;27(suppl):239A.
7. Yao J, Cao QL, Masani N, Delabays A, Magni G, Acar P, Laskari C, Pandian NG. Three-dimensional echocardiographic estimation of infarct mass based on quantification of dysfunctional left ventricular mass. *Circulation* 1997;96(5):1660-1666.
8. Rehr RB, Peshock RM, Malloy CR, Keller AM, Parkey RW, Buja LM, Nunnanlly RL, Willerson JT. Improved in vivo magnetic resonance imaging of acute myocardial infarction after intravenous paramagnetic contrast agent administration. *Am J Cardiol* 1986;57:864-868.
9. Nishimura T, Kobajaski H, Ohara Y, Yamada N., Haze K, Takamiya M, Hiramori K. Serial assessment of myocardial infarction by using gated MR imaging and Gd-DTPA. *Am J Radiol* 1989;153:715-720.
10. Pflugfelder PW, Sechtem U, White RD, Higging CB. Quantitation of regional myocardial function by rapid cine MR imaging. *Am J Radiol* 1988;150:523-520.
11. Bland JM, Altman DG. Statistical method for assessing agreement between two methods of clinical measurements. *Lancet* 1086;i:307-310.
12. Hegger JJ, weyman AE, Wann LS, Dillon JC, Feigenbaum H. Cross-sectional echocardiography in acute myocardial infarction: detection and localization of regional left ventricular dyssynergy. *Circulation* 1979;60:531-535.
13. Hegger JJ, weyman AE, Wann LS, Rogers EW, Dillon JC, Feigenbaum H. Cross-sectional echocardiographic analysis of the extent of left ventricular asynergy in acute myocardial infarction. *Circulation* 1980;61:1113-1118.
14. Fujii J, Sawada H, Aizawa T, Kato K, Onoe M, Kuno Y. Computer analysis of Cross-sectional echocardiogram for quantitative evaluation of left ventricular asynergy in myocardial infarction. *Br Heart J* 1984;51:139-148.
15. Pandian NG, Skorton DJ, Collins SM, Koyanagi S, Kieso R, Marcus ML, Kerber RE. Myocardial infarct size threshold for two-dimensional echocardiographic detection: Sensitivity of systolic wall thickening and endocardial motion abnormalities in small versus large infarcts. Am J Cardiol 1985;55:551-555.

CHAPTER 6
QUANTITATIVE THREE-DIMENSIONAL CONTRAST ECHOCARDIOGRAPHIC DETERMINATION OF MYOCARDIAL MASS AT RISK AND RESIDUAL INFARCT MASS AFTER REPERFUSION: EXPERIMENTAL CANINE STUDIES WITH AN INTRAVENOUS CONTRAST AGENT - NC100100

Jiefen Yao, MD; Claudius Teupe, MD; Masaaki Takeuchi, MD; Erick Avelar, MD; Malachi Sheahan, MD, Raymond Connolly, PhD, Jonny Ostensen, PhD and Natesa G. Pandian, MD

Submitted

Quantitative Three-Dimensional Contrast Echocardiographic Determination of Myocardial Mass at Risk and Residual Infarct Mass After Reperfusion: Experimental Canine Studies With An Intravenous Contrast Agent - NC100100

Jiefen Yao, MD; Claudius Teupe, MD; Masaaki Takeuchi, MD; Erick Avelar, MD; Malachi Sheahan, MD, Raymond Connolly, PhD, Jonny Ostensen, PhD and Natesa G. Pandian, MD

Background. Accurate assessment of the efficacy of reperfusion therapy aids in the management of patients with acute myocardial ischemia. The aim of this study was to examine the quantitative value of contrast three-dimensional echocardiography (3DE) in estimating myocardial mass at risk (RM), salvaged mass (SM) and residual infarct mass (IM). **Methods and Results.** We created 2-3 hour coronary occlusion followed by 2-4 hour reperfusion in 10 dogs. 3DE data with and without contrast were acquired at the end of each stage. The RM was determined using Evans Blue dye method and IM by 2,3,5 triphenyltetrazolium chloride (TTC) staining. From the 3DE data set, the perfusion defect mass (PDM) and dysfunctional mass (DFM) were measured. The RM during coronary occlusion (x) (27.1±14.6g or 23.8±9.7% of LV) correlated well with PDM (y) both in weight (y= 0.5x+8.9, r= 0.90, p<0.001, mean difference= -4.8±8.1g, p= NS) and in % of LV (y= 0.7x+6.5, r= 0.83, p< 0.01, mean difference= -0.1±5.4%, p= NS); and with DFM (y) in weight (y= 0.6x+7.6, r= 0.89, p< 0.005, mean difference= -3.7±7.5g, p= NS) and in % of LV (y= 0.9x+2.3, r= 0.95, p< 0.0001, mean difference= 1.3±3.0%, p= NS). After reperfusion, the IM (x) (9.3±8.1g or 9.1±8.8 % of LV) correlated well with PDM (y) in weight (y= 1.2x+1.2, r= 0.93, p< 0.001, mean difference= 2.3±4.0g, p= NS) and in % of LV (y= 1.3x, r= 0.98, p< 0.0001, mean difference= 2.7±3.7%, p= NS); and moderately well with DFM in weight (y) (y= 0.7x+7.9, r= 0.79, p<0.05, mean difference= 5.6±5.0g, p= NS) and in % of LV (y= 0.8x+6.5, r= 0.83, p< 0.05 mean difference= 5.9±5.7%, p=NS). The SM was 13.6±11.0% of LV from anatomic methods and 14.2±13.0% by contrast 3DE. **Conclusion:** Myocardial contrast 3DE using intravenous contrast injection could quantify the actual RM during acute ischemia and the residual IM in the setting of reperfusion. Thus, the SM and the efficacy of reperfusion can be evaluated as well.

Key words: Contrast echocardiography, coronary disease, myocardial infarction, three-dimensional echocardiography, reperfusion

In the management of patients with acute myocardial ischemia/infarction, accurate estimation of the myocardial mass at risk (RM) and the residual infarct mass (IM) following revascularization procedures is essential for assessing the efficacy of reperfusion and assisting in clinical decision making.[1-3] Though conventional two-dimensional echocardiography (2DE) is able to display regional wall motion abnormalities, differentiation between ischemic, stunned or infarcted myocardium has been difficult.[4-6] Pharmacologic stress echocardiography, nuclear imaging techniques and contrast enhanced magnetic resonance imaging and computed tomography have shown to be helpful in differentiating viable versus non-viable regions. Their availability and potential for repetitive studies could be limited in acute clinical settings.[7-12]

Microbubbles have been used in myocardial contrast echocardiography based on the phenomenon that they exhibit backscatter and resonance. Early ultrasound contrast agents could not pass through the pulmonary circulation and had to be injected directly into the coronary artery, aortic root or left atrium, requiring catheterization procedures.[13-16] Recently, a new generation of contrast agents have been developed that can trespass the pulmonary circulation to reach the left heart after peripheral venous administration. Such agents provide us with a new means to study the myocardial perfusion using a non-invasive technique.[17,18] Two-dimensional myocardial contrast echocardiography has been shown capable of defining perfusion abnormalities. It is diffi-

cult, however, to quantify the actual myocardial mass affected by hypoperfusion by using one or only a few selected views of the left ventricle (LV). As demonstrated in studies of regional wall motion analysis, three-dimensional echocardiography (3DE) can be used in quantifying regional dysfunctional myocardial mass (DFM), without the need of geometric assumptions.[19,20] Two recent studies proved the feasibility and accuracy of myocardial contrast 3DE in estimating myocardial perfusion defect mass (PDM) using contrast injection directly in the left atrium. These approaches are invasive, requiring left heart catheterization.[21,22] Our earlier studies using contrast infusion directly into the aortic root and recently, using intravenous contrast injection during 3DE data acquisition indicated that IM can be accurately estimated following coronary occlusion.[23,24] In the present study, we sought to validate the accuracy of 3DE in quantifying RM during acute ischemia and residual IM following reperfusion therapy using intravenous contrast injection.

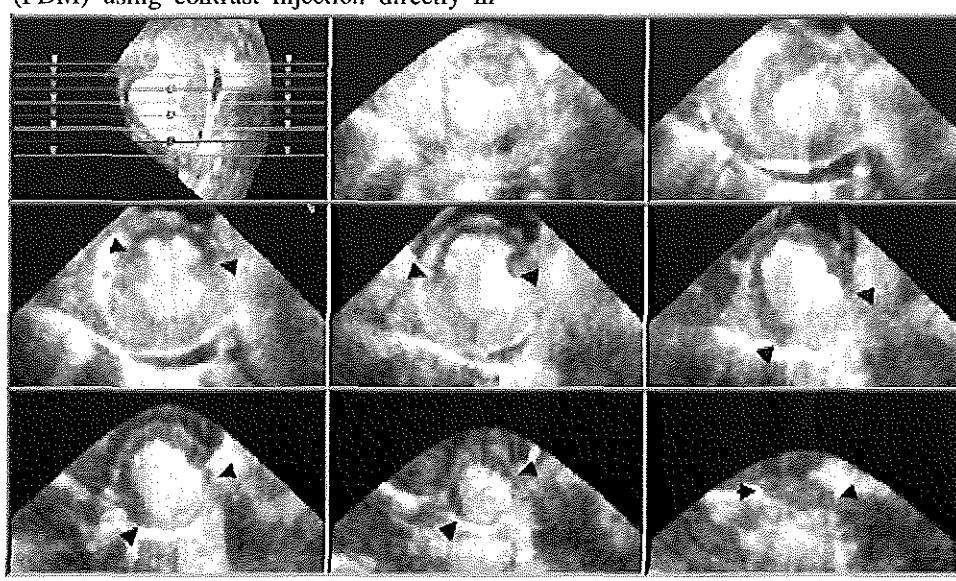

Figure 1. Myocardial perfusion demonstrated in multiple parallel equidistant short-axis views of LV reconstructed from a 3DE data set. The LV long-axis view in the upper left corner was used as a reference image to produce true short-axis views of LV. The transverse lines across the reference image represent the levels of the cutting planes. The regions of perfusion defects are demarcated by black arrows.

Methods

Myocardial contrast 3DE was performed in an open-chest canine model of acute ischemia followed by reperfusion. A contrast agent, NC100100, was administered intravenously as a bolus and 3DE data were acquired in a rotational scanning format. The RM during acute ischemia and residual IM following reperfusion were estimated from the PDM by 3DE and were compared with that measured anatomically by Evens blue dye and 2,3,5 triphenyltetrazolium chloride (TTC) staining methods. This study was carried out in conformity

with the American

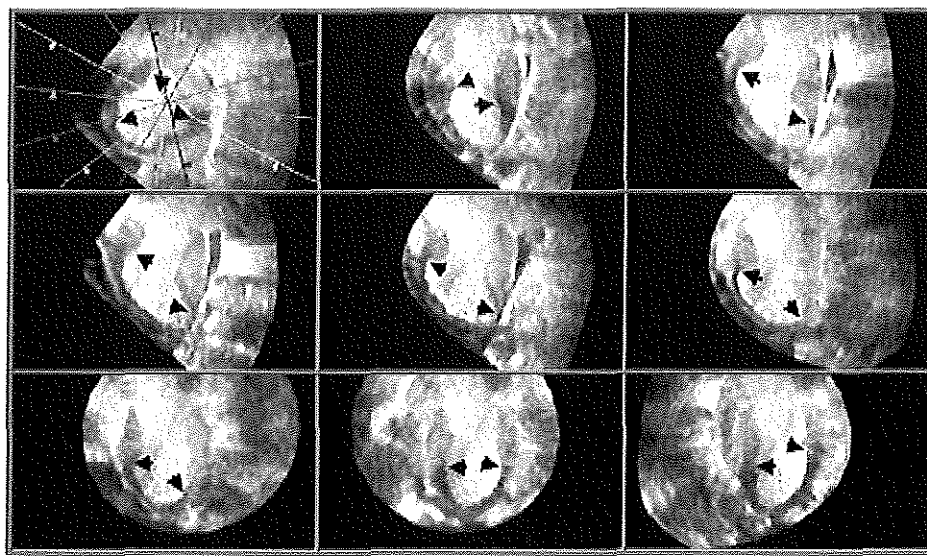

Figure 2. Myocardial perfusion demonstrated in multiple long-axis views of LV. As shown in the upper left reference image, the long-axis views were derived from equally spaced cutting intervals (angles) of LV, represented by the radiating lines. The regions of perfusion defects are demarcated by black arrows.

Association for Accreditation of Laboratory Animal Care guidelines for the use of animals in research and followed the regulations of and was approved by the Institutional Animal Research Committee at New England Medical Center, Tufts University.

Animal Preparation and imaging protocol

Ten mongrel dogs (weighed 21-34 kg, mean 27±5 kg) were used in this study. The dog was sedated with intramuscular acepromazine (20-30 mg) and was anesthetized with intravenous sodium pentobarbital (20-25 mg/kg). Additional doses were given when necessary during the experiment. It was then intubated and ventilated mechanically with room air using a volume cycle respirator. An intravenous line was open for fluid and medicine administration. A fluid-filled catheter was introduced into a femoral artery for continuous blood pressure monitoring and another into a femoral vein for contrast agent administration. Lead II electrocardiogram and $\%O_2$ saturation was monitored throughout the experiment. The chest was opened by mid-line sternotomy. The pericardium was cut and suspended to form a cradle. Either the left anterior descending coronary artery (in 6 dogs) or the circumflex coronary artery (in 4 dogs) was isolated and occluded with a silk snare. Lidocaine was given intravenously to prevent ventricular fibrillation (1 mg/kg bolus injection before coronary occlusion followed by 0.5 mg/min continuous infusion till the end of study). After 2 to 3 hours of coronary occlusion, a water-bath was arranged above the pericardial cradle for ultrasound transmission. 3DE data were acquired twice, once in a continuous mode without contrast and once in triggered mode after intrave-

nous contrast administration. Then the silk snare that occluded the coronary artery was released but not removed to allow complete opening of the artery and to assure later reocclusion at the same site. 2 to 4 hours was allowed for reperfusion before 3DE data acquisition was repeated in continuous mode and in triggered mode with contrast following intravenous dipyridamole (0.84 mg/kg infused in a period of 6 minutes). The time allowed for occlusion and reperfusion and the level of coronary occlusion varied among the dogs to produce various sizes of risk and infarct regions. At the end of each experiment, the coronary artery was reoccluded at the same site followed by injection of 50 ml of Evans Blue dye into the left atrium. Normal circulation was allowed for 10 minutes before the dog was euthanized with an overdose of potassium chloride. The heart was then removed for measurements of the RM from Evans Blue Dye staining and IM from TTC staining.

Intravenous contrast agent, NC100100

NC100100 (Nycomed, Oslo, Norway) is an investigational ultrasound contrast agent. It contains microbubbles filled with a perflourocarbon gas, stored under room temperature as a dry powder. It is reconstituted using sterile water to form a suspension of 10 µl/ml microbubbles with a median diameter of 3 µm. For 3DE data acquisition, a bolus of 0.2 ml NC100100 was administered intravenously, followed by 3ml saline.

Three-dimensional echocardiography

Data acquisition. A commercially available ultrasound unit (HP Sonos 5500, Hewlett-Packard, Andover, Massachusetts), with the ability of harmonic triggered imaging, was interfaced with a commercially available 3DE image processing system (EchoScan, version 3.1, TomTec Imaging Systems, GmbH, Munich, Germany) for 3DE data acquisition. A rotational motor device was mounted onto the ultrasound imaging transducer (transmitting frequency at 1.8 or 2.1 MHz and receiving frequency at 3.6 or 4.2 MHz). The images were acquired from an anterior epicardial orientation. Rotation of the transducer was controlled by the 3DE system at 3° intervals through 180° with electrocardiographic and respiratory gating. Continuous imaging without contrast agent was used for regional wall motion analysis and triggered imaging (one in every cardiac cycle) following intravenous contrast agent was used for analysis of myocardial perfusion abnormalities. A low ultrasound output power with a mechanical index of 0.3 was used to minimize microbubble destruction and to prolong the persistence of the agent in the circulation. Collection of images was started when the LV cavity was filled with microbubbles and the myocardium was brightened, with no significant attenuation in the far field. The acquired data were calibrated, processed and stored onto optical magnetic disks.

Data analysis. The 3DE data were reviewed off-line by blinded observers. From the static contrast 3DE data, the LV was reconstructed in multiple two-dimensional short-axis and long-axis views for delineation of the extent of perfusion abnormalities (figures 1 and 2). From dynamic 3DE data, the LV was reconstructed and viewed in multiple parallel short-axis images and the site and extent of regional dysfunction were appraised. From 8 parallel, equi-distant short-axis slices of the LV, the volume of a given myocardial region (e.g. dysfunctional or hypoperfused zone) was measured on each slice by manually tracing and applying a volumetric label to that region (volume = area x slice thickness). Using "summation

of discs" method, the total volume of that region on all slices was derived. The myocardial mass was calculated from its volume and the specific gravity of the myocardium (1.04g/ml).

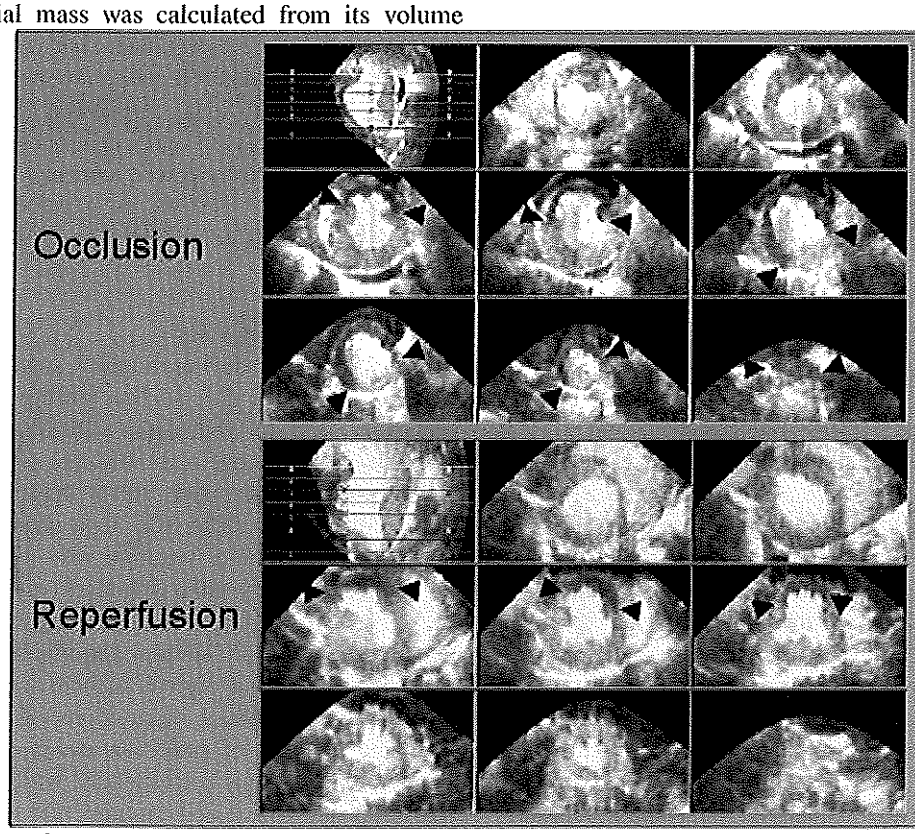

Figure 3. An example of myocardial perfusion abnormalities (arrows) in a dog during occlusion of the left anterior descending coronary artery (top) and following reperfusion (bottom). Note the decrease in the extent of the perfusion defects on multiple short-axis views of LV.

The PDM was measured from the 3DE data obtained during coronary occlusion and after reperfusion, respectively. Each short-axis slice of the LV reconstructed from the contrast data was examined. Dark areas of the LV myocardium were considered regions of perfusion defect in comparison to normally perfused myocardium, which appeared bright due to contrast enhancement (figures 3 and 4). These regions were traced and labeled on all slices to derive the PDM. The total LV mass was obtained by contouring the whole myocardial area on all LV slices. The percent of LV involved in perfusion defect was calculated as well. The salvaged myocardial mass (SM) by reperfusion was estimated from contrast 3DE by subtracting the PDM following reperfusion from the PDM during coronary occlusion. The DFM was also measured from the dynamic 3DE data acquired at each stage. By examining all the slices, the akinetic or dyskinetic region of the myocardium on each slice was defined and labeled to derive the

total DFM and the percent of LV involved in dysfunction.[19]

Each labeled region of the LV was extracted and reconstructed. For example, the normally perfused myocardium could be displayed as if the perfusion defect region had been removed. Side-by-side display of the perfused and non-perfused regions facilitated the visual appreciation of the extent of perfusion abnormalities (figure 5).

Anatomical determination of myocardial mass at risk and infarct mass

After the heart was removed, the atrial tissue was excised and the ventricles were sectioned parallel to the mitral annulus into 1cm thick slices. The myocardial territory of the occluded coronary artery was void of Evans Blue dye, representing the RM. The normally perfused myocardium was stained blue. The risk area and the total LV myocardial region on both sides of the slice were plotted onto transparencies. The percent of LV at risk of infarction was calculated from the unstained area and the total LV myocardial area, which was used later to calculate the weight of the RM from the total LV mass.

After finishing the above measurements, the ventricular slices were bathed in 1.2% TTC solution at 37°C for 20 minutes. All the slices were inspected on both sides. The infarct region was defined visually based on its pale appearance in contrast to the non-infarct area stained red by TTC. Both the infarct region and the total myocardial region were plotted onto transparencies. Then the right ventricular tissue was removed and the total LV mass was weighed in grams. The infarct zones on all slices were then dissected after carefully examining both sides and weighed to derive IM. The percentage of LV involved in infarction was calculated from the total LV mass and the IM.

Statistics

All data were expressed as mean ± standard deviation. Results from 3DE measurements were compared with anatomical data using simple linear regression. The differences and limits of agreement between them were analyzed by paired student *t* test and Bland-Altman analysis. A p value of <0.05 was considered statistically significant.

Results

One dog died during the early stage of coronary occlusion and another during reperfusion, due to ventricular fibrillation. Therefore, only 9 dogs had 3DE data at the end of coronary occlusion and 8 dogs following reperfusion. The 3DE data acquisition time was around 1 minute (45 to 75 seconds). Two-dimensional images of the LV reconstructed from 3DE data sets delineated regional wall motion abnormalities and perfusion defect regions in both transverse and longitudinal orientations of the LV. The location of perfusion defect and dysfunctional regions corresponded with the territories of the occluded coronary arteries.

Myocardial mass at risk of infarction

The RM during coronary occlusion determined by Evans Blue dye staining (x) was 27.1±14.6g or 23.8±9.7% of LV. The PDM from 3DE data (y) was 22.3±7.9g ($y=0.5x+8.9$, $r=0.90$, $p<0.001$, mean difference=-4.8±8.1g, p=NS) or 23.6±8.4% of LV ($y=0.7x+6.5$, $r=0.83$, $p<0.01$, mean difference=-0.1±5.4%, p=NS) (figure 6). The DFM during coronary occlusion by 3DE (y) was 23±10g ($y=0.6x+7.6$, $r=0.89$, $p<0.005$, mean difference=-3.7±7.5g, p=NS) or 25.1±9.8% of LV ($y=0.9x+2.3$, $r=0.95$, $p<0.0001$, mean difference=1.3±3.0%, p=NS) (figure 7). Good correlation was also

obtained between DFM (y) and PDM (x) from 3DE, either in weight (y=1.1x-1.4, r=0.92, p<0.001, mean diffenrence = 1.1± 3.8g, p=NS) or in % of LV (y=1.1x+0.2, r=0.91, p<0.001, mean differrence= 1.5± 4.1%, p=NS).

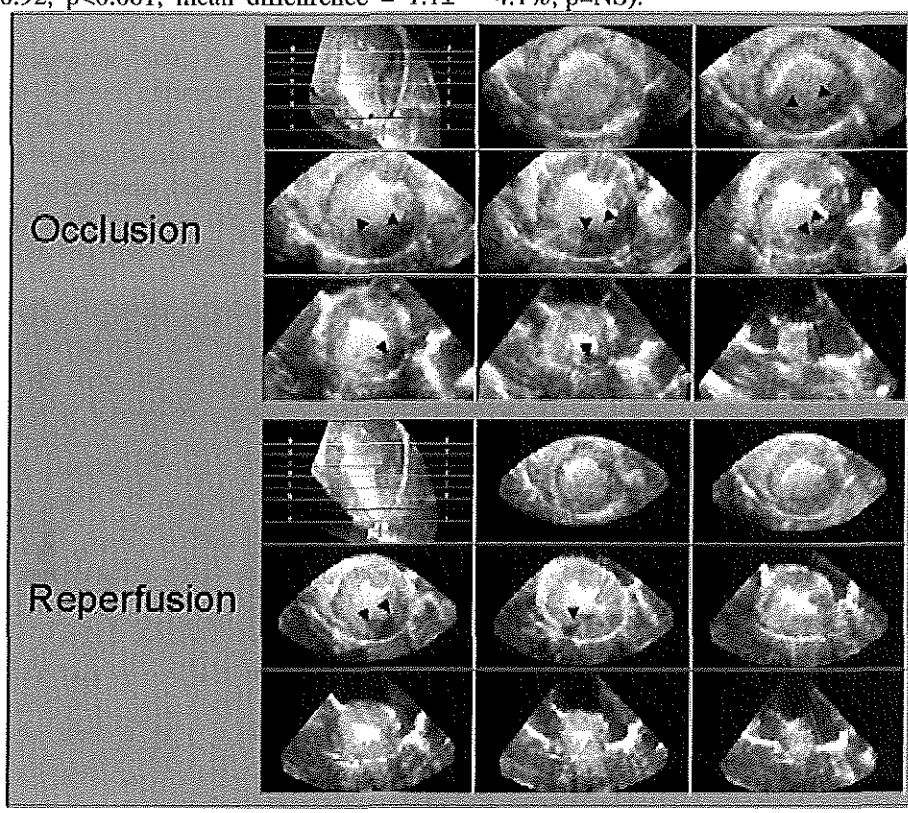

Figure 4. An example of myocardial perfusion abnormalities (arrows) in a dog during occlusion of the circumflex coronary artery (top) and following reperfusion (bottom). During coronary artery occlusion phase, the second slice of the LV from the base (upper right image) showed subendocardial perfusion defect, which also indicates that the defect was not caused by ultrasound attenuation. After reperfusion, both the longitudinal and circumferential extent of the perfusion defect decreased.

Residual infarct mass following reperfusion

The residual IM determined by TTC staining (x) was 9.3±8.1g or 9.1±8.8% of the total LV mass. The PDM from 3DE (y) was 12.2±10.3g (y=1.2x+1.2, r=0.93, p<0.001, mean difference=2.3±4.0g, p=NS) or 11.7±11.6% of LV mass (y=1.3x, r=0.98, p<0.0001, mean difference=2.7±3.7%, p=NS) (figure 8). The DFM from 3DE following reperfusion (y) was 14.8±7.5g (y= 0.7x+7.9, r=0.79, p<0.05, mean difference=5.6±5.0g, p=NS) or 14.1±8.9% of LV (y=0.8x+6.5, r=0.83, p<0.05 mean difference=5.9±5.7%, p=NS) (figure 9). Only moderate correlation was obtained between DFM (y) and PDM (x), either in weight (y=0.5x-8.3, r=0.74, p<0.05, mean diffenrence=2.6±6.9g, p=NS) or in % of LV (y=0.6x+6.9, r=0.81, p<0.05, mean diffen-

rence=2.4±6.9%, p=NS).

Salvaged myocardial mass

From the above measurements, the SM could be arrived at in each study, calculated from the RM or PDM during coronary occlusion subtracted by the residual IM or PDM following reperfusion. According to the anatomic measurements, 13.6±11.0% of LV was salvaged by reperfusion. From 3DE measurements of the PDM, 14.2±13.0% of LV was salvaged, close to anatomical measurements. 3DE measured dysfunctional mass also decreased in 10.2±7.0% of LV (figure 10).

Validation of left ventricular mass measurement

The accuracy of 3DE measurement was validated by comparing the LV mass following reperfusion by 3DE (113.4±26.7g) (y) with LV mass by anatomic measurement (109.8±29.1g) (x). Good correlation was obtained between the two (y=0.8x+26.6, r=0.86, p<0.005, mean difference=3.5± 14.9g, p=NS).

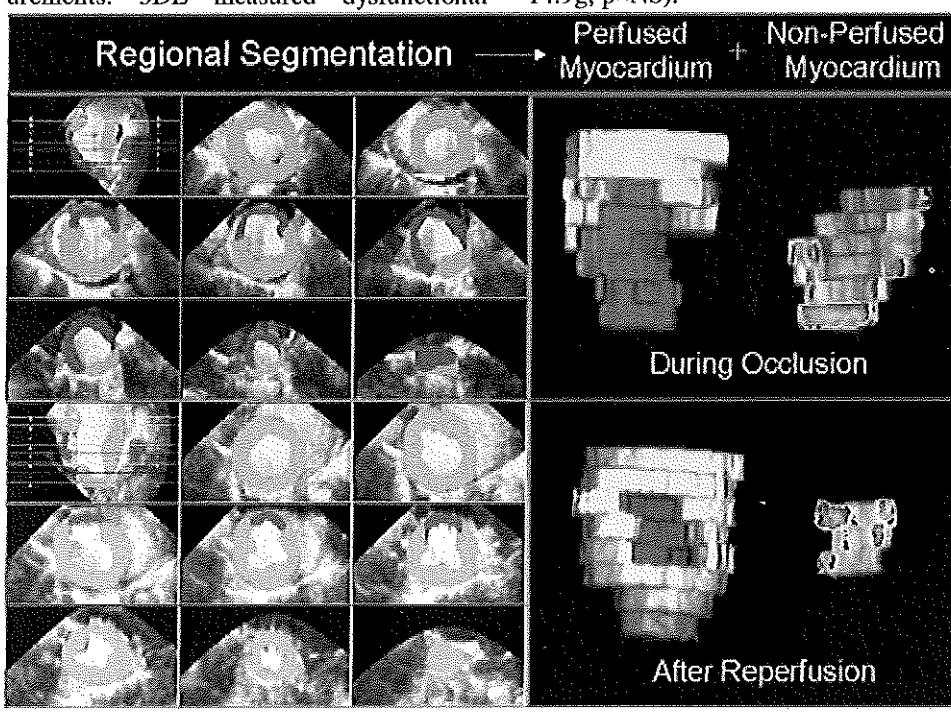

Figure 5. A representative example of the efficacy of reperfusion in a dog with anterior descending coronary artery occlusion (top panels) followed by reperfusion (bottom panels). As shown in the left images with multiple short-axis slices of LV, the regions with perfusion defect were contoured and a dark gray label was applied. The normally perfused regions were labeled in light gray. Not only the volume of each labeled area was calculated by the computer, the volumetric labels could be extracted and displayed individually, as shown here, demonstrating the size of the PDM in contrast to the normally perfused mass, during occlusion and reperfusion stages respectively.

Discussion

Our observations in this experimental study indicate that 3DE using an intravenous contrast agent, NC 100100 in this case, is able to estimate the RM during coronary occlusion and the residual IM after reperfusion by quantifying the PDM. The DFM may represent the RM during acute

ischemia. If reperfusion therapy is instituted, the accuracy of DFM in predicting the residual IM decreases.

Accurate assessment of the RM and the residual IM following revascularization is very helpful in clinical evaluation of the efficacy of reperfusion therapy. 3DE has been used for evaluating global LV function and regional wall motion abnormalities. In the setting of acute myocardial infarction, the myocardial mass that is akinetic or dyskinetic may represent the IM.[19] As it is already well known, if revascularization procedure is performed at this time, the ischiemic myocardium can be salvaged, but the function of the salvaged region does not recover immediately. In other words, after reperfusion therapy, the DFM no longer represents the exact IM.[6]

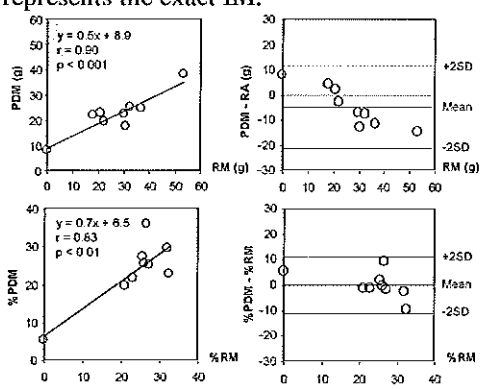

Figure 6. Linear regression (left panels) and Bland-Altman analysis (right panels) of the correlation and disagreement between PDM during coronary occlusion by 3DE and the RM by Evans Blue dye method, both in grams (top) and in percent of LV (bottom).

The development of transpulmonary microbubbles and the evolution of new ultrasound techniques make it possible to evaluate the myocardial perfusion noninvasively.[17,18] A combination of the function and perfusion study should be able to differentiate viable from nonviable dysfunctional myocardial regions.[25] Though studies with 2DE have proven that myocardial perfusion imaging can define the extent of perfusion defect following peripheral administration of contrast agents, the accuracy of 3DE with intravenous contrast injection was not known.

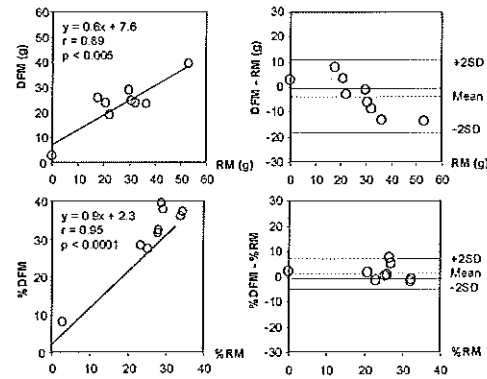

Figure 7. Linear regression (left panels) and Bland-Altman analysis (right panels) of the correlation and disagreement between DFM) during coronary occlusion by 3DE and the RM by Evans Blue dye method, in grams (top) and in percent of LV (bottom).

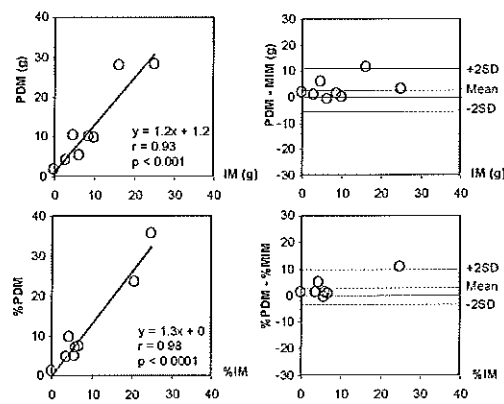

Figure 8. Linear regression (left panels) and Bland-Altman analysis (right panels) of the correlation and disagreement between PDM following reperfusion by 3DE and the residual IM by TTC staining, in grams (top) and in percent of LV (bottom).

Myocardial contrast echocardiography

2DE studies have indicated that con-

trast microbubbles are susceptible to damage by ultrasound.[26] The persistence of microbubbles in the circulation is inversely related to the time of exposure to ultrasound and the transmitting power of ultrasound. Therefore, triggered or transient imaging is used in most of the current studies.[27] Harmonic imaging

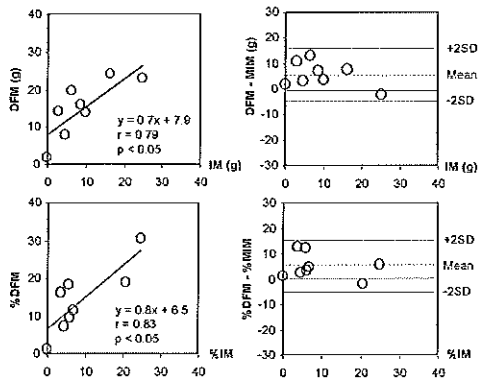

Figure 9. Linear regression (left panels) and Bland-Altman analysis (right panels) of the correlation and disagreement between DFM following reperfusion by 3DE and the residual IM by TTC staining, in grams (top) and in percent of LV (bottom).

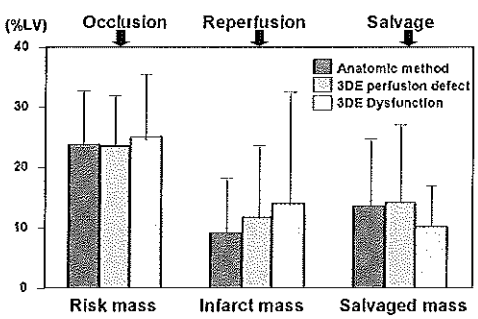

Figure 10. Bar graph showing 3DE estimation of RM during coronary occlusion, residual IM after reperfusion and SM, from PDM or DFM, in comparison with the anatomic measurements.

increases the signal to noise ratio of the contrast images, reduces the optimal transmitting power of ultrasound, decreases the dose of contrast agent and minimizes the attenuation effect of microbubbles.[28] It is worthwhile to point out that in most 2DE perfusion studies, the trigger interval for transient imaging is usually longer than one heart beat (2 to 8 beats, or even longer) to allow for sufficient time for microbubble replenishment. However, it is not possible currently to perform 3DE data acquisition with trigger intervals longer than one heart beat. Besides, 3DE data acquisition time is limited upon a bolus administration of contrast agent and may not allow for longer trigger intervals. Interestingly, the images we obtained from 3DE using 1 to 1 triggering under a low mechanical index showed very good perfusion of the myocardium in the normally perfused regions and clearly delineated perfusion defects in the territory of occluded coronary artery or infarct region. Our explanation is that though 1 to 1 triggering was used for 3DE data acquisition, each of the original images was scanned from a different cutting plane, similar to the result of transient imaging. Besides, the low ultrasound output power may also have contributed to minimizing destruction of microbubbles. Another problem often encountered in contrast echocardiography is the attenuation of signals in the far field (in this experimental setting, the posterior wall). This problem was minimized in this study by slow administration of the contrast agent and the following saline flush, avoiding too high dose of contrast and initiating data acquisition after the early attenuation phase. The contrast agent we employed in this study, NC100100, had minimal attenuation artifacts.

Rationale for three-dimensional contrast echocardiography

The LV is a three-dimensional structure and its cavity size and shape may vary

in different time period of ischemia, infarction or intervention due to physiological remodeling. Besides, the coronary territories are irregular in shape and varies in size attributed to different coronary branches at different levels. Although 2DE, by integrating information from various views of the LV, is able to provide a qualitative or semiquantitative assessment of the extent of myocardium with regional wall motion or perfusion abnormalities, accurate delineation of the topography of a perfusion defect region or quantitation of PDM is not possible by using only one or a few views. To examine the efficacy of reperfusion therapies, a more reproducible method, which should be independent of the acoustic window and cutting plane variation, independent of data acquisition operator and able to provide accurate location and quantitative data of the abnormalities before and after reperfusion, is needed. 3DE could be the method that might be able to fulfill the above requirements. It allows reconstruction of images in any orientation independent of the acoustic window for data acquisition, provides quantitative information of global or regional myocardial region without the need of geometric assumptions and is reproducible on data acquired at different times or by different operators, or analyzed by different observers.[19,29,30] Two studies have demonstrated that contrast 3DE is able to quantify RM or IM accurately.[21,22] These studies, however, employed deposit microspheres (mean diameter = 10 • m) that could not pass the pulmonary circulation and had to be injected into the left atrium using cardiac catheters. We had also demonstrated the feasibility of 3DE using central and peripheral contrast administration in quantifying small and large perfusion defects in acute coronary occlusion models.[23,24] The present study further validated the feasibility and accuracy of 3DE using an intravenous contrast agent in the estimation of RM during coronary occlusion and residual IM following reperfusion by quantifying PDM in each stage. Techniques currently employed to assess myocardial viability include stress echocardiography and stress nuclear imaging.[8,31] Following reperfusion therapy, the functional status of the myocardium may not reflect the presence or absence of viability, contrast echocardiography may show normal perfusion pattern in the viable area.[32] Contrast 3DE may allow for more accurate quantification.

Discrepancy between regional wall motion and perfusion abnormalities

As shown in our study, the DFM and PDM during coronary occlusion had good agreements with each other and with anatomically measured RM. However, following reperfusion, the mean difference between DFM and PDM became larger. The DFM was bigger than both the PDM and the true IM. Following reperfusion, the DFM correlated less well with the PDM and the real IM than it did during the occlusion phase. The PDM measured following flow restoration, however, correlated more closely with the residual IM, indicating that contrast imaging is of great value in assessing SM.

We were still surprised by the fact that there was correlation at all between the DFM and the residual IM following reperfusion and the over-estimation of the IM based on analysis of DFM was not significantly high. Previous two-dimensional studies suggested that the DFM significantly overestimate the true infarct size after revascularization procedures due to stunning of the reperfused myocardium.[6] Part of the reason might be that the dysfunctional myocardium

in this study was defined as the akinetic or dyskinetic regions only and regions that were hypokinetic were excluded.

Critique of our study

There are several limitations in this study that need to be aware of when applying this technique to clinical scenarios since significant difference may exist between experimental and clinical settings. Besides the physical and anatomical differences between species, the acute coronary occlusion and reperfusion canine model was produced in normal animals free of pre-existing coronary artery disease, while patients suffering from acute myocardial ischemia/infarction often have various degrees of atherosclerosis preceding the event or even history of previous myocardial infarctions. Therefore, the human physiological response to coronary artery occlusion and revascularization (including mobilization of coronary reserve and collaterals) and thus, the regional wall motion and myocardial perfusion may differ from our animal model.

Adequate myocardial perfusion time following a bolus intravenous administration of contrast agent was obtained for 3DE data acquisition in this experimental study, which was relatively short comparing with the time required in most clinical studies. How well this method could be applicable in human studies needs to be examined. If not, continuous intravenous infusion of the contrast agent may be considered. Real-time 3DE is able in on-line display of multiple cross-sectional views (orthogonal or parallel) of the heart at the same time and allows for ultra-fast 3DE data acquisition. However, the image quality from this approach has not been satisfactory and, furthermore, it also need post-acquisition processing to develop three-dimensional images.

3DE requires post-processing of the raw image data in our approach as well. Progress is being made in speeding up this process. Due to interpolation of the original images during data processing, the resolution of reconstructed images decreases compared to the original 2DE images. Quantitative data analysis still requires manual tracing. Automatic thresholding technique by calibrating gray-scales of the data may make the analysis easier and more objective,[22]

3DE data were obtained only once at each end of occlusion and reperfusion stages. Perfusion patterns and functional behavior of the LV may change over time following reperfusion therapy. This aspect was not explored in this study. Evaluation of the influences of duration of coronary occlusion and duration of reperfusion requires a more extended study in different groups of animals. We chose to use dipyridamole following reperfusion to magnify the difference between normally perfused regions (which might have hyperemic reactions) and the hypoperfused regions (which should have less or no hyperemic reactions or even more deteriorated hypoperfusion due to "steal of flow" phenomenon") in contrast enhancement. How well it might work with dobutamine was not tested in this study and it would be interesting to examine.

Conclusion

This experimental study demonstrated that myocardial contrast 3DE using intravenous NC100100 could estimate accurately the RM during acute ischemia and the residual IM following reperfusion. Although both PDM and DFM during acute ischemia could represent the RM, examination of myocardial perfusion abnormalities appeared superior to wall motion analysis in

evaluation of residual IM in the setting of reperfusion and, thus, the SM and the efficacy of reperfusion.

1. Mahmarian JJ. Prediction of myocardium at risk. Clinical significance during acute infarction and in evaluating subsequent prognosis. *Cardiol Clin* 1995;13(3):355-378.
2. Kaul S, Villanueva FS. Is the determination of myocardial perfusion necessary to evaluate the success of reperfusion when the infarct-related artery is open? *Circulation* 1992;85(5):1942-1944.
3. Kaul S, Glasheen WP, Ruddy TD, Pandian NG, Weyman AE, Okada RD. The importance of defining left ventricular area at risk in vivo during acute myocardial infarction: an experimental evaluation with myocardial contrast two-dimensional echocardiography. *Circulation* 1987;75:1249-1260.
4. Taylor AL, Kieso RA, Melton J, Hite P, Pandian NG, Kerber RE. Echocardiographically detected dyskinesis, myocardial infarct size, and coronary risk region relationships in reperfused canine myocardium. *Circulation* 1985;71(6):1292-1300.
5. Kerber RE, Marcus ML, Ehrhardt J, Wilson R, Abboud FM. Correlation between echocardiographically demonstrated segmental dyskinesis and regional myocardial perfusion. *Circulation* 1975;52(6):1097-1104.
6. Johnston BJ, Blinston GE, Jugdutt BI. Overestimation of myocardial infarct size due to remodeling of the infarct zone. *Can J Cardiol* 1994;10:77-86.
7. Kaul S. Dobutamine echocardiography for determining myocardial viability after reperfusion: experimental and clinical observations. *Eur Heart J* 1995;16 Suppl M:17-23.
8. Charney R, Schwinger ME, Chun J, Cohen MV, Nanna M, Menegus MA, Wexler J, Franco HS, Greenberg MA. Dobutamine echocardiography and resting-redistribution thallium-201 scintigraphy predicts recovery of hibernating myocardium after coronary revascularization. *Am Heart J* 1994;128(5):864-869.
9. Santoro GM, Bisi G, Sciagra R, Leoncini M, Fazzini PF, Meldolesi U. Single photon emission computed tomography with technetium-99m hexakis 2-methoxyisobutyl isonitrile in acute myocardial infarction before and after thrombolytic treatment: assessment of salvaged myocardium and prediction of late functional recovery. *J Am Coll Cardiol* 1990;15(2):301-314.
10. Ryan T, Tarver RD, Duerk JL, Sawada SG, Hollenkamp NC. Distinguishing viable from infarcted myocardium after experimental ischemia and reperfusion by using nuclear magnetic resonance imaging. *J Am Coll Cardiol* 1990;15(6):1355-1364.
11. Rumberger JA, Bell MR. Measurement of myocardial perfusion and cardiac output using intravenous injection methods by ultrafast (cine) computed tomography. *Invest Radiol* 1992;27 Suppl 2:S40-6.
12. Dilsizian V, Bonow RO. Current diagnostic techniques of assessing myocardial viability in patients with hibernating and stunned myocardium. *Circulation* 1993;87(1):1-20.
13. Kaul S, Pandian NG, Okada RD, Pohost GM, Weyman AE. Contrast echocardiography in acute myocardial ischemia. I. In vivo determination of total left ventricular "area at risk". *J Am Coll Cardiol* 1984;4:1272-1282.
14. Kaul S, Gillam LD, Weyman AE. Contrast echocardiography in acute myocardial ischemia. II. The effect of site of injection of contrast agent on the estimation of area at risk for necrosis after coronary occlusion. *J Am Coll Cardiol* 1985;6:825-830.
15. Reisner SA, Ong LS, Lichtenberg GS, Amico AF, Shapiro JR, Allen MN, Meltzer RS. Myocardial perfusion imaging by contrast echocardiography with use of intracoronary sonicated albumin in humans. *J Am Coll Cardiol* 1989;14(3):660-665.
16. Skyba DM, Jayaweera AR, Goodman NC, Ismail S, Camarano G, Kaul S. Quantification of myocardial perfusion with myocardial contrast echocardiography during left atrial injection of contrast. Implications for venous injection. *Circulation* 1994;90:1513-1521.
17. Grayburn PA, Erickson JM, Escobar J, Womack L, Velasco CE. Peripheral intravenous myocardial contrast echocardiography using a 2% dodecafluoropentane emulsion: identification of myocardial risk area and infarct size in the canine model of ischemia. *J Am Coll Cardiol* 1995;26(5):1340-1347.
18. Firschke C, Lindner JR, Wei K, Goodman NC, Skyba DM, Kaul S. Myocardial perfusion imaging in the setting of coronary artery stenosis and acute myocardial infarction using venous injection of a second generation echocardiographic contrast agent. *Circulation* 1997;96(3):959-967.
19. Yao J, Cao QL, Masani N, Delabays A, Magni G, Acar P, Laskari C, Pandian NG. Three-dimensional echocardiographic estimation of infarct mass based on quantification of dysfunctional left ventricular mass. *Circulation* 1997;96(5):1660-6
20. De Castro S, Yao J, Magni G, Cacciotti L, Trambaiolo P, De Sanctis M, Fedele F. Three-dimensional echocardiographic assessment of the extension of dysfunctional mass in patients with coronary artery disease. *Am J Cardiol* 1998;81:103G-106G
21. Linka AZ, Ates G, Wei K, Firoozan S, Skyba DM, Kaul S. Three-dimensional myocardial contrast echocardiography: validation of in vivo risk and infarct volumes. *J Am Coll Cardiol*

1997;30(7):1892-1899.
22. Kasprzak JD, Vletter WB, Roelandt JRTC, van Meegen JR, Johnson R, Ten Cate FJ. Visualization and quantification of myocardial mass at risk using three-dimensional contrast echocardiography. *Cardiovasc res.* 1998;40:314-21.
23. Delabays A, Cao QL, Yao J, Magni G, Kanojia A, Acar P, Laskari C, Masani N, Schwartz S, Pandian N: Contrast three-dimensional echocardiography in acute myocardial infarction: 3-D reconstruction of perfusion defects yields accurate estimate of infarct mass and extent. (abstract 718-4) JACC 1996;27(2) [suppl A]:63A
24. Masani ND, Yao J, Cao QL, Vannan MA, Meija LD, Johnson D, Ostensen J, Pandian NG. Accurate infarct size estimation using NC100100 in mixed coronary territories: increased accuracy of three-dimensional echo vs. two-dimensional echo. (abstract 1185) *Circulation* 1997;96(8):I-214
25. Nanto S, Lim YJ, Masuyama T, Hori M, Nagata S. Diagnostic performance of myocardial contrast echocardiography for detection of stunned myocardium. *J Am Soc Echocardiogr* 1996;9(3):314-319.
26. Villarraga HR, Foley DA, Aeschbacher BC, Klarich KW, Mulvagh SL. Destruction of contrast microbubbles during ultrasound imaging at conventional power output. *J Am Soc Echocardiogr* 1997;10(8):783-91.
27. Porter TR, Li S, Kricsfeld D, Armbruster RW. Detection of myocardial perfusion in multiple echocardiographic windows with one intravenous injection of microbubbles using transient response second harmonic imaging. *J Am Coll Cardiol* 1997;29(4):791-9.
28. Wei K, Skyba DM, Firschke C, Jayaweera AR, Lindner JR, Kaul S. Interactions between microbubbles and ultrasound: In vitro and in vivo observations. *J Am Coll Cardiol* 1997;29:1081-1088
29. Nosir YFM, Lequin MH, Kasprzak JD, van Domburg RT, Vletter WB, Yao J, Stoker J, Ten Cate FJ, Roelandt JRTC. Measurements and day-to-day variabilities of left ventricular volumes and ejection fraction by three-dimensional echocardiography and comparison with magnetic resonance imaging. *Am J Cardiol* 1998;82:209-214
30. Nosir YFM, Fioretti PM, Vletter WB, Boersma E, Salustri A, Postma JT, Reijs AEM, Ten Cate FJ, Roelandt JRTC. Accurate measurement of left ventricular ejection fraction by three-dimensional echocardiography. A comparison with radionuclide angiography. *Circulation* 1996;94:460-466.
31. Picano E. Dipyridamole-echocardiography test: the historical background and the physiologic basis. *Eur Heart J* 1989;10:365-376
32. Sklenar J, Camarano G, Goodman NC, Ismail S, Jayaweera AR, Kaul S. Contractile versus microvascular reserve for the determination of the extent of myocardial salvage after reperfusion. The effect of residual coronary stenosis. *Circulation* 1996;94(6):1430-1440

CHAPTER 7

USEFULNESS OF THREE-DIMENSIONAL TRANSESOPHAGEAL ECHOCARDIOGRAPHIC IMAGING FOR EVALUATING NARROWING IN THE CORONARY ARTERIES

Jiefen Yao, MD; Meindert A. Taams, MD; Jaroslaw D. Kasprzak, MD;
Pim J. de Feijter, MD; Folkert J. ten Cate, MD; Lex A. Van Herwerden, MD;
Jos R.T.C. Roelandt, MD.

Am J Cardiol **1999;84: (in press)**

Usefulness of Three-Dimensional Transesophageal Echocardiographic Imaging for Evaluating Narrowing in the Coronary Arteries

Jiefen Yao, MD; Meindert A. Taams, MD; Jaroslaw D. Kasprzak, MD; Pim J. de Feijter, MD; Folkert J. ten Cate, MD; Lex A. Van Herwerden, MD; Jos R.T.C. Roelandt, MD.

Coronary artery (CA) imaging has relied upon invasive techniques for diagnosis of stenotic lesions. Two-dimensional techniques are limited in obtaining optimal longitudinal views of all segments of the CA, due to their spatial orientations. Three-dimensional echocardiography (3DE) may produce any desired cross-sectional views and reconstruct 3-dimensional images from a volumetric data set. Its role in CA imaging has not been fully explored. The aim of this study was to evaluate the potential of 3DE in visualizing CA and in assessing the severity of stenosis. We performed transesophageal 3DE in 46 patients. Images were collected sequentially with the transducer rotated through 180°. From the 3DE data sets of all 46 patients, cross-sectional views and 3-dimensional images of CA were reconstructed. For segment-by-segment comparison between CA angiography and 3DE in semi-quantitatively analysis of coronary stenosis, 5 segments were defined for the proximal CA tree in 20 patients who had both procedures. The left main, anterior descending, circumflex and right CA were visualized from 3DE in 100%, 100%, 98%, and 72%. The available lengths of these segments from 3DE were 12±4 (4-22), 15±6 (6-36), 30±12 (13-60) and 18±9 (6-36) mm, respectively. Comparison between 3DE and CA angiography in semi-quantitative estimation of CA stenosis resulted in complete agreement in 83% of the segments (Kappa value = 0.7). The sensitivity and specificity of 3DE in detecting significant stenosis (≥50%) were 84% and 97%. In conclusion, transesophageal 3DE allows imaging of the proximal CA, detection of stenotic lesions and estimation of the severity of stenosis.

Key Words: Three-dimensional Echocardiography, coronary artery disease, transesophageal echocardiography

Imaging of the coronary artery (CA) and diagnosis of stenosis have relied mainly on invasive techniques including coronary angiography and intravascular ultrasound. A number of noninvasive techniques, including 2-dimensional echocardiography, fluoroscopy, magnetic resonance imaging and computer tomographic scanning, have also been explored in evaluating CA stenosis.[1-9] Among them, 2-dimensional echocardiography is one of the most widely investigated methods. It is limited in the number of available views due to restricted transducer orientation and beat-to-beat variation of the images caused by the movements of the heart. Volume-rendered 3-dimensional echocardiography (3DE) provides good delineation of not only gross anatomy but also delicate structures of the heart.[10,11] Previous study has demonstrated its feasibility in visualizing proximal CA.[12] However, the qualitative and quantitative abilities of this potentially useful tool have not been fully explored and a systematic study is required to evaluate this technique. We explored various approaches in CA reconstruction and analyzed the severity of CA stenosis in each segment.

METHODS

Patient Population

We recruited 46 patients (32 men, 14 women, age 58±14 years old, ranged from 18 to 85 years), who were referred for transesophageal echocardiography with various clinical indications (valvular diseases in 15, diseases of aorta in 7 and congenital defects or rule out thrombus in 3) or requested intra-operative monitoring (valvuloplasty or replacement in 5, coronary bypass in 15 and pericardiectomy in 1). Of them, 20 had both 3DE and CA angiography within 3 months (46±35 days, range: 6-90 days). These 20 patients formed the subgroup for comparison between these two techniques in semi-

quantitative segmental evaluation of CA stenosis. All patients were in sinus rhythm, except 5 in artificially paced rhythm. Informed consent was obtained from each patient.

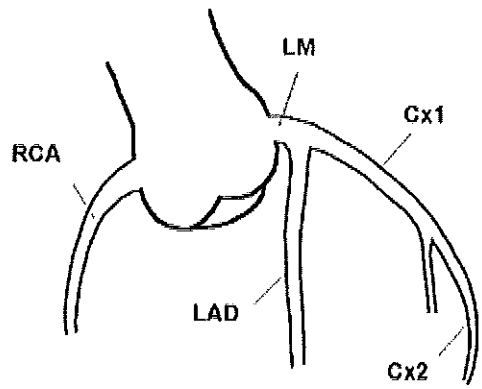

Figure 1. Schematic drawing demonstrating the definition of proximal CA segments for comparison between 3DE and CAA in semi-quantitative evaluation of CA stenosis. LM = left main CA, LAD = proximal left anterior descending CA, Cx1 = the first segment of left circumflex CA before the first marginal branch, Cx2 = the second segment of the circumflex CA distal to the first marginal branch, and RCA = proximal right CA.

Definition of the proximal CA segments

For the convenience of blind analysis and comparison between 3DE and CA angiography in semi-quantitative evaluation of the severity of CA stenosis, 5 segments of the proximal CA was defined. They included left main, proximal 2cm of left anterior descending, the first and second segments of left circumflex (before and 2cm after the first marginal branch) and proximal 2cm of right CA (Fig. 1). Only these segments were analyzed in the semi-quantitative study, though more were available sometimes.

CA angiography

Selective CA angiography of both left and right CA was performed in multiple projections in a standard manner. The angiograms were reviewed by an observer blinded to the results of 3DE. Each CA segment was observed from multiple projections to decide the presence or absence and the severity of stenosis. Visual estimation of the severity of stenosis was graded into 0% (normal), 0-50%, 50-90% and >90%. Significant stenosis was defined when reduction of the CA lumen was more than 50%.

Three-DE

Data acquisition and processing. A commercially available ultrasound unit (HP, SONOS 2500, Hewlett-Packard), incorporated with 3DE data acquisition software, was employed for both 2-dimensional examination and 3DE data acquisition using a 5 MHz multiplane transesophageal transducer. 3DE data acquisition was initiated when the transducer was advanced to the mid-esophagus level, with the aortic root slightly to the left of the mid-line in the image sector, with no effort in searching for the CA. With the probe in a fixed position, the transducer was steered from 0 through 180° at 3° intervals. Images were collected at each step with electrocardiogram and respiratory gating and stored onto a magnetic optical disk for off-line processing, reconstruction and data analysis using a dedicated 3DE processing computer (EchoView 3.1, TomTec Imaging Inc.). Gaps between the original images were filled automatically using a cylindrical interpolating algorithm to produce a voxel-based volumetric 3DE data set.

Methods of reconstruction. From the 3DE data sets, images of CA were reconstructed and displayed in 3 formats. They included: 1) anyplane cross-sectional images; 2) volume-rendered 3DE images and; 3) extracted CA lumen in 3-dimensions.

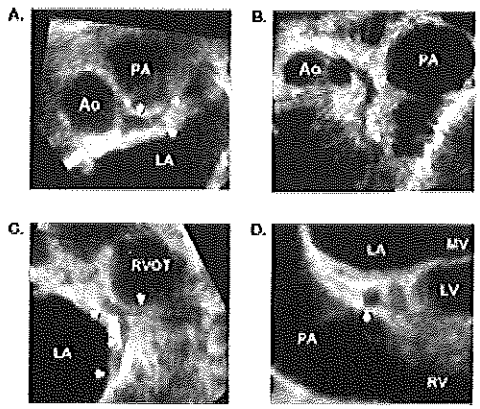

Figure 2. Multiple cross-sectional images of CA (arrows) reconstructed from a 3DE data set. **A.** Longitudinal image of the left main CA bifurcating into anterior descending and circumflex arteries. **B.** A different view of the left main CA extending into the anterior descending CA. **C.** Cross-sectional images of the distal left main CA and proximal segments of circumflex and anterior descending arteries. **D.** Cross-sectional view of the left main CA. PA indicates pulmonary artery; Ao = aortic root; LA = left atrium; RVOT = right ventricular outflow tract; MV = mitral valve, LV = left ventricle; RV = right ventricle.

Secondary cross-sectional images were reconstructed from the 3DE data sets, independent of the position and orientation of the transducer during data acquisition. Using anyplane method, the cutting plane could be steered in arbitrary directions to produce optimal views of each CA segment (Fig. 2). Employing segmentation, thresholding and gray-scale shading techniques, 3DE images of CA along with other cardiac structures were reconstructed in various projections and displayed dynamically. The ostia of CA were viewed *en face* from within the aortic root as if aortotomy had been performed. Each CA segment was reconstructed in longitudinal and cross-sectional views (Fig. 3). The CA lumen was manually traced in 1mm thick slices on multiple parallel images. A volumetric label was applied to the traced region to extract and reconstruct images of the CA lumen, delineating spatial CA anatomy (Fig. 4).

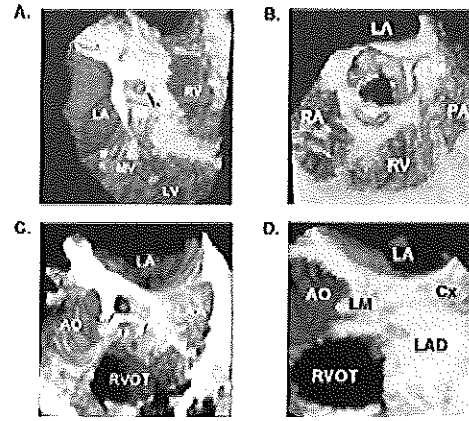

Figure 3. Volume-rendered 3D images of CA (arrows). **A.** An *en face* view of the ostium of left main CA from within the aortic root. **B.** Proximal segment of the left main CA (LM) arising from the left coronary sinus. **C.** Longitudinal view of the middle and distal portions of left main CA. **D.** Longitudinal view of the left main CA extending into circumflex (Cx) and anterior descending CA (LAD). LA indicates left atrium, MV = mitral valve, LV = left ventricle, RV = right ventricle, RA = right atrium, PA = pulmonary artery, AO = aortic root; LAA = left atrial appendage, RVOT = right ventricular outflow tract.

Data analysis. The proximal CA was examined using different reconstruction methods mentioned above. The lengths of all available CA segments were measured at end-diastole. The diameter of the left main CA was measured at 3 different levels of the stem and an average value was taken. Two independent observers, unaware of the CA angiographic results, analyzed the 3DE data of those 20 patients who underwent both CA angiography and 3DE. The presence or absence and the severity of stenotic lesions in each designated segment were evaluated (Fig. 5). The severity of stenosis was estimated visually, by integrating the information obtained from multiple cross-sectional and 3DE images, as percent narrowing of the CA lumen. Similar to angiographic

analysis, the severity of stenosis was assessed as 0%, 0-50%, 50-90% and >90%. Significant stenosis in a CA segment was diagnosed when a reduction of lumen size was >50%. Inter- and intra-observer variabilities in semi-quantitative assessment of CA stenosis were also studied.

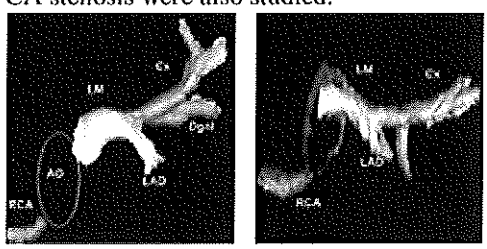

Figure 4. Two examples of 3-dimensional images of extracted CA lumen. RCA indicates right CA; AO = aortic root; LM = left main CA, LAD = left anterior descending CA; Dgnl = diagonal branch of left CA.

Statistical methods

All measurements were expressed as mean±SD. The severity of CA stenosis derived from 3DE and that from angiography were presented in 2-way tables and compared using Kappa analysis. Kappa values less than 0.40 were defined as poor agreement between the two, values between 0.40 and 0.75 as fair to good agreement and values above 0.75 as strong agreement. Compared to CA angiography, the sensitivity, specificity and positive and negative predictive values of 3DE in diagnosis of significant CA stenosis were obtained.

RESULTS

Feasibility of CA imaging by 3DE

Three-DE data was available in all studied patients. It took 2 to 5 minutes for 3DE data acquisition, 10 to 15 minutes for data processing and 10 to 40 minutes for image reconstruction and semiquantitative analysis of CA lesions. Various lengths of CA were obtained from transesophageal 3DE in all 46 patients (100%). The left main, anterior descending, circumflex and right CA were observed in 100%, 100%, 98%, and 72% of patients. Their lengths measured 12±4 (4-22) mm, 15±6 (6-36) mm, 30±12 (13-60) mm and 18±9 (6-36) mm, respectively. The diameter of the left main ranged from 3.0 to 5.2 mm (4.1±0.6 mm). In 30 of 46 patients, stenotic lesions of various severity and locations were observed from reconstructed cross-sectional or 3DE images.

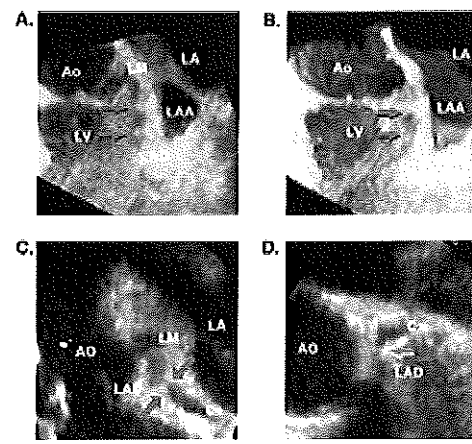

Figure 5. Reconstructed cross-sectional (A, C and D) and 3-dimensional CA images showing stenotic lesions (arrows). **A.** Reconstructed cross-sectional image of the left main (LM) and anterior descending (LAD) showing two eccentric stenotic lesions. **B.** Volumetric 3-dimensional reconstruction of the same lesions as in panel A. **C.** Cross-sectional image of a concentric stenosis at the beginning of the circumflex CA (Cx). **D.** Cross-sectional view showing an eccentric stenosis in LAD. Ao indicates aortic root, LA = left atrium, LAA = left atrial appendage, LV = left ventricle.

Segmental semi-quantitative evaluation of CA stenosis

In the subgroup of 20 patients, who underwent both 3DE and angiography within 3 months, the severity of CA stenosis was compared segment-by-segment between the 2 techniques. With 5 segments in each patient, a total of 100 segments of the proxi-

mal CA were analyzed from angiography, but 13 of them were excluded due to their absence or inadequate lengths in the 3DE data sets. Therefore, a total of 87 segments remained for comparison between 3DE and angiography in the evaluation of CA stenosis. Of these 87 segments, stenoses of various degrees were diagnosed in 34 (19 significant stenoses) by angiography and 35 (18 significant) by 3DE. Compared to angiography, the sensitivity, specificity, positive predictive value and negative predictive value of 3DE were 91%, 92%, 89% and 94% (92% agreement) in detecting all CA stenoses and were 84%, 97%, 89% and 96% (94% agreement) in defining significant stenosis (table 1). Complete agreement between these 2 techniques was obtained in 83% of the segments in defining the severity of stenosis. A value of 0.70 was obtained from Kappa analysis, representing good agreement between them (table 2). Both intra- and inter-observer 3DE analyses of the severity of CA stenosis resulted in good agreements, with Kappa values of 0.66 and 0.60, respectively (table 3).

Table I. 3DE in evaluation of CA stenosis in comparison with angiography.

		Angiography			Angiography	
		-	+		Non-significant	Significant
3DE	-	49	3	3DE Non-significant	66	3
	+	4	31	3DE Significant	2	16
sensitivity	91%			84%		
specificity	92%			97%		
PPV	89%			89%		
NPV	94%			96%		
overall accuracy	92%			94%		

Additional information from 3DE

Using various formats of image reconstruction and display, the proximal CA segments could be studied comprehensively. The spatial distribution of the CA tree and its relationship with other cardiac structures (such as aortic root, right ventricular outflow tract, and the left atrial appendage) were demonstrated and easily appreciated (Fig. 3 and 4). The location, extension and eccentricity of CA plaques were delineated nicely in both cross-sectional and 3-dimensional images (Fig. 5).

Table II. Segmental semi-quantitative analysis of CA stenosis by 3DE and angiography.

		Angiography				
		0%	<50%	50-90%	>90%	Sum
3	0%	49	3	0	0	52
D	<50%	4	10	2	1	17
E	50-90%	0	2	9	1	12
	>90%	0	0	2	4	6
	Sum	53	15	13	6	87

DISCUSSION

Significant proximal CA stenosis is known to be associated with ischemic events, including myocardial infarction, and higher mortality rates in patients undergoing major interventional procedures.[13,14] Most of them are also markers of diffuse CA disease. Accurate evaluation of these lesions may lead to important clinical decision making. Three-DE can be easily coupled with clinically indicated 2-dimensional examinations and could be a potentially useful method for evaluating proximal CA lesions.

Previous techniques for coronary artery imaging

CA angiography remains the "gold standard" and the most widely used method in assessing CA lesions.[15,16] However, its discrepancy in evaluating the severity of CA stenosis, especially lesions in left main CA,

has been shown by both pathological and intracoronary ultrasound studies.[17-21] Even with multiple projections, angiography can not overcome the problems of foreshortening and overlapping on planar projections. It indirectly displays the plaques from the lumen silhouette.[22] Intra-coronary ultrasound provides direct information of the plaques and is accurate in assessing CA stenosis. It is limited by the invasiveness and highly cost. Among noninvasive techniques, fluoroscopy and computer tomography are only sensitive to calcified plaques. Non-calcified lesions require the use of contrast. Magnetic resonance imaging has also shown encouraging results. These techniques are expensive and not widely available.[5-9] Two-dimensional echocardiography is applied daily in various clinical settings for a variety of indications. Promising results have been achieved with the development of newer imaging modalities.[2,4] Nevertheless, 2-dimensional echocardiography is highly operator dependent for obtaining satisfactory views due to the restriction in acoustic windows and movement of the heart.

Rationale and feasibility of 3DE in CA imaging

Volume-rendered 3DE provides a volumetric data set of the heart. With the ability of anyplane display, it extends the potential of 2-dimensional echocardiography in CA imaging by creating unconventional views. The ability of 3DE in still frame analysis makes CA examination easier. Three-DE demonstrates spatial anatomic relationships between CA and other cardiac structures, which may provide important information for interventional procedures such as CA bypass surgery or intra-coronary stent placement.

Table III. Intra- and inter-observer agreements in 3DE analyses of CA stenosis.

		Ob-1A				agreement	Kappa
		0%	<50%	50-90%	>90%		
	0%	48	3	0	0		
Ob-1B	<50%	6	11	1	0	84%	0.66
	50-90%	0	2	8	1		
	>90%	0	0	1	4		
		0%	<50%	50-90%	>90%		
	0%	47	4	2	0		
Ob-2	<50%	4	10	3	0	78%	0.60
	50-90%	0	1	4	3		
	>90%	0	0	1	2		

Evaluation of CA stenosis by 3DE

Free placement of the cutting plane in 3DE helps us in avoiding foreshortened views of CA. This may avoid over- or under-estimation of the severity of CA lesions. From this study, good agreement was obtained between 3DE and angiography. While agreement was obtained in 83% of the segments, the discrepancy in most of the other segments was 1 grade (Table 4). No systemic over- or under-estimation of the severity of CA stenosis was observed. In addition, 3DE also provided information of other cardiac structures. Whether the echogenicity of the plaques could represent the degree of calcification needs to be studied in future investigations.

Limitations of this study

Only patients with sinus rhythm or pacemaker rhythm were investigated. Atrial fibrillation, particularly with significant variability of heart rate, may have extended

3DE data acquisition time. Therefore, the accuracy of 3DE in evaluating CA disease in patients with atrial fibrillation is not known. Among a total number of 46 patients in the feasibility study, only 20 were eligible in the semiquantitative study, since we didn't request angiographic studies in those with no clinical indications. The number of stenotic CA lesions was not sufficient to allow a further subdivision by sites to study the accuracy of 3DE in each segment. A future study in a large cohort of patients with various cardiac rhythms and a wide spectrum of CA lesions would be helpful in addressing some of the limitations. We did not compare 2-dimenssional and 3DE methods in evaluating CA lesions, which would have extended the time of examination and increased the discomfort of the patients. The lengths of the left anterior descending and right CA were limited in this 3DE study, due to decreased image resolution in the far ultrasound field, yet the total lengths of CA from 3DE exceeded that in most of the previous 2-dimensional studies. Importantly, symptomatic stenotic lesions occur more often in the proximal segments. Requirement of data processing prevents 3DE from real-time visualization of CA. Analysis of 3DE data is time consuming and requires experience of the observer. There was considerable inter- and intra-observer variability in this study in analyzing CA lesions, though most of the discrepancies were small. It would be ideal to perform quantitative analysis of coronary stenosis from 3DE data and compare with another quantitative technique. However, in daily clinical practice, semiquantitative angiographic assessment of the narrowing of coronary arteries is being used more often. Although this "eyeballing" method has considerable observer variability, when coupled with clinical symptoms it has proven very helpful in clinical decision making.

1. Weyman AE, Feigenbaum H, Dillon JC, Johnston KW, Eggleton RC. Noninvasive visualization of the left main coronary artery by cross-sectional echocardiography. *Circulation* 1976;54:169-174.
2. Ryan T, Armstrong WF, Feigenbaum H. Prospective evaluation of the left main coronary artery using digital two-dimensional echocardiography. *J Am Coll Cardiol* 1986;7:807-812.
3. Taams MA, Gussenhoven EJ, Cornel JH, The SH, Roelandt JR, Lancee CT, v.d. Brand M. Detection of left coronary artery stenosis by transesophageal echocardiography. *Eur Heart J* 1988;9:1162-1166.
4. Ross JJ Jr, Mintz GS, Chandrasekaran K. Transthoracic two-dimensional high-frequency (7.5MHz) ultrasonic visualization of the distal left anterior descending coronary artery. *J Am Coll Cardiol* 1990;15:373-377.
5. Detrano R, Markovic D, Simpfendorfer C, Franco I, Hollman J, Grigera F, Stewart W, Ratcliff N, Salcedo EE, Leatherman J. Digital subtraction fluoroscopy: a new method of detecting coronary calcifications with improved sensitivity for the prediction of coronary disease. *Circulation* 1985;71:725-732.
6. Manning WJ, Li W, Boyle NG, Edelman RR. Fat-suppressed breath-hold magnetic resonance coronary angiography. *Circulation* 1993;87:94-104.
7. Kajinami K, Seki H, Takekoshi N, Mabuchi H. Noninvasive prediction of coronary atherosclerosis by quantification of coronary artery calcification using electron beam computed tomography: comparison with electrocardiographic and thallium exercise stress test results. *J Am Coll Cardiol* 1995;26:1209-1221.
8. Simons DB, Schwartz RS, Edwards WD, Sheedy PF, Breen JF, Rumberger JA. Noninvasive definition of anatomic coronary artery disease by ultrafast computed tomographic scanning: a quantitative pathologic comparison study. *J Am Coll Cardiol* 1992;20:1118-1126.
9. Achenbach S, Moshage W, Bachmann K. Detection of high-grade restenosis after PTCA using contrast enhanced electron beam CT. *Circulation* 1997;96:2785-2788.
10. Roelandt JRTC, Ten Cate FJ, Vletter WB, Taams MA. Ultrasonic dynamic three-dimensional visualization of the heart with a multiplane transesophageal imaging transducer. *J Am Soc Echocadiogr* 1994;7:217-229.
11. Salustri A, Becker AE, Van Herwerden L, Vletter WB, Ten Cate FJ, Roelandt JRTC. Three-dimensional echocardiography of normal and pathologic mitral valve: A comparison with two-

dimensional transesophageal echocardiography. *J Am Coll Cardiol* 1996;27:1502-1510.
12. El-Rahman SMA, Khatri G, Nanda N, Agrawal G, Nanda A, Nanda A, McGiffin DC, Kirklin JK, Pacifico AD, Li ZA, Wang XF. Transesophageal three-dimensional echocardiographic assessment of normal and stenosed coronary arteries. *Echocardiography* 1996;13:503-510.
13. Devlin G, Lazzam L, Schwartz L: Mortality related to diagnostic cardiac catheterization: the importance of left main coronary disease and catheter induced trauma. *Int J Cardiac Imaging* 1997;13:379-384.
14. Kennedey JW, Baxley WA, Bunnel IL, Gensini GG, Messer JV, Mudd JG, Noto TJ, Paulin Pichard AD, Sheldon WC, Cohen M. Mortality related to cardiac catheterization and angiography. *Cathet Cardivasc Diagn* 1982;8:323-340.
15. Conti CR, Selby JH, Christie LG, Pepine CJ, Curry RC Jr, Nichols WW, Conetta DG, Feldman RL, Mehta J, Alexander JA. Left main coronary artery stenosis: clinical spectrum, pathophysiology and management. *Prog Cardiovasc Dis* 1979;22:73-106.
16. Abbas SA, Morris RS, Heller GV. Correlation of symptoms, myocardial perfusion imaging, and anatomic narrowing of the left anterior descending artery. *J Nucl Cardiol* 1996;3:363-364.
17. Vlodaver Z, Frech R, Van Tassel RA, Edwards Je. Correlation of the antemortem coronary arteriogram and the postmortem specimen. *Circulation* 1973;47:162-169.
18. Mintz GS, Popma JJ, Pichard AD, Kent KM, Satler LF, Chuang YC, DeFalco RA, Leon MB. Limitations of angiography in the assessment of plaque distribution in coronary artery disease: a systematic study of target lesion eccentricity in 1446 lesions. *Circulation* 1996;93:924-931.
19. Isner JM, Kishel J, Kent KM, Ronan JA Jr., Ross AM, Roberts WC. Accuracy of angiographic determination of left main coronary artery narrowing. Angiographic-histologic correlative analysis in 28 patients. *Circulation* 1981;63:1056-1064.
20. Hermiller JB, Buller CE, Tenaglia AN, Kisslo KB, Phillips HR, Bashore TM, Stack RS, Davidson CJ. Unrecognized left coronary artery disease in patients undergoing interventional procedures. *Am J Cardiol* 1993;71:173-176.
21. Ge J, Liu F, Görge G, Haude M, Baumgart D, Erbel R. Angiographically "silent" plaque in the left main coronary artery detected by intravascular ultrasound. *Cor Art Dis* 1995;6:805-810.
22. Topol EJ, Nissen SE. Our preoccupation with coronary luminology. The dissociation between clinical and angiographic findings in ischemic heart disease. *Circulation* 1995;92:2333-2342.

CHAPTER 8

THREE-DIMENSIONAL ULTRASOUND STUDY OF CAROTID ARTERIES BEFORE AND AFTER ENDARTERECTOMY: ANALYSIS OF STENOTIC LESIONS AND SURGICAL IMPACT ON THE VESSEL

Jiefen Yao, MD; Marc R.H.M. van Sambeek, MD; Anita Dall'Agata, MD;
Lukas C. van Dijk, MD; Micheala Kozakova, MD; Peter J. Koudstaal, MD, PhD;
Jos R.T.C. Roelandt, MD, PhD

Stroke **1998;29:2026-2031**

Three-dimensional Ultrasound Study of Carotid Arteries Before and After Endarterectomy:
Analysis of Stenotic Lesions and Surgical Impact on the Vessel

Jiefen Yao, MD; Marc R.H.M. van Sambeek, MD; Anita Dall'Agata, MD; Lukas C. van Dijk, MD; Micheala Kozakova, MD; Peter J. Koudstaal, MD, PhD; Jos R.T.C. Roelandt, MD, PhD

Background and Purpose It has been proven that symptomatic patients with severe carotid stenosis benefit from endarterectomy. Currently used methods for quantitation of the severity of carotid stenosis have limitations and the impact of endarterectomy on the operated region of carotid artery remains unknown. The purpose of this study was to examine the accuracy of a three-dimensional ultrasound system for quantitation of stenotic lesions and to evaluate changes in regional vessel volume and cross-sectional area after carotid endarterectomy. **Methods** 14 patients were studied with both carotid angiography and three-dimensional ultrasound. Of 13 patients underwent surgery, 12 were reexamined with three-dimensional ultrasound after surgery. The length and volume of 20 random selected plaques were measured from three-dimensional data sets. The severity of stenosis was quantified by three-dimensional ultrasound using both diameter method and area method on cross-sectional views at the most stenotic site and the results were compared with that by carotid angiography. The segmental vessel volume and average cross-sectional area of the operated artery both before and after endarterectomy were measured from three-dimensional ultrasound data. **Results** Good correlation was obtained between three-dimensional ultrasound and carotid angiography in quantitative analysis of carotid stenosis (SEE=12.4%, r=0.76, mean difference=-7.0±12.3% using the diameter method and SEE=105%, r=0.82, mean difference = 1.8±10.5% using the area method by three-dimensional ultrasound). Three-dimensional ultrasound had excellent reproducibility and small intra- and inter-observer variability in plaque length and volume measurements. No significant change in segmental vessel volume and average cross-sectional area of the operated artery was observed after surgery in patients with suture closure. However, a significant increase in segmental vessel volume was obtained in patients with polyfluorethylene patches applied to the surgical opening of the artery. **Conclusions** Three-dimensional ultrasound can be used for both qualitative and quantitative analysis of plaques in the carotid artery and to detect and quantify significant carotid stenosis. Its volumetric potential has important clinical implications in serial follow-up studies for observing the progression or regression of stenotic lesions and for evaluating the outcome of interventional procedures such as endarterectomy or stent placement.

Key words: carotid arteries, atherosclerosis, carotid stenosis, ultrasonics, carotid endarterectomy

It has been proven that symptomatic patients with severe carotid artery stenosis (≥70%) benefit from endarterectomy.[1-2] Selection of candidates for surgery mostly relies on carotid angiography.[3-6] Because of the invasiveness and the associated complications and mortality of this technique, noninvasive procedures have been employed for evaluating the severity of carotid artery stenosis.[7-22] Two-dimensional ultrasound scanning, in combination with Doppler, has been used either as an adjuvant or as the decisive examination for surgical candidate selection.[11-16] One of the major limitations of the two-dimensional method is that it requires mental reconstruction of the shape of the plaque and the stenotic vessel lumen from limited cross-sectional views. Three-dimensional reconstruction technique has been investigated in carotid artery imaging employing various modalities and demonstrated some encouraging findings.[23-26] Whether volume-rendered three-dimensional ultrasound reconstruction could allow better appreciation of the stenotic lesions and accu-

rate assessment of the severity of stenosis of the cervical carotid artery is not known. Neither is the impact of endarterectomy on the volumetric properties of the regional carotid artery fully understood.[27] We have employed a prototype three-dimensional vascular ultrasound reconstruction system to evaluate its reproducibility in the measurement of plaque length and volume and its value in quantitative assessment of the severity of stenosis compared with angiography. The changes in segmental vessel volume and average cross-sectional area of the carotid artery before and after endarterectomy were evaluated as well.

Subjects and Methods

Patients

In this study, we recruited 14 patients (4 females, mean age 64 years, ranged from 41 to 77 years), each with a recent TIA or minor stroke. Carotid angiography showed at least one severe stenosis (≥70%) of the carotid artery. All were considered candidates for carotid endarterectomy. Three-dimensional ultrasound of both carotid arteries were performed within 3 months of carotid angiography or less than three weeks before surgery (baseline study). 13 of these patients underwent carotid endarterectomy. Three-dimensional ultrasound of the operated artery was repeated in 12 patients within one week after surgery (post-operative study). Informed consent for this study was obtained from each patient.

Carotid artery angiography

Selective carotid artery angiography was performed in standard manners employing Seldinger technique. Each carotid artery was imaged from multiple projections. All angiograms were reviewed by an experienced independent observer to assess the site and severity of carotid artery stenosis with the method used in European Carotid Surgery Trial.[1] A decrease of ≥50% of the estimated original lumen was defined as significant stenosis. Severe stenosis was diagnosed when the lumen diminishment was ≥70%.

Carotid endarterectomy

Carotid endarterectomy was performed in the classic way.[28-29] During the procedure, the cerebral perfusion was monitored with electroencephalography (EEG). A shunt was used only on indication of ischemia, when the EEG became asymmetric. After exposure and clamping, the artery was dissected longitudinally to expose the lumen and the intima-media complex of the stenotic segment was excised. After close examination to ascertain that there was no debris left in the lumen, the artery was primarily closed with a running suture. In case the operated segment was of small diameter, the incision was closed using a polytetrafluorethylene patch to prevent the lumen from being too much narrowed.

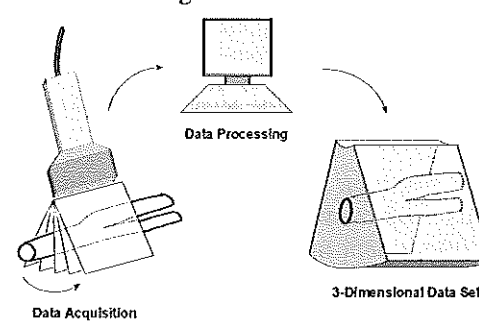

Figure1. Schematics showing the principle of three-dimensional ultrasound data acquisition and production of a volumetric data set of the carotid artery.

Three-dimensional ultrasound of carotid arteries

Instrumentation. A commercially available ultrasound system with a prototype probe

and computer software for three-dimensional data acquisition and reconstruction (AU3 Partner, Esaote Biomedica, S.p.A., Florence, Italy) was used for imaging of the carotid arteries. The prototype probe has a dual frequency of 10/5 MHz with the transducer steered in a fan-like fashion by an internally incorporated motoring device. The transducer frequency of 10 MHz was used for three-dimensional data acquisition. A prism three-dimensional ultrasound data set can be acquired by automatic sequential collection of images in a push button manner with the probe held in a fixed position. Two-dimensional images could be collected consecutively without ECG gating to produce a static data set, or a dynamic data set could be obtained by registration of ECG gated images to their correspondent cardiac phases. The range of transducer movement can be predetermined at 30 to 65°. The probe also has the ability of two-dimensional and spectral and color Doppler imaging.

Data acquisition and processing. In each patient, both carotid arteries were imaged. Two-dimensional ultrasound imaging and color and spectral Doppler were performed first to select the optimal acoustic window for three-dimensional data acquisition. A multitude of two-dimensional images of the carotid artery were collected sequentially at equal intervals by steering the transducer through 65 degrees without ECG gating. Spaces between the images were filled automatically by the computer using a specific interpolation algorithm during data processing to produce a volumetric three-dimensional data set (Figure 1). The three-dimensional data were stored in a digital format for off-line analysis. Images of the two-dimensional ultrasound before and during three-dimensional data acquisition were stored onto VHS videotapes for necessary review.

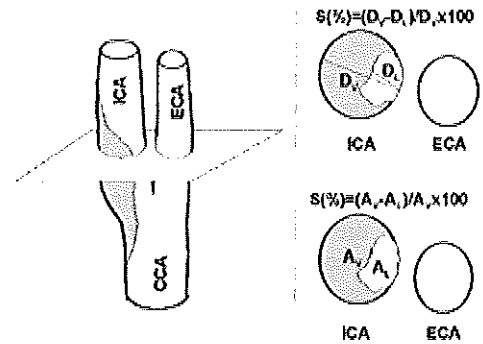

Figure 2. A schematic description of the diameter method and the area method for measuring the severity of carotid stenosis on the cross-sectional image reconstructed from a three-dimensional ultrasound data set. ICA indicates internal carotid artery; ECA, external carotid artery; CCA, common carotid artery; S, stenosis; D_L, minimal diameter of the free lumen; D_V, diameter of the original vessel; A_L, minimal area of the free lumen; A_V, cross-sectional area of original vessel.

Data analysis. The three-dimensional data sets were reviewed by an independent observer, unaware of angiographic results, to determine the presence or absence of plaques and the site of stenosis. Measurement of plaque length and volume and severity of stenosis were performed separately by two blinded observers and repeated by one of them with intervals of one week or longer.

By moving the cutting plane through the three-dimensional data set in various directions, multiple views of the carotid artery were produced. The length of a plaque was measured in a longitudinal view of the vessel. By defining both ends of the plaque, multiple (as many as 20) equidistant cross-sectional cutting planes perpendicular to the longitudinal view of the plaque were generated automatically.

Volume of the plaque was computed by manual tracing of the plaque on each cross-sectional image. The severity of stenosis was computed from measurements on the cross-sectional image with the smallest lumen area using two methods. With the diameter method, the severity of stenosis was derived from measurements of the smallest free lumen diameter and the diameter of the original vessel lumen. With the area method it was derived from the cross-sectional free lumen area and the original vessel lumen area (Figure 2).

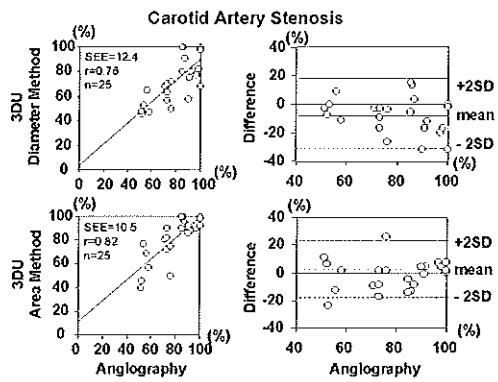

Figure 3. Linear regression (left) and Bland-Altman analysis (right) between the severity of carotid stenosis measured from angiography and that from three-dimensional ultrasound using the diameter method (top) and the area method (bottom).

In patients who underwent carotid endarterectomy, segmental vessel volume of the carotid artery bifurcation was measured before and after surgery. A longitudinal cutting plane of the carotid artery bifurcation showing the common, internal and external carotid arteries was selected as a reference image from the three-dimensional data set. A segment of 2 cm of the vessel, including 1 cm of the common carotid artery proximal and 1 cm of both internal and external carotid arteries distal from the bifurcation, was defined. 20 parallel equidistant cross-sectional images of this segment was automatically generated. The area of the carotid artery within the adventitia, ignoring any plaques if present, was traced manually on each image to derive the segmental vessel volume. Divided by the predefined length of the segment (2 cm), an average cross-sectional area of the carotid bifurcation was also computed.

Statistics

All data were expressed as mean ± standard deviation (M±SD). Comparison between measurements by three-dimensional ultrasound and angiography, before and after surgery and intra- and inter-observer variability were examined using linear regression, paired student *t* test and Bland-Altman analysis. A p value of less than 0.05 was defined as statistically significant.

Results

Carotid Endarterectomy

Endarterectomy was successful in all 13 patients who underwent this procedure. Among the 12 patients who had three-dimensional ultrasound both before and after surgery, 3 required intraoperative shunt, 3 had polytetrafluorethylene patches upon closure of the arterial incision. 2 patients suffered from post-operative bleeding that required re-operation within 24 hours after surgery. There were no other major peri-operative event.

Carotid artery angiography

In all 14 patients, 26 significant stenoses (51-100%, 82±17%) were found in 19 of 28 examined vessels by carotid artery angiography. Eight of these stenoses were located in internal, 8 in external, 1 in common carotid artery and 9 at the bifurcation extending from

common to internal carotid artery. Of these stenoses, 21 were severe (≥70%).

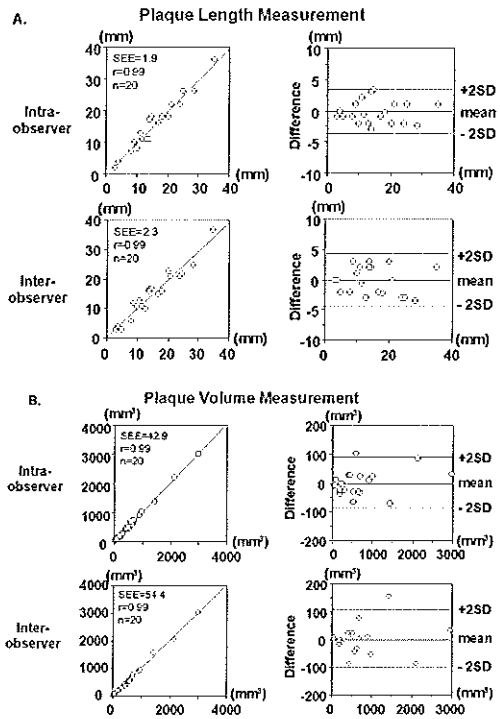

Figure 4. A. Comparison between intra-observer (top) and inter-observer (bottom) measurements of the lengths of 20 randomly selected plaques. **B.** Comparison between intra-observer (top) and inter-observer (bottom) volume measurements of 20 randomly selected plaques.

Three-dimensional ultrasound of carotid artery

Three-dimensional ultrasound was successful in all 14 patients in baseline studies and 12 patients in post-operative studies. It took less than 2 seconds for acquisition of each three-dimensional data set.

Carotid Stenosis. All the significant stenoses diagnosed from angiography were recognized from three-dimensional ultrasound except one in external carotid artery due to sub-optimal image quality. The severity of stenosis measured from three-dimensional ultrasound ranged from 45 to 100% (74±19%) using the diameter method and 40 to 100% (83±18%) using the area method. The correlation between the percentage of stenosis measured from angiogram and that measured from three-dimensional ultrasound using the area method (SEE=10.5%, r=0.82, mean difference=1.8±10.5%) was better than that using the diameter method (SEE=12.4%, r=0.76, mean difference =-7.0±12.3%) (Figure 3). The sensitivity, specificity, positive predictive value and negative predictive value of three-dimensional ultrasound in defining severe carotid stenosis were 65%, 100%, 100% and 65% using the diameter method and 90%, 92%, 95% and 86% using the area method.

Plaques. From three-dimensional ultrasound data sets of the carotid artery, the length and volume of 20 randomly selected plaques were measured. They ranged from 3 to 35 mm (15±8 mm) in length and 45 to 2980 mm^3 (703±734 mm^3) in volume. There was excellent correlation for both intra- and inter- observer measurements (Figures 4A and 4B).

Surgical impact. At the most stenotic site, the cross-sectional area of the carotid artery free lumen changed from 6.4±6.3mm^2 before endarterectomy to 50.6±18.8 mm^2 afterwards. The segmental vessel volume and the average cross-sectional area of the operated artery (2cm long including the bifurcation) changed in average from 2227 mm^3 (874 to 3240 mm^3) and 111 mm^2 (44 to 162 mm^2) before surgery to 2318 mm^3 (1648 to 3368 mm^3) and 115 mm^2 (82 to 168 mm^2) after surgery with a slight but non-significant increase (Figure 5). By dividing the patients into a group with

patches applied during surgery and a group without patch, a significant increase was observed in the segmental volume in the former group. In the later group of patients without patch, the segmental volume had no significant change, although the average value slightly decreased (Figure 6).

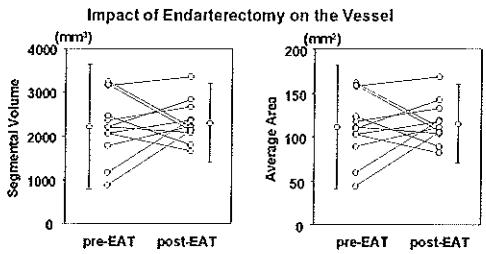

Figure 5. Graphs showing changes in segmental vessel volume (left) and average cross-sectional area (right) of the carotid artery before endarterectomy (pre-EAT) and after (post-EAT). Since the lengths of all the measured segments were the same (2cm), the changes in segmental volume and in cross-sectional area are proportional.

Additional information. Besides the quantitative information of the carotid artery and stenotic lesions, we were able to obtain some incremental information of the carotid artery, plaques and surrounding structures from three-dimensional ultrasound. Not only the longitudinal, but also the circumferential extent of the plaque was well appreciated at various levels. The eccentricity of the plaque distribution and the cross-sectional area and shape of the free vessel lumen were better portrayed throughout the segment of the carotid artery that was within the three-dimensional data set (Figure 7). Presence or absence of calcification in the plaque or the vessel wall could be predicted from the intensity of the ultrasound signal in comparison with surrounding tissues with the calcified plaque or vessel wall appeared brighter and usually caused shadows or ultrasound attenuation.

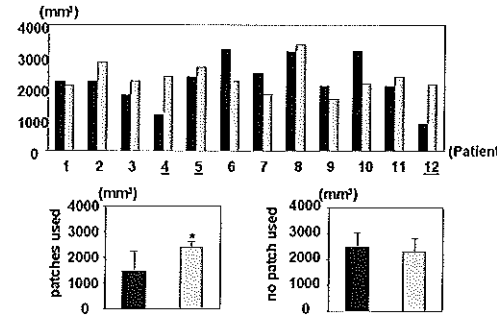

Figure 6. Plots showing changes of segmental vessel volume at baseline (black bars) and post-operative (gray bars) in each individual patient (top) and in the groups of patients with (bottom left) and without (bottom right) polytetrafluorethylene patches during endarterectomy upon closure of the artery. Patient 4, 5 and 12 was applied with patches (underlined). The post-operative segmental vessel volume in the group of patients with patches had significant increase compared with baseline measurement (*).

Discussion

Imaging techniques for the carotid artery

Among the techniques that have been used for evaluation of carotid artery stenosis, angiography is the most widely used and accepted one for selection of candidates for carotid endarterectomy, as it was in the American Symptomatic Carotid Endarterectomy Trial (NASCET) and the European Carotid Surgery Trial (ECST).[1-6] However, carotid angiography is an invasive procedure which has non-negligible complications and peri-procedure risk, especially in patients with severe stenosis.[7-8, 30-31] Besides, the technique provides solely free lumen projections ignoring details of the plaques, the vessel wall and the surrounding tissues and structures. Therefore, the assessment of the percentage of carotid artery

narrowing at the stenotic site requires either extrapolation of the original diameter of the vessel lumen at the same site (ECST) or measurement of vessel diameter at a reference site such as the segment of the vessel distal to the stenosis (NASCET) or the common carotid artery.[1-6, 32] Two-dimensional ultrasound is able to overcome some of the drawbacks of carotid angiography and has proven reliable in some studies in evaluating carotid artery stenosis, especially when combined with Doppler imaging.[11-16] However, its feasibility and accuracy has been challenged by the physical inaccessibility of some cutting planes which, in some circumstances, might be the optimal ones. Besides, two-dimensional ultrasound is technically operator dependent to acquire all the useful information on-line. Magnetic resonance angiography and computed tomographic angiography of the carotid artery have been investigated as well.[17-22] Both techniques are not available at bedside and are expensive. The later also requires contrast injection. Therefore, they are limited in routine application. Experience with intravascular ultrasound in carotid artery imaging is very preliminary.[33] Although it may provide information of the arterial wall and stenotic lesions on cross-sectional views, it gives less information on the longitudinal extension of the lesions. Besides its invasiveness and expensive cost, intravascular ultrasound is limited in use in severe carotid stenosis.

Three-dimensional ultrasound of the carotid artery

Three-dimensional surface ultrasound is realized by sequential collection of two-dimensional images of the carotid artery to produce a volumetric digital data set. There are several advantages of this technique. First, it is noninvasive and can be performed in various clinical settings. Second, it may minimize the discomfort for the patient caused by a routine two-dimensional ultrasound study by reducing the examination time and probe manipulation. A three-dimensional data set of the carotid artery can be collected within 2 seconds with the probe hold in a fixed position. Close examination of the carotid artery can be achieved off-line and images of the carotid artery can be reconstructed in unrestricted directions from the three-dimensional data set. Third, it provides volumetric information of not only the free lumen of the carotid artery, but also the plaques, the vessel wall and the adjacent tissue and structures such as the jugular vein. Information of the shape and distribution of plaques and the degree of calcification may be helpful in clinical management of the patients such as selection of appropriate interventional methods. And last, three-dimensional ultrasound permits volume quantification of either a plaque or a segment of free lumen or original vessel lumen. The reproducibility of plaque length and volume measurements was excellent in this study both from the same observer and from different observers. This may have important clinical implications in serial follow-up studies. For example, it may provide a reliable method for observation of the progression or regression of a plaque and/or changes in the severity of stenosis in a segment of the carotid artery. It may also provide a reliable method in follow-up studies after interventional procedures such as carotid endarterectomy or endoluminal stenting to observe the local vessel change, plaque reformation or stent dysfunction such as inadequate expansion or recoil.

Changes of the segmental vessel volume and, therefore, the average cross-sectional area

of the original carotid artery (ignoring the plagues) increased after endarterectomy in patients with patches used upon closing of the

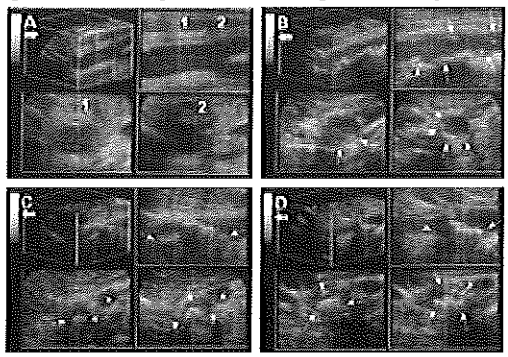

Figure 7. Images reconstructed from three-dimensional ultrasound of the carotid arteries in different patients labeled A, B, C and D. The thick arrow in each panel under the capital letter indicates the direction of carotid artery from proximal to distal. Four images are shown in each panel as they appear on the screen of the three-dimensional ultrasound unit. The upper left image shows the orientation of the volumetric data set in a cube. A cross-sectional cutting plane of the carotid artery can be reconstructed guided by a spatial coordinate system (upper right image). At the same time, two other cutting planes perpendicular to the first are displayed automatically and their positions are indicated by two vertical lines (1 and 2). Panel A shows three-dimensional reconstruction of a carotid artery after endarterectomy. Panels B, C and D are examples of multiple plaques with different shapes and distribution (thin arrows). While the longitudinal extent of the plaques are shown in the upper right images, the lower images display their circumferential involvement of the vessel and the cross-sectional view of the free carotid lumen as well as the shape of the plaques.

artery as can be expected. In patients without application of patches, changes in segmental vessel volumes after surgery were less significant and varied from decrement to increment. This is an interesting observation, although the answer to it is not clear. We believe that the change in segmental vessel volume of the carotid artery after surgery is multi-factor dependent. On the one hand, the suture might decrease the size of the vessel, resulting in decrease of segmental vessel volume and cross-sectional area. On the other hand, removal of the intima-media complex and the plaque, especially those calcified ones, might increase the distensibility and decrease the recoil force of the involved segment of the vessel, resulting in increase of both segmental volume and cross-sectional area. Better understanding of the impact of endarterectomy upon the carotid artery requires further investigation with bigger number of patients.

Limitations of this study

There were several limitations of this study. First, carotid angiography was used as the reference method for quantitation of carotid stenosis. However, it has its own potential limitations in the accuracy of estimating a three-dimensional stenotic lesion by using a two-dimensional projection of the lumen silhouette and by presuming the original lumen size of the vessel at the diseased site. Therefore, although in this study the severity of carotid stenosis measured by three-dimensional ultrasound using the area method correlated better with the results from carotid angiography than using the diameter method, care must taken in interpretation of the results. Second, some problems of the two-dimensional ultrasound could not be overcome by three-dimensional reconstruction. For instance, image quality of two-dimensional ultrasound could not be improved by three-dimensional reconstruction. On the contrary, interpolation of the spaces between the original two-dimensional images further decreases the image resolution. Ultrasound artifacts in two-dimensional images will remain in the three-dimensional data set which also affect the re-

constructed images. Finally, the number of patients examined in this study was small. However, the number of vessels we studied was considerable. Further studies in a larger population woth a wider range of carotid abnormalities is necessary to validate the results from this study.

Conclusions

Three-dimensional ultrasound of the carotid arteries can be used to detect and quantify significant and severe carotid stenosis. Its potential in volumetric measurements indicates important clinical implications. Quantification of plaque and vessel volume allows serial follow-up studies of the progression or regression of stenotic lesions and evaluation of interventional procedures.

1. European Carotid Surgery Trialists' Collaborative Group. MRC European Carotid Surgery Trial : interim results for symptomatic patients with severe (70-99%) or with mild (0-29%) carotid stenosis. *Lancet* 1991;337:1235-1243.
2. Eliasziw M, Smith RF, Singh N, Holdsworth DW, Fox AJ, Barnet HJM, for the North American Symptomatic Carotid Endarterectomy Trial (NASCET) Group. Further comments on the measurement of carotid stenosis from angiograms. *Stroke* 1994;25:2445-2449.
3. Rothwell PM, Gibson RJ, Slattery J, Sellar RJ, Warlow CP. Equivalence of measurements of carotid stenosis. A comparison of three methods on 1001 angiograms. European Carotid Surgery Trialists' Collaborative Group. *Stroke* 1994;25:2435-2439.
4. Rothwell PM, Gibson RJ, Slattery J, Warlow CP. Prognostic value and reproducibility of measurements of carotid stenosis. A comparison of three methods on 1001 angiograms. European Carotid Surgery Trialists' Collaborative Group. *Stroke* 1994;25:2440-2444.
5. Streifler JY, Eliasziw M, Fox AJ, Benavente OR, Hachinski VC, Ferguson GG, Barnett HJ, for the North American Symptomatic Carotid Endarterectomy Trial. Angiographic detection of carotid plaque ulceration. Comparison with surgical observations in a multicenter study. *Stroke* 1994;25:1130-1132.
6. Gagne PJ, Matchett J, MacFarland D, Hauer-Jensen M, Barone GW, Eidt JF, Barnes RW. Can the NASCET technique for measuring carotid stenosis be reliably applied outside the trial? *J Vasc Surg* 1996;24:449-455.
7. Zhu CZ, Norris JW. Complications of carotid angiography. *J Neurol Neurosurg Psychiatry* 1991;54:758-759.
8. Gerraty RP, Bowser DN, Infeld B, Mitchell PJ, Davis SM. Microemboli during carotid angiography. Association with stroke risk factors or subsequent magnetic resonance imaging changes? *Stroke* 1996;27:1543-547.
9. MacFarland HR, Pinkerton JA Jr. Comparison of non-invasive carotid tests with angiography in assessing carotid stenosis. *Mo Med* 1987;84:653-655.
10. Mittl RL Jr, Broderick M, Carpenter JP, Goldberg HI, Listerud J, Mishkin MM, Berkowitz HD, Atlas SW. Blinded-reader comparison of magnetic resonance angiography and duplex ultrasonography for carotid artery bifurcation stenosis. *Stroke* 1994;25:4-10.
11. Boyle MJ, Wolinski AP, Grimley RP. Accuracy of duplex versus angiography in patients undergoing carotid surgery. *J R Soc Med* 1995;88:20-23.
12. Hansen F, Bergqvist D, Lindblad B, Lindh M, Matzsch T, Lanne T. Accuracy of duplex sonography before carotid endarterectomy - a comparison with angiography. *Eur J Vasc Endovasc Surg* 1996;12:331-336.
13. Prestigiacomo CJ, Connoly ES Jr, Quest DO. Use of carotid ultrasound as a preoperative assessment of extracranial carotid artery blood flow and vascular anatomy. *Nerosurg Clin N Am* 1996;7:577-587.
14. Cartier R, Cartier P, Fontaine A. Carotid endarterectomy without angiography. The reliability of Doppler ultrasonography and duplex scanning in preoperative assessment. *Can J Surg* 1993;36:411-416.
15. Dawson DL, Zierler RE, Strandness DE Jr, Clowes AW, Kohler TR. The role of duplex scanning and arteriography before carotid endarterectomy: a prospective study. *J Vasc Surg* 1993;18:673-680.
16. McKittrick JE, Cisek PL, Pojunas KW, Blum GM, Ortgiesen P, Lim RA. Are both color-flow duplex scanning and cerebral arteriography required prior to carotid endarterectomy? *Ann Vasc Surg* 1993;7:311-316.
17. Rubinstein D. MR imaging and the evaluation of extracranial carotid stenosis. *Am J Roentgenol* 1994;163:1213-1214.

18. De Marco JK, Nesbit GM, Wesbey GE, Richardson D. Prospective evaluation of extracranial carotid stenosis: MR angiography with maximum-intensity projections and multiplanar reformation compared with conventional angiography. *Am J Roentgenol* 1994;163:1205-1212.
19. Furuya Y, Isoda H, Hasegawa S, Takahashi M, Kaneko M, Uemura K. Magnetic resonance angiography of extracranial carotid and vertebral arteries, including their origins: comparison with digital subtraction angiography. *Neuroradiology* 1992;35:42-45.
20. Dillon EH, van Leeuwen MS, Arancha Fernandez M, Eikelboom BC, Mali WT. Computed tomographic angiography for carotid imaging [letter]. *Lancet* 1992;340:1286.
21. Dillon EH, van Leeuwen MS, Arancha Fernandez M, Mali WT, Eikelboom BC. Carotid artery imaging with computed tomography angiography [letter]. *J Vasc Surg* 1993;17:624-625.
22. Goldenberg M. Computed tomographic evaluation of cervical carotid plaque complications [letter]. Stroke 1986;17:779.
23. Pretorius DH, Nelson TR, Jaffe JS. 3-dimensional sonographic analysis based on color flow Doppler and gray scale image data: a preliminary report. *J Ultrasound Med* 1992;11:225-232.
24. Rosenfield K, Boffetti P, Kaufman J, Weinstein R, Razvi S, Isner JM. Three-dimensional reconstruction of human carotid arteries from images obtained during noninvasive B-mode ultrasound examination. *Am J Cardiol* 1992;70:379-384.
25. Tarjan Z, Pozzi Mucelli F, Frezza F, Pozzi Mucelli R. Three-dimensional reconstruction of carotid bifurcation from CT images: evaluation of different rendering methods. *Eur Radiol* 1996;6:326-333.
26. Wilkerson DK, Keller I, Mezrich R, Schroder WB, Sebok D, Gronlund-Jacobs J, Conway R, Zatina MA. The comparative evaluation of three-dimensional magnetic resonance for carotid artery disease. *J Vasc Surg* 1991;14:803-809.
27. van Alphen HA, Polman CH. Carotid endarterectomy: how does it work? A clinical and angiographic evaluation. *Stroke* 1986;17:1251-1253.
28. Thompson JE, Talkington CM. Carotid endarterectomy. *Adv Surg* 1993;26:99-131.
29. Steiger HJ. Carotid endarterectomy - when to do it, how to do it? *Acta Neurochir (Wien)* 1995;137:121-127.
30. Hankey GJ, Warlow CP, Sellar RJ. Cerebral angiographic risk in patients with mild cerebrovascular disease. *Stroke* 1990;21:209-222.
31. Davies KN, Humphrey PR. Complications of cerebral angiography in patients with symptomatic carotid territory ischaemia screened by carotid ultrasound. *J Neurol Neurosurg Psychiatry* 1993;56:967-972.
32. Williams MA, Nicoliades AN. Predicting the normal dimensions of the internal and external carotid arteries from the diameter of the common carotid. *Eur J Vasc Surg* 1987;1:91-96
33. Karnik R, Ammerer HP, Winkler WB, Valentin A, Slany J. Initial experience with intravascular ultrasound imaging during carotid endarterectomy. *Stroke* 1994;25:35-39.

CHAPTER 9

EVALUATION OF CARDIOVASCULAR MASS LESIONS BY THREE-DIMENSIONAL ECHOCARDIOGRAPHY

Jiefen Yao, MD; Anita Dall'Agata, MD; Jaroslaw D. Kasprzak, MD; Lissa Sugeng, MD; Natesa G. Pandian, MD; Jos R.T.C. Roelandt, MD, PhD

Submitted

Evaluation of Cardiovascular Mass Lesions by Three-Dimensional Echocardiography

Jiefen Yao, MD; Anita Dall'Agata, MD; Jaroslaw D. Kasprzak, MD; Lissa Sugeng, MD; Natesa G. Pandian, MD; Jos R.T.C. Roelandt, MD, PhD

Two-dimensional echocardiography (2DE) has been the most commonly used tool in diagnosis and evaluation of abnormal mass lesions. We sought to examine whether three-dimensional echocardiography (3DE) could provide incremental information for clinical evaluation of these masses and could quantify their volumes reliably. Both 2DE and 3DE were performed in 37 patients with 48 various kinds of masses including tumors, thrombi, atheromas, vegetations, parasitic cysts and abscesses. From 3DE, dynamic cross-sectional views and three-dimensional images were reconstructed, the site, size, shape and number of masses and other concomitant cardiac abnormalities were analyzed. These were compared with information obtained from 2DE. Reproducibility of 3DE volume measurement were examined in 20 randomly selected masses. Excellent correlation and small limits of agreement were observed between intra-observer (r=0.99, SEE=2.1 ml, difference=0.9±2.4 ml) and inter-observer (r=0.99, SEE=2.7 ml, difference=0.4±2.7 ml) measurements. 3DE aided in better delineation of the masses in 24/37 (65%) of the cases. In conclusion, 3DE provided incremental information to 2DE approach for both qualitative and quantitative evaluation of mass lesions.

Key words: echocardiography, three-dimensional echocardiography, cardiac mass lesions

Abnormal mass lesions such as tumors, vegetations or thrombi may reside either within or adjacent to the cardiovascular structures.[1-6] Accurate evaluation of the size, attachment, and mobility of the masses and their anatomical relationship with the cardiac structures may be helpful for clinical diagnosis and management.[7-11] Among all cardiac imaging techniques, two-dimensional echocardiography (2DE) has been the most widely used method for this purpose. However, limitations for a comprehensive study of the masses with 2DE exist when a mass lesion has remote attachment, small in size, complex in shape, or highly mobile. Three-dimensional echocardiography (3DE), by obtaining a volumetric data set of the heart, is able to produce arbitrary cross-sectional views and dynamic three-dimensional (3D) images of any projections. Different from 2DE technique, which only produces images of an object when cutting through it, 3DE enables the observer to look at an object from a distance (*en face* views).[12-17] The aim of this study was to examine the qualitative and quantitative potential and incremental value of 3DE in comprehensive assessment of various cardiovascular mass lesions.

METHODS

Patient population

3DE was performed in 37 patients (21 males, 16 females, age 51±18 years, range: 24-82 years) diagnosed with cardiovascular mass lesions (including tumors, vegetations, thrombi, parasitic cysts and abscesses) by 2DE. 22 cases were studied with transesophageal and 15 with transthoracic approach. A variety of other cardiac abnormalities, either related or unrelated with the masses, were also examined. They include valvular diseases (stenosis, insufficiency, prolapse or perforation), ischemic heart disease or cardiomyopathy (regional or global myocardial wall motion abnormalities or aneurysm), aortic diseases (dissection, dilatation or aneurysm) and pericardial effusion. Surgery was performed in 23 cases. Pathology of the masses that were surgically removed was studied. The other masses were treated medically or closely observed. One patient was in atrial fibrillation, one had an artificial pacemaker and all other patients were in sinus rhythm.

Data acquisition

2DE examination (either transthoracic or transesophageal) was carried out in standard manners. Multiple imaging planes, including off-axis views, were used to delineate the mass lesions and their relationship with cardiac structures. Images were recorded onto ½ VHS videotapes for archiving and off-line analysis.

3DE data acquisition was performed within 24 hours of 2DE examination. A dedicated 3DE processing computer (TomTec, EchoScan 3.0, TomTec Imaging System GmbH, Munich, Germany) was connected to the ultrasound unit for image collection. Image processing, reconstruction and data analysis were performed off-line using the same computer. The imaging window for 3DE data acquisition was optimized in each patient to get maximal amount of information of the mass lesions. Using a motor device attached to the ultrasound probe, the imaging plane was steered in a rotational manner. Images were collected sequentially from 0 through 180°, at 2° or 3° intervals, gated to ECG and respiration. They were then calibrated and stored in the computer for later off-line analysis. The acquired images were registered automatically according to their spatial and temporal relationships. Spaces between the images were filled by the computer using a cylindrical interpolating algorithm. Thus, the processed 3D data set contains voxel-based information, from which secondary cross-sectional views and dynamic 3D images can be reconstructed.

Data analysis

Both 2DE and 3DE studies were analyzed by two cardiologists, experienced in both techniques, to obtain a consensus in defining the location, attachment, morphology (size and shape) and number of mass lesions in each case. Other cardiac abnormalities were evaluated as well. While doing so, they also decided whether 3DE provided any incremental information for better understanding and evaluating the location, attachment and number of masses and other cardiovascular abnormalities in each case. To test the accuracy and reproducibility of volume measurement in mass lesions, 20 masses of various sizes, textures and locations were selected and their volumes quantified by two independent observers. One of them repeated the measurements two weeks later.

Qualitative 3DE. One way of reviewing the 3D data was to reconstruct "anyplane" cross-sectional images from the volumetric data set.[12] A combination of several methods was used to improve the flexibility and comprehensiveness in data analysis. They include anyplane, paraplane, long-axis and short-axis methods. With anyplane method, a cutting plane was steered in unlimited directions guided by 3 perpendicular axis of the Cartesian coordinate system, similar to the flight navigating system, to create arbitrary cross-sectional views. With paraplane method, a group of cutting planes loafing the data set into a number of equidistant slices were created parallel to a selected image. By defining any two points in the data set, an artificial axis was generated and images around (long-axis method) or perpendicular (short-axis method) to this axis were delivered in equal intervals. Another way of reviewing the 3D data was to reconstruct dynamic volume-rendered 3D images, using the above mentioned methods in selecting appropriate cutting planes from the volumetric data set. The mass lesions and their correlation with other cardiac structures were displayed in multiple projections.

Comparing the information provided by 3DE with that by 2DE, the observers were to gauge whether incremental information of the mass lesions could be obtained. Care was taken in the following findings: 1) site and extension of mass attachment; 2) size and

shape of mass lesions; 3) number of masses and; 4) other cardiac abnormalities.

Quantitative 3DE. A group of 20 masses (including 5 vegetations, 6 tumors, 6 thrombi, 2 cysts and 1 abscess) were randomly selected for volume measurement. The volume of each mass was measured from 3D data set using modified Simpson's rule or "summation of discs" method. The object to be measured was electronically sectioned into multiple equi-distant slices (6 to 12 slices) using paraplane or short-axis method. The slice thickness (0.5 to 10 mm) was determined according to the size and regularity of the mass lesion in each case. The mass was manually traced on each cross-sectional view and its total volume on all slices was summed up automatically by the computer.

Statistics

Volumes of the masses were expressed as mean ± standard deviation (M±SD). Reproducibility between intra- and inter-observer volume measurements was examined by linear regression, paired student t test and Bland-Altman analysis. A p value < 0.05 was defined statistically significant.

RESULTS

From 3DE data of all 37 patients, 48 masses were observed. They include 16 tumors (4 myxomas, 6 rhabdomyosarcomas, and 6 metastatic tumors), 8 thrombi, 3 atheromas, 18 vegetations, 2 hydatid echinococcal cysts and 1 intra-myocardial abscess. The masses were located in various sites of the cardiovascular system including all cardiac chambers and valves, pericardial cavity, myocardium and aorta (Table). Of these masses, all except two small vegetations were also defined from 2DE.

Table. Details of the masses.

Location of masses	No. of masses	No. of Patients	Category of masses				
			tumor	vegetation	thrombi	cyst	abscess
Left ventricle	6	5	3	1	1	-	-
Right ventricle	6	5	2	3	-	1	-
Left atrium	7	7	3	-	4	-	-
Right atrium	3	3	3	-	-	-	-
Aortic valve	8	5	-	8	-	-	-
Pulmonary valve	1	1	-	1	-	-	-
Mitral valve	6	4	0	6	1	-	-
Tricuspid valve	2	1	2	-	-	-	-
Pericardial cavity	3	2	3	-	-	1	-
Intra-myocardium	1	1	-	-	-	-	1
Aorta	5	5	-	-	5	-	-
Subtotal	48	37	16	19	11	2	1

Comparison between 2DE and 3DE

In comparison to 2DE, 3DE provided incremental information for better evaluation of the masses in 24 of 37 (65%) cases in either the site of attachment (14%), extent of attachment (22%), size of the masses (41%), shape of the masses (49%) or number of masses (9%). In 59% of cases, 3DE was able to provide additional information useful for assessment of other cardiovascular abnormalities other than the masses. These abnormalities include valvular diseases (stenosis, prolapse, flail or perforation) regional wall motion abnormalities in aneurysmal left ventricle, congenital anomalies such as bicuspid aortic valve and double outlet right

ventricle, diseases of aorta (aneurysm, dilatation and dissection), pericardial effusion and pacemaker lead dislocation.

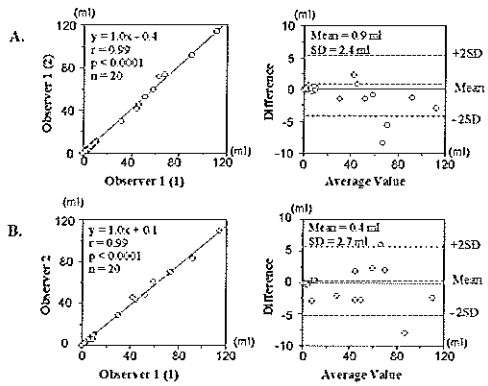

Figure 1. Graphs showing intra- and inter-observer variability in 3DE volume measurement of mass lesions. A. Comparison of intra-observer measurements by linear regression (left) and Bland-Altman analysis (right). B. Comparison of inter-observer measurements by linear regression (left) and Bland-Altman analysis (right).

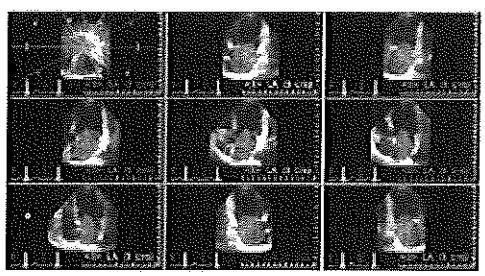

Figure 2. Multiple cross-sectional images of a left atrial myxoma reconstructed from 3DE data using long-axis method. Its size, location and relationship with the left atrium are well depicted.

Volume quantitation from 3DE

Volumes of the 20 masses measured from 3DE ranged from 0.1 ml to 111 ml (31±34 ml). Excellent correlation and small limits of agreement were observed between intra-observer (r=0.99, SEE=2.1ml; difference=0.9±2.4ml) and inter-observer (r=0.99, SEE=2.7; differnece=0.4±2.7) measurements (Fig. 1A and 1B).

Representative cases

Figure 2 demonstrates multiple cross-sectional views of a left atrial myxoma reconstructed from 3DE data set using long-axis method. Not only the size and shape of the tumor, but also the size of the left atrium and free spaces around the tumor are well appreciated in multiple longitudinal views. When displayed dynamically in multiple images simultaneously, its mobility and extent of movement were better delineated. In another patient with left atrial myxoma, 3D volume-rendered images crisply portrayed the site of the pedicle attached to the atrial septum (figure 3).

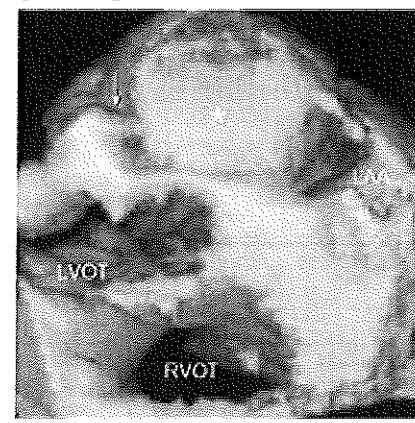

Figure 3. Volume-rendered 3DE image of a left atrial myxoma (*) obtained by transesophageal imaging. Its size, shape and the pedicle (arrow) are crisply displayed. LVOT = left ventricular outflow tract; RVOT = right ventricular outflow tract; LAA = left atrial appendage.

Figure 4 shows 3D images from a patient with aortic valve vegetations. It was difficult to decide the exact number of vegetations from 2DE due to their mobility and small sizes. Using 3D reconstruction, the vegetations on either side of the valve could be appreciated from a distance without cutting through them, which was not possible from 2D approach. In addition, two small perfo-

rations were also observed on a 3D *en face* view. They were missed by 2DE examination, even though aortic regurgitation was diagnosed from color Doppler imaging. The perforations were later validated by surgery and the aortic valve was replaced with a prosthesis.

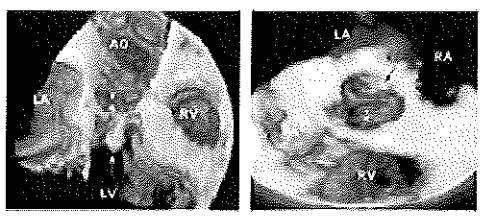

Figure 4. 3D images from a patient with aortic valve endocarditis. The left image was reconstructed in a longitudinal view of the ascending aorta. Two vegetations (big arrows) were clearly located on the right and non-coronary cusps. The smaller one was missed by 2DE examination. The right image was reconstructed in an *en face* view of the aortic valve from above. Not only the vegetation (big arrow) on the non-coronary cusp, but also two adjacent perforations (small arrows) were demonstrated. AO = aorta; LA = left atrium; RV = right ventricle; LV = left ventricle; PA = pulmonary artery; RA = right atrium.

Thrombi or atheromas were observed in various locations in this study. Figure 5 demonstrates two examples. The mural thrombus in the left image is located in the dyskinetic apex and is relatively immobile. The thrombus in the right image arises from the ascending aorta and was highly mobile in a dynamic display.

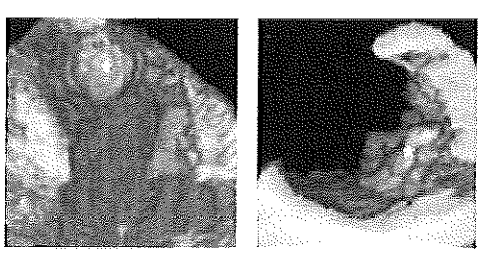

Figure 5. 3DE reconstruction of thrombi from two patients. The left image demonstrates a thrombus (*) lying in the dyskinetic apex of the left ventricle. The right image shows a thrombus (*) in the ascending aorta.

Parasitic cysts were observed in two patients in this study. In one patient, who had pleural effusion, 3DE data acquisition was performed using an unconventional acoustic window, a posterior intercostal space. The cyst was found next to the posterior wall of the left ventricle as shown in multiple parallel images in figure 6. Because of the irregular shape of the cyst, its volume could not be decided accurately by 2DE. Free from geometrical limitations, 3DE was able to provide its volume (91 ml), which closely resembled the volume measured during surgery (89 ml).

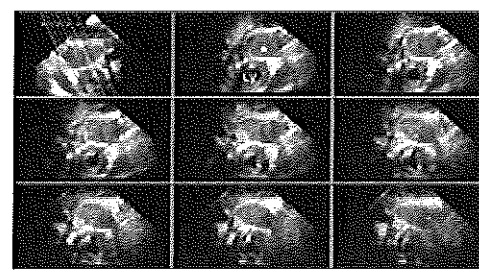

Figure 6. Parallel equi-distant images of a pericardial parasitic cyst (*) derived from a 3DE data set. The cyst was situated next to the posterior wall of the left ventricle (LV). The 3DE data was acquired from the posterior intercostal space of a patient with pleural effusion.

DISCUSSION

Abnormal masses have been sporadically reported in various locations of the cardiovascular system, mostly in case reports diagnosed by various imaging techniques. The patients may show various symptoms based on the location, size and invasiveness of the mass lesions and, accordingly, require different treatment. Cardiac tumors have been reported *in situ* or metastasized from other organs. They frequently involve the pericardium and the right heart[2, 5, 8]. Dislodging of vegetations may cause bacterial embolism elsewhere and lead to severe consequences[1, 6, 11]. Thrombi may occur in various cardiac chambers and is an important source of embolism. Aortic atheromas and thrombi, either

isolated or coexisting, are significantly associated with vascular events[3, 4, 18, 19]. Parasitic masses, though occur less frequently in the heart, may cause lethal allergic reactions upon rupture[20]. Therefore, once a mass lesion is suspected, prompt and accurate assessment of it is important for clinical management.

2DE and 3DE Imaging

Development in cardiac imaging techniques, particularly in echocardiography, has greatly facilitated the assessment of mass lesions in the cardiovascular system. Numerous reports on intracardiac and intravascular tumors, vegetations or thrombi have been documented using 2DE [1-11]. Although it can provide information on the location, attachment, dimensions and number of the masses in most cases, its ability for a comprehensive evaluation of the mass lesion is often restricted by using only a limited number cross-sectional views. It is more so with small and mobile masses (such as valvular vegetations) than with big and less mobile ones (such as mural thrombi and intramyocardial tumors). Small mobile masses are often viewed in and out of the cutting plane during the cardiac cycle with 2DE, making it difficult to determine the number, size or even a definite presence of a mass or masses. 3DE, on the other hand, contains volumetric information of the heart, from which unlimited cutting planes can be generated. Not only conventional but also unconventional views can be obtained that may help to easily locate the optimal cutting planes for studying the mass lesions. In addition, multiple cross-sectional images of the heart can be reconstructed from 3DE data set and viewed simultaneously. Dynamic display of volume-rendered 3D images from various projections allow the viewer to perceive realistic *in vivo* appearance and spatial relationship of the masses and cardiac structures noninvasively[12-17]. This study collected masses of various sizes, shapes and origins in the cardiovascular system. In the majority of cases, 3DE could provide incremental information to 2DE for better understanding and evaluating the mass lesions. Observation of the progression or involution of the mass lesions is important in clinical management. 3DE has proven to be able of accurate volume quantification without the need of any geometric assumptions[21, 22]. Our results also confirmed its excellent reproducibility in volumetric measurement of various mass lesions in vivo.

Limitations of this study

We need to point out a few limitations existed in this study. Although various kinds of mass lesions in the cardiovascular system were collected in this study, the number of masses is not sufficient for further subdivisions according to different categories such as histology, residing chambers and so on, for more detailed analysis. This study is in part a retrospective review of many previous examinations. Volume validation of the masses was not carried out in all surgical patients except a few. The accuracy of 3DE in measuring volumes of both regular and irregular shaped objects has been well proved before. Our understanding was that the reproducibility of volume measurement of the mass lesions was more important in clinical management.

Conclusion

3DE is able to deliver incremental information for better evaluation of the attachment, size, shape and spatial correlation of cardiovascular mass lesions and for better delineation of other cardiac abnormalities. Accurate and reproducible volume measurement of the masses may be useful for close observation of their clinical course. It may be regarded as an important adjuvant tool to 2D imaging when additional information is required.

1. Henderson RA, Palmer TJ. Echocardiographic diagnosis of infective endocarditis of all four cardiac valves. *Int J Cardiol* 1991;33:173-175
2. Vargas-Barron J, Romero-Cardenas A, Villegas M, Keirns C, Gomez-Jaume A, Delong R, Malo-Camacho R. Transthoracic and transesophageal echocardiographic diagnosis of myxomas in the four cardiac cavities. *Am Heart J* 1991;121:931-933
3. Chapoutot L, Nazeyrollas P, Metz D, et al. Floating right heart thrombi and pulmonary embolism: diagnosis, outcome and therapeutic management. *Cardiology* 1996;87:169-174
4. Dressler FA, Labovitz AJ. Systemic arterial emboli and cardiac masses. Assessment with transesophageal echocardiography. *Cardiol Clin* 1993;11:447-460
5. Tse HF, Lau CP, Lau YK, Lai CL. Transesophageal echocardiography in the detection of inferior vena cava and cardiac metastasis in hepatocellular carcinoma. *Clin Cardiol* 1996;19:211-213
6. Shapiro SM, Young E, Ginzton LE, Bayer AS. Pulmonary valve endocarditis as an underdiagnosed disease: role of transesophageal echocardiography. *J Am Soc Echocardiogr* 1992;5:48-51
7. Louie EK. Cardiovascular imaging: new applications, new insights, and new choices in the diagnosis and treatment of vascular embolism. *Am J Card Imaging* 1994;8:8-12
8. Singh I, Jacobs LE, Kotler MN, Ioli A. The utility of transesophageal echocardiography in the management of renal cell carcinoma with intracardiac extension. *J Am Soc Echocardiogr* 1995;8:245-250
9. Edwards LC 3rd, Louie EK. Transthoracic and transesophageal echocardiography for the evaluation of cardiac tumors, thrombi and valvular vegetations. *Am J Card Imaging* 1994;8:45-58
10. Cooke RA, Chambers JB. The role of echocardiography in the diagnosis and management of infective endocarditis. *Br J Clin Pract* 1992;46:111-115
11. Mugge A, Daniel WG, Frank G, Lichtlen PR. Echocardiography in infective endocarditis: reassessment of prognostic implications of vegetation size determined by the transthoracic and transesophageal approach. *J Am Coll Cardiol* 1989;14:631-638
12. Roelandt JRTC, Ten Cate FJ, Vletter WB, Taams MA. Ultrasonic dynamic three-dimensional visualization of the heart with a multiplane transesophageal imaging transducer. *J Am Soc Echocadiogr* 1994;7:217-229
13. Pandian NG, Cao QL, Vogel M, Ludomirski A, Schwartz SL. Clinical potential of three-dimensional echocardiography in endocarditis. *Echocardiography* 1995;12:631-635
14. Borges AC, Witt C, Bartel T, Muller S, Konertz W, Baumann G. Preoperative two- and three-dimensional transesophageal echocardiographic assessment of heart tumors. *Annals Thoracic Surgery* 1996;61:1163-1167
15. Kasprzak JD, Salustri A, Roelandt JR, Cornel JH. Comprehensive analysis of aortic valve vegetation with anyplane, paraplane, and three-dimensional echocardiography. [letter] *European Heart J* 1996;17:318-320
16. Kupferwasser I, Mohr-Kahaly S, Erbel R, et al. Three-dimensional imaging of cardiac mass lesions by transesophageal echocardiographic computed tomography. *J Am Soc Echocardiogr* 1994;7:561-570
17. Nanda NC, Abd-El Rahman SM, Khatri G, et al. Incremental value of three-dimensional echocardiography over transesophageal multiplane two-dimensional echocardiography in qualitative and quantitative assessment of cardiac masses and defects. *Echocardiography* 1995;12:619-628
18. Tunick PA, Rosenzweig BP, Katz ES, Freedberg RS, Perez JL, Kronzon I. High risk for vascular events in patients with protruding aortic atheromas: a prospective study. *J Am Coll Cardiol* 1994;23:1085-1090
19. Witteman JC, Kannel WB, Wolf PA, et al. Aortic calcified plaques and cardiovascular disease (the Framingham study). *Am J Cardiol* 1990;66:1060-1064
20. Dighiero J, Canabal EJ, Aguirre CV, Hazan J, Horjales JO. Echinococcus disease of the heart. *Circulation* 1958;17:127-132
21. Vogel M, Gutberlet M, Dittrich S, Hosten N, Lange PE. Comparison of transthoracic three dimensional echocardiography with magnetic resonance imaging in the assessment of right ventricular volume and mass. *Heart* 1997;78:127-130
22. Nosir YFM, Fioretti PM, Vletter WB, et al. Accurate measurement of left ventricular ejection fraction by three-dimensional echocardiography. A comparison with radionuclide angiography. *Circulation* 1996;94:460-466

CHAPTER 10

CLINICAL APPLICATION OF TRANSTHORACIC VOLUME-RENDERED THREE-DIMENSIONAL ECHOCARDIOGRAPHY IN THE ASSESSMENT OF MITRAL REGURGITATION

Jiefen Yao, MD; Navroz D. Masani, MBBS, Qi-Ling Cao, MD; Peter Nikuta, MD; Natesa G. Pandian, MD

Am J Cardiol **1998;82:189-196**

Clinical Application of Transthoracic Volume-Rendered Three-Dimensional Echocardiography in The Assessment of Mitral Valve Regurgitation

Jiefen Yao, MD; Navroz D. Masani, MBBS; Qi-Ling Cao, MD; Peter Nikuta, MD; Natesa G. Pandian, MD

Two-dimensional echocardiography (2DE) and Doppler methods are generally used for assessing mechanisms and severity of mitral regurgitation (MR). Recently, 3-dimensional echocardiography (3DE) has been applied successfully in various cardiac disorders, but its value in evaluating the mechanism and the severity of MR are not known. We studied 30 patients with MR using 2DE and 3DE. Volume-rendered gray-scale 3DE images of the mitral valve apparatus and MR jets were reconstructed. Maximal volume of the MR jet by 3DE was compared to mitral regurgitant volume and fraction, regurgitant jet area and the ratio of jet area to left atrial area and semiquantitative grading derived from 2DE methods. Our results demonstrated that 3DE aided in a better depiction of the mitral apparatus and its abnormalities in 70% of the patients. The origin, direction and morphology of MR jet were better delineated in 3DE volumetric display. Quantitative analysis, however, showed only weak to moderate correlation between 3DE maximal MR jet volume and 2DE mitral regurgitant volume (y=.5x+11.4, r=.7), regurgitant fraction (y=.5x+8.2, r=.65), mitral regurgitant jet area (y=.2x+5, r=.51), jet area to left atrial area ratio (y=.53x+7.6, r=.54), and semi-quantitative grading of MR (y=9.1x-1.8, r=.74). In conclusion, 3DE aids in a better understanding of the mechanisms of MR and morphology of the regurgitant jets. Its quantitative ability, when reconstruction of the jet alone is used, may be limited.

Key words: echocardiography, three-dimensional echocardiography, mitral valve regurgitation

Accurate estimation of the severity of mitral regurgitation (MR) by 2-dimensional echocardiography (2DE) is limited because of various factors.[1-8] The mitral valve apparatus, regurgitant jets and related cardiac chambers are all complex 3-dimensional structures. Discrepancy exists in 2DE methods for quantitative volume and function analysis by using geometric assumptions. Three-dimensional echocardiography (3DE) applied in various cardiac abnormalities, provides additional information to 2DE and accurate assessment of chamber volume and myocardial mass without geometric assumptions.[9-13] We have shown previously that it is also possible to reconstruct regurgitant jets in multi-dimensions from color Doppler flow imaging.[14] Whether 3DE can be used in a better understanding of the mechanisms and severity of MR is not known.

Methods

Patient Population

Thirty patients (age 26 to 85 years, mean±SD: 65±15 years) with MR were examined using both 2DE and 3DE. Underlying pathology included rheumatic valvular disease (7 cases), age-related fibrocalcific valvular disease (6 cases), mitral valve prolapse or billowing (6 cases), coronary artery disease (9 cases), dilated cardiomyopathy (1 case) and obstructive hypertrophic cardiomyopathy (1 case). Three patients had atrial fibrillation. All the rest were in sinus rhythm.

Two-dimensional echocardiography

Data acquisition. A commercially available ultrasound unit (SONOS 1500 or 2500, Hewlett-Packard, Andover, MA) was used for both 2DE and 3DE data acquisition. Routine procedures of 2DE study were performed in every patient to disclose all possible abnormalities. Parasternal long-axis and apical 4- and 2-chamber views

were imaged for measurement of the diameter of the left ventricular outflow tract and planimetry of left ventricular cavity. Pulsed wave Doppler was performed in apical views with the sample volume placed at mitral valve tip, in the left ventricular outflow tract and in pulmonary veins. Color Doppler was performed in apical views for planimetry of MR jet area. Electrocardiogram was monitored throughout the study. All 2DE images were recorded onto ½-inch VHS video tapes for off-line analysis.

Data analysis. A cardiologist unaware of the 3DE results reviewed the 2DE data. The possible mechanisms of MR considering the morphology and function of the mitral valve apparatus and left heart chambers were evaluated. Quantitative parameters of MR were obtained from an average of 3 consecutive heart beats in patients with sinus rhythm and 5 beats in those with atrial fibrillation.

The endocardium of left ventricle was traced (excluding the papillary muscles) in apical 4- and 2-chamber views to obtain end-diastolic and end-systolic volumes using biplane Simpson's method. Subtracting end-systolic from end-diastolic left ventricular volume derived the total left ventricular stroke volume (including both forward stroke volume and mitral regurgitant volume). The forward stroke volume was computed from the diameter of left ventricular outflow tract and the time-velocity integral of pulsed wave Doppler profile at that site. The total left ventricular stroke volume minus forward stroke volume yielded mitral regurgitant volume. Mitral regurgitant volume divided by the total left ventricular stroke volume resulted in mitral regurgitant fraction. MR color Doppler jet area was measured in apical 2- and 4-chamber views by manual tracing. Area of the left atrium was traced in the same views. The ratio of the MR jet area to left atrial area was calculated. The severity of MR was also analyzed semi-quantitatively by incorporating multiple parameters including cardiac chamber sizes, MR jet area, mitral inflow velocity, pulmonary venous flow pattern and the intensity of MR jet signals on spectral Doppler.[15-18] Grade 1 to 4 was assigned to MR of mild to severe degrees.

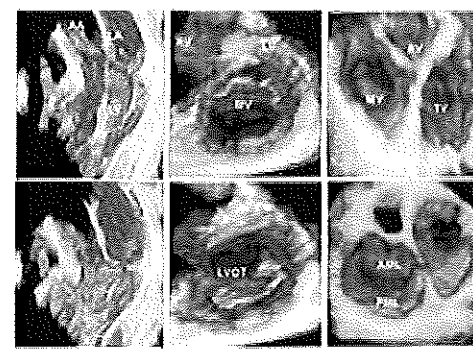

Figure 1. Representative images showing various 3DE projections of mitral valve in diastole (upper row) and in systole (lower row). Left images: longitudinal views allow observation of mitral valve and subvalvular apparatus as well as of cardiac chambers; middle images: Views from the left ventricle demonstrating the opening and coaptation of the mitral valve; and right: views from the left atrium showing the superior surface of the mitral leaflets as well as aortic and tricuspid valves. AA indicates ascending aorta; LA = left atrium; LV = left ventricle; RV = right ventricle; MV = mitral valve; LVOT = left ventricular outflow tract; AV = aortic valve; TV = tricuspid valve; AML = anterior mitral leaflet; PML = posterior mitral leaflet.

Three-dimensional echocardiography

Data acquisition and processing. 3DE was performed on the same day following the 2DE examination. A dedicated 3DE processing computer (EchoScan 3.0, TomTec Imaging Systems GmbH, Munich, Germany) was connected with the ultrasound unit for data acquisition. 2DE color Doppler images of the MR jet were collected via rotational transthoracic imaging at the apical window and 2DE images of the mi-

tral apparatus at apical or parasternal window. A computer controlled motoring device was attached to the probe to steer the imaging plane through 180° at 3° intervals. Images of one cardiac cycle were collected at each step gated to electrocardiogram and respiration. The gates were set to those heart beats in expiratory phase with regular R-R intervals on electrocardiogram in patients with sinus rhythm and the average R-R intervals without exceeding 200 ms in patients with atrial fibrillation. Images that failed to fit into the gates were rejected from the data set. After appropriate processing employing various algorithms including image realignment, space interpolation and digital transformation, a gray-scale volume-rendered 3DE data set was formed.

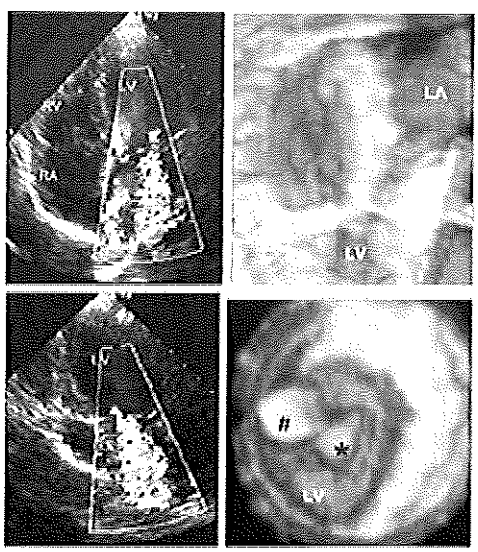

Figure 2 Selected 2DE color Doppler (left) and 3DE (right) images of MR jet. The right upper image shows the MR jet in a longitudinal view. The *en face* view of the proximal flow convergence region viewed from the left ventricle is shown in the lower right picture. RA indicates right atrium; * = flow convergence; # = LVOT flow; The rest of the abbreviations are same as in figure 1.

Reconstruction and display of 3DE images. Applying optimal gray-scale threshold and shading techniques, dynamic volume-rendered 3DE images of the mitral valve apparatus, cardiac chambers and intracardiac blood flows were reconstructed and displayed in various projections. For example, both *en face* and longitudinal views of the mitral valve and different views of the subvalvular apparatus were reconstructed and viewed to define structural and functional abnormalities [Fig. 1]. MR jet was reconstructed in various projections to demonstrate its origin, direction and spatial distribution. In addition, its proximal flow convergence region was also reconstructed in longitudinal as well as in *en face* views from the left ventricle [Fig. 2].

Quantitation of MR jet volume. The volume of the reconstructed color Doppler MR jet was measured from the 3DE data set using "summation of discs" method. With frame-by-frame review of the reference image, 1 frame with the maximal size of MR jet was chosen for volume measurement. After a "axis" of the jet was defined arbitrarily, multiple parallel equidistant (3-mm) "short-axis" images of the jet were derived automatically. The border of the regugitant jet was manually traced on each magnified image. The area of the traced region and the volume of that region on each slice were automatically calculated by the computer. Summation of volumes of all slices yields MR jet volume. The jet was extracted using a labeling system and was reconstructed alone, free from visual obstruction by other cardiac structures [Fig. 3].

Statistic analysis

All data were expressed as mean ± standard deviation. Simple linear regression method, Student *t* test and Bland-Altman analysis were employed to compare MR jet volume from 3DE with other measurements from 2DE. A p value smaller than 0.05 was

considered statistically significant. Inter- and intra-observer variability for 3DE MR jet volume measurement was expressed as mean difference and degree of variance.

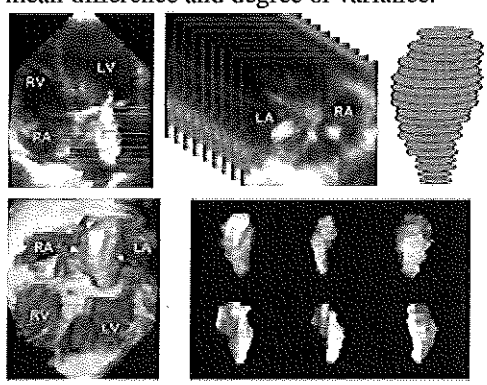

Figure 3. Schematic images demonstrating 3DE method for displaying MR jet and for measuring MR jet volume. On the upper left is a reference image of MR in a four-chamber format used to derive multiple parallel short-axis cross-sectional views of the MR jet. The boundaries of the MR jet on these views are traced manually (upper middle images). The upper right schematic drawing resembles the computation algorithm of the MR jet volume calculated automatically by the computer, i.e. Jet volume = ∑Area • Slice thickness. The lower left 3DE image images portrays the MR jet (arrows) as well as the cardiac chambers. Multiple 3DE images of the extracted MR jet are demonstrated on the lower right panel reconstructed in a rotational manner, the morphology of the jet can be appreciated from different vantage views. The abbreviations are same as in figure 1.

Results

Dynamic 3DE display of mitral valve apparatus and mechanism of MR

In all 30 patients, reconstruction of volume-rendered 3DE images demonstrated the dynamic anatomy of mitral valve apparatus and the cardiac chambers in multiple projections. Views from the left ventricle allowed delineation of the thickness and movement of the leaflets, morphology of the commissures and size of the mitral valve opening. Views from the left atrium portrayed the size, shape and movement of mitral annulus and left atrial appendage, as well as systolic coaptation of mitral leaflets. In patients with mitral valve prolapse, the exact portion or scallop of the leaflets that bulged into the left atrium during systole could be displayed [Fig. 4]. Longitudinal views of the mitral valve allowed better appreciation of the morphology and function of the subvalvular apparatus, the severity of mitral valve displacement if present, as well as the size and function of cardiac chambers [Fig. 1]. In addition, the 3DE data set could be reviewed by reconstruction of arbitrary cross-sectional images of the mitral valve and many of them are physically inaccessible from conventional 2DE.

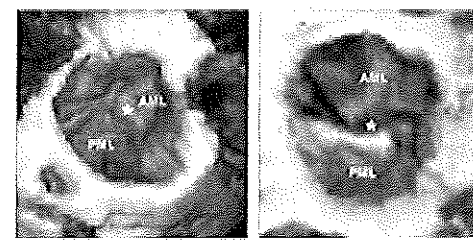

Figure 4. 3DE images of mitral valve from a patient with MR due to anterior mitral leaflet prolapse. When viewed from above (left), the prolapse portion of mitral leaflet (*) is portrayed as a protrusion into the left atrium. While looked from below (right), the prolapse is depicted as a depression. The abbreviations are same as in figure 1.

From 3DE, mitral valve prolapse was observed in 4 patients. 2 patients had billowing anterior mitral leaflets. 13 showed degenerative changes (fibro-calcification) in mitral annulus (6 patients) or thickened and deformed mitral leaflets registered as rheumatic valvular disease (7 patients) that affected coaptation of the mitral leaflets. 10 showed normal mitral valve structure with decreased mitral valve opening, abnormal left ventricular function and dilated left atrium and/or left ventricle. These patients were registered with either coronary artery disease (9 patients) or dilated cardiomy-

opathy (1 patient). One patient with obstructive hypertrophic cardiomyopathy showed systolic anterior motion of the anterior mitral leaflet. Compared with 2DE, 3DE provided incremental information in 70% (21/30) of the patients on anatomical and functional changes of the mitral valve apparatus concerned with the mechanisms of MR (Table 1).

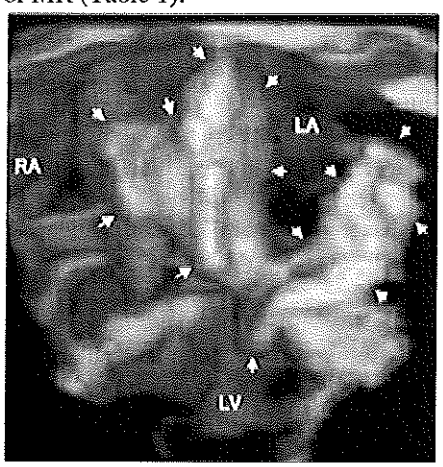

Figure 5. Reconstruction of multiple MR jets (arrows) in a patient with mitral valve prolapse. The distribution and morphology of the jets are easily appreciated in 3DE. The abbreviations are same as in figure 1 and 2.

In all patients, dynamic volume-rendered 3DE images of MR jets clearly showed the site of origin of the jet, the direction or its trajectory, the spatial distribution and its relationship with the left atrial wall [Fig. 5]. In 17 patients, the MR jets were free from left atrial wall (central jets). In 13, the jets touched the left atrial wall in various degrees (wall jets). Morphology of MR jets varied from patient to patient. Wall jets (happened more likely in-patients with deformity or malcoaptation of the leaflets) were usually more flattened and irregular in shape than central jets (seen more likely in patients with incomplete central coaptation of the leaflets). The proximal flow convergence region of MR showed various sizes and shapes besides hemisphere [Fig. 6].

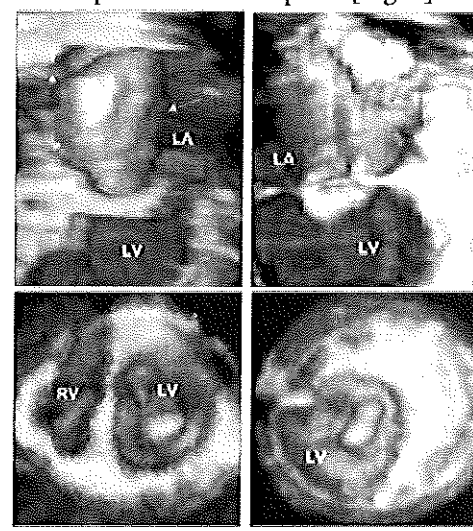

Figure 6. Volume-rendered 3DE images of MR jet (upper panels) and the proximal flow convergence region (lower panels) from patients with central (left) and wall-hugging (right) MR jets. The abbreviations are same as in figure 1.

Quantitative and semi-quantitative assessment of MR by 2DE and 3DE

Mitral regurgitant volume by 2DE method was 26.2 ± 15.1 ml (4.2 to 57.3ml). Mitral regurgitant fraction was 36% ±16% (7.1 to 68.7%). Mitral regurgitant jet area by color Doppler planimetry was 10 ± 4.4 cm^2 (1.6 to 24.9cm^2). Mitral regurgitant jet area to left atrial area ratio was 33% ± 11% % (8 to 51%). The severity of MR varied from grade 1 through grade 4 (the number of patients with grade 1, 2, 3 and 4 of MR was 2, 7, 12 and 9, respectively). 3DE measured maximum color Doppler jet volume of MR was 25 ± 11 ml (6 - 53 ml). The difference between 2 independent measurements by the same observer (intra-observer difference) was 1.6 ± 5.4 ml. The difference between 2 independent observers (inter-observer difference) was 1.9 ± 12.3 ml. In-

tra- and inter-observer variability of the measurements were 5.8% and 7.8%, respectively.

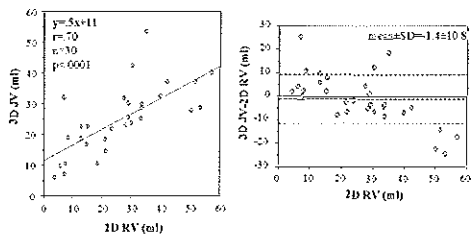

Figure 7. Comparison between MR jet volume by 3DE (3D JV) and mitral regurgitant volume by 2DE (2D RV). On the left (A) is the linear regression plot. On the right (B) is the scattergram of Bland-Altman analysis.

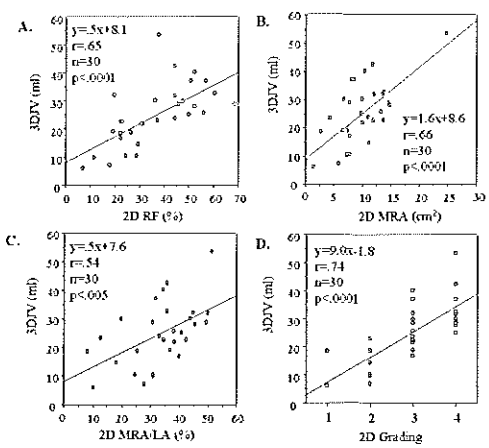

Figure 8. Linear regression plots showing correlation between MR jet volume measured from 3DE (3D JV) and mitral regurgitant fraction (2D RF) (A), MR jet area (2D MRA) (B), regurgitant jet area to left atrial area ratio (2D MRA/LA) (C), and semi-quantitative grading of MR (2D Grading) (D) derived from 2DE.

Comparison of 3DE and 2DE in assessment of the severity of MR

Correlation between the MR jet volume measured from 3DE and mitral regurgitant volume, regurgitant fraction, jet area, jet area to left atrial area ratio and semiquantitative grading of MR from 2DE methods were summarized in Table 2. A great extent of disagreement between MR jet volume from 3DE measurement and mitral regurgitant volume from 2DE method existed (1.8±10.8ml) [Fig. 7A and 8]. There was a wide spread of the data points from the line of regression. A tendency for over-estimation at smaller regurgitant volumes and under-estimation at bigger regurgitant volumes by 3DE measurement was present [Fig. 7B].

Analysis of quantitative methods for free jets and wall jets

No significant difference was found between free MR jets and wall jets in the correlation between 3DE MR jet volume and 2DE measurements of MR, nor among different 2DE methods (Table 3).

Discussion

This study shows that 3DE displays MR and the mitral apparatus more comprehensively than 2DE color Doppler; it aids in a better appraisal of the mechanism of MR, but 3DE measurement of MR jet volume alone does not provide a reliable estimate of MR severity. Although 2DE may provide adequate information in most cases, 3DE, as an adjuvant examination, may add incremental information on the pathology and function of the mitral valve apparatus and related cardiac chambers as well as the morphology of the MR jets. 3DE has been used successfully in various cardiac abnormalities and in measurement of cardiac chamber volumes and myocardial mass.[9-13] Initial studies also demonstrated its ability in displaying intra-cardiac blood flow.[14,19,20]

Evaluation of MR by 3DE

Our study resulted in good 3DE images for both mitral valve apparatus and MR jets acquired from transthoracic imaging. Although transesophageal window may produce superior images, the small distance

between the esophagus and left atrium and the angular limitation of the image sector may result in truncating of the MR jets in many cases. In this study, 3DE data obtained at the apical window enclosed the left ventricle, all the mitral valve apparatus and the left atrium, and thus the whole MR jet. Although the 3DE images of cardiac structures and intracardiac flows were both in gray-scale format, MR jet could always be differentiated from the surrounding structures because of its brighter appearance. With its high velocity, it also stood out from other normal intracardiac flows, such as pulmonary venous flow jets.

Table 1. Incremental information obtained from 3DE for better understanding the mechanisms of MR.

Etiology of MR	No. of Pts	Incremental Information from 3DE	No. of Pts
Mitral valve prolapse	4	Site and extension of prolapse	4
Mitral valve billowing	2	Enlarged size of anterior mitral leaflet	1
Mitral annulus calcification (MAC)	6	Extent of MAC and mobility of mitral valve	4
Rheumatic heart disease	7	Deformity of mitral apparatus	6
Coronary artery disease	9	Size and shape of mitral annulus	5
Dilated cardiomyopathy	1	No	0
Obstructive hypertrophic cardiomyopathy	1	Eccentric coaptation of mitral valve	1
Total No. of Pts.	**30**	-	**21**

Table 2. Correlation between MR jet volume from 3DE and measurements of MR from 2DE

2DE Measurement	Regression Equation	r	p
Regurgitant Volume	y=0.5x+11.4	0.70	<0.0001
Regurgitant Fraction	y=0.5x+8.2	0.65	<0.0001
Jet Area	y=0.2x+5.0	0.51	<0.01
Jet Area/Left Atrial Area	y=0.5x+7.6	0.54	<0.005
Grading	y=9.1x-1.8	0.74	<0.0001

Observations in this study raise a number of questions about the quantitative accuracy of 3DE in estimating MR volume and also about the accuracy of proximal flow convergence approach by 2D color Doppler. Although statistically significant correlations were observed between 3DE jet volume and MR parameters from 2DE, a close examination of the results indicates that 3DE measured MR jet volume does not provide a reliable evaluation of the severity of MR. Various shapes of the proximal flow convergence regions observed in 3DE images in this study indicate possible errors in the geometric assumptions while quantifying MR volume by the 2DE color Doppler method. 3DE could have the potential to avoid geometric assumptions of the flow convergence region by direct measurement of its surface area. No significant difference in measurements between free and wall jets was found in this study by both 2DE and 3DE methods. This observation is inconsistent, however, with the previous reports[21-23], and may be due to the similar impact of the eccentricity of the jet on the measurement approach by both techniques. Further studies in a larger population with various degrees and eccentricity of MR are necessary to address this issue.

2DE methods for estimation of MR

The most accurate noninvasive method presently available for measuring mitral regurgitant volume is 2DE and Doppler method. The traditional method is to subtract the stroke volume calculated from the

left ventricular outflow tract from the stroke volume of mitral inflow obtained at mitral annulus level.[24] In the present study, we used another method in which the left ventricular stroke volume was computed from the difference between end-diastolic and end-systolic left ventricular volumes.[25] The advantage of the later method is that it is not affected by aortic regurgitation. Although proven to be accurate, both methods use geometric assumptions for left ventricular outflow tract, mitral annulus and left ventricle and thus inaccuracy may occur when suboptimal image planes are used for measurements. Color Doppler flow imaging has been used for quantifying MR by regurgitant jet and left atrium planimetry.[26] However, the results are not always satisfactory.[6,27] This is not surprising since the direction and shape of the regurgitant jets vary in different views. The same problem is encountered when calculating regurgitant jet area to left atrial area ratio since the biggest regurgitant jet area does not necessarily happen in the standard cutting planes for the left atrium. 3DE reconstruction of the whole MR jet and left atrium should be able to provide more accurate information. Another quantitative method for assessing the severity of MR employs the surface area of the proximal flow convergence zone which requires geometric assumption for its shape.[7, 28] This method is highly technique-dependent; further inappropriate assumption of the shape of the proximal flow convergence region may lead to errors in calculation. Semi-quantitative grading of MR which integrates multiple indices from two-dimensional, spectral Doppler and color Doppler imaging remains for all practical reasons the most commonly used technique in clinical practice[18-21].

Table 3. Comparison between 3DE and 2DE methods for evaluating free MR jets and wall jets.

Methods Used for Comparison			Free Jets n = 17		Wall Jets n = 13	
			r	p	r	p
3DJV	vs.	2DRV	.69	<.005	.74	<.005
3DJV	vs.	2DRF	.71	<.005	.61	<.05
3DJV	vs.	2DJA	.69	<.005	.76	<.005
3DJV	vs.	2Dgrading	.80	<.001	.70	<.01
2DJA	vs.	2DRV	.47	>.05	.32	>.05
2DJA	vs.	2DRF	.22	>.05	.30	>.05
2DRV	vs.	2Dgrading	.55	<.05	.58	<.05

2Dgrading = semi-quantitative grading of MR into Grade 1 to 4; 2DJA = color Doppler jet area; 2DRF = mitral regurgitant fraction; 2DRV = mitral regurgitant volume measured using 2DE method; 3DJV = MR jet volume measured with 3DE.

Limitations of the study

Due to various limitations of the currently used methods, this study lacks a gold standard for quantifying the severity of MR. Quantitative analysis using 2DE methods has been shown to be a good method based on validation studies using magnetic flow meter measurements and hence we elected to use it as a gold standard.[27] MR jet volume measured by 3DE method, correlated with the measurements of MR by 2DE methods only moderately and with significant variability, and thus dose not appear to be satisfactory for accurate evaluation of the severity of MR.

Mitral regurgitant jet area and volume in 2DE and 3DE approaches are derived from color Doppler velocity signals, not the real

blood flow. The size and shape of MR jets may be affected by many factors such as compliance and pressure of the receiving chamber, concurrent flows (e.g. pulmonary venous flows), impact of the receiving chamber walls in cases of wall jets, and color scale and gain settings of the ultrasound machine.[5] The jet volume measured in one frame represents just the temporal size of the jet, other factors such as the persisting time of regurgitation and variations in regurgitant flow rate are not incorporated.

Clinical implications

Although as an adjuvant examination to 2DE, 3DE reconstruction provides additional information on mitral apparatus and the mechanisms of MR. This could allow its application in a variety of complex MV diseases. On the other hand, our study points out that caution should be exercised in using 3DE jet volume for MR quantitation. Quantitative potential of 3DE needs to be evaluated by exploring indices from proximal flow convergence and vena contracta, coupled with spectral Doppler measured time-velocity integral. Preliminary animal investigations suggest that these approaches may have potential in quantifying valvular regurgitation.[29] Technical advances in acquiring true color Doppler velocity data by 3DE (rather than using gray-scale data for reconstruction) could further aid in expanding the value of 3DE.

1. Stewart WJ, Currie PJ, Salcedo EE, Klein AL, Marwick T, Agler DA, Homa D, Cosgrove DM. Evaluation of mitral leaflet motion by echocardiography and jet direction by color Doppler flow mapping to determine the mechanisms of mitral regurgitation. *J Am Coll Cardiol* 1992;20:1353-1361.
2. Dent JM, Spotnitz WD, Kaul S. Echocardiographic evaluation of the mechanisms of ischemic mitral regurgitation. *Coron Artery Dis* 1996;7:188-195.
3. Enriquez-Sarano M, Bailey KR, Seward JB, Tajik AJ, Krohn MJ, Mays JM. Quantitative Doppler assessment of valvular regurgitation. *Circulation* 1993;87:841-848.
4. Chen C, Koschyk D, Brockhoff C, Heik S, Hamm C, Bleifeld W, Kupper W. Noninvasive estimation of regurgitant flow rate and volume in patients with mitral regurgitation by Doppler color mapping of accelerating flow field. *J Am Coll Cardiol* 1993;21:374-383.
5. Grimes RY, Burleson A, Levine RA, Yoganathan AP. Quantification of cardiac jets: Theory and limitations. *Echocardiography* 1994;11:267-280.
6. McCully RB, Enriquez-Sarano M, Tajik AJ, Seward JB. Overestimation of severity of ischemic/functional mitral regurgitation by color Doppler jet area. *Am J Cardiol* 1994;74:790-793.
7. Grossmann G, Giesler M, Schmidt A, Kochs M, Wieshammer S, Eggeling T, Felder C, Hombach V. Quantification of mitral regurgitation by color flow Doppler imaging - value of the "proximal isovelocity surface area" method. *International J Cardiol* 1993;42:165-173
8. Cape EG, Yoganathan AP, Weyman AE, Levine RA. Adjacent solid boundaries alter the size of regurgitant jets on Doppler flow maps. *J Am Coll Cardiol* 1991;17:1094-1102
9. Pandian NG, Nanda NC, Schwartz SL, Fan P, Cao QL, Sanyal R, Hsu TL, Mumm B, Wollschlager, Weintraub A. Three-dimensional and four-dimensional transesophageal echocardiographic imaging of the heart and aorta in humans using a computed tomographic imaging probe. *Echocardiography* 1992;9:677-687.
10. Marx G, Fulton DR, Pandian NG, Vogel M, Cao QL, Ludomirski A, Delabays A, Sugeng L, Klas B. Delineation of site, relative size and dynamic geometry of atrial septal defects by real-time three-dimensional echocardiography. *J Am Coll Cardiol* 1995;25:482-490.
11. Schwartz SL, Cao QL, Azevedo J, Pandian NG. Simulation of intraoperative visualization of cardiac structures and study of dynamic surgical anatomy with real-time three-dimensional echocardiography. *Am J Cardiol* 1994;73:501-507 .
12. Salustri A, Becker AE, Van Herwerden L, Vletter WB, Ten Cate FJ, Roelandt JRTC. Three-dimensional echocardiography of normal and pathologic mitral valve: A comparison with two-dimensional transesophageal echocardiography. *J Am Coll Cardiol* 1996;27:1502-1510.
13. Nosir YFM, Fioretti PM, Vletter WB, Boersma E, Salustri A, Postma JT, Reijs AEM, Ten Cate FJ, Roelandt JRTC. Accurate measurement of left ventricular ejection fraction by three-dimensional echo-

cardiography. A comparison with radionuclide angiography. *Circulation* 1996;94:460-466.
14. Delabays A, Sugeng L, Pandian NG, Tsu TL, Ho SL, Chen CH, Marx GR, Schwartz SL, Cao QL. Dynamic three-dimensional echocardiographic assessment of intracardiac blood flow jets. *Am J Cardiol* 1995;76:1053-1058.
15. Rivera JM, Vandervoort PM, Morris E, Weyman AE, Thomas JD. Visual assessment of valvular regurgitation: comparison with quantitative Doppler measurements. *J Am Soc Echo* 1994;7:480-487.
16. Burwash IG, Blackmore GL, Koilpillai CJ. Usefulness of left atrial and left ventricular chamber sizes as predictors of the severity of mitral regurgitation. *Am J Cardiol* 1992;70:774-779.
17. Kamp O, Huitink H, van Eenige MJ, Visser CA, Roos JP. Value of pulmonary venous flow characteristics in the assessment of severity of native mitral valve regurgitation: an angiographic correlated study. *J Am Soc Echo* 1992;5:239-246.
18. Utsunomiya T, Patel D, Doshi R, Quan M, Gardin JM. Can signal intensity of the continuous wave Doppler regurgitant jet estimate severity of mitral regurgitation? *Am Heart J* 1992;123:166-171.
19. Belohlavek M, Foley DA, Gerber TC, Grennleaf JF, Seward JB. Three-dimensional reconstruction of color Doppler jets in the human heart. *J Am Soc Echocardiogr* 1994;7:553-560.
20. Shiota T, Sinclair B, Ishii M, Zhou X, Ge S, Teien DE, Gharib M, Sahn DJ. Three-dimensional reconstruction of color Doppler flow convergence regions and regurgitant jets: an in vitro quantitative study. *J Am Coll Cardiol* 1996;27:1511-1518.
21. Chen CG, Thomas JD, Anconina J, Harrigan P. Impact of impinging wall jet on color Doppler quantitation of mitral regurgitation. *Circulation* 1991;84:712-720.
22. Shiota T, Sinclair B, Ishii M, Zhou X, Ge S, Teien DE, Gharib M, Sahn DJ. Three-dimensional reconstruction of color Doppler flow convergence regions and regurgitant jets: an in vitro quantitative study. *J Am Coll Cardiol* 1996;27:1511-1518.
23. Enriquez-Sarano M, Tajik AJ, Bailey KR, Seward JB. Color flow imaging compared with quantitative Doppler assessment of severity of mitral regurgitation: influence of eccentricity of jet and mechanism of regurgitation. *J Am Coll Cardiol* 1993;21:1211-1219.
24. Ascah KJ, Stewart WJ, Jiang L, Guerrero JL, Newell JB, Gillam LD, Weyman AE. A Doppler-two-dimensional echocardiographic method for quantitation of mitral regurgitation. *Circulation* 1985;72:377-383.
25. Keren G, Katz S, Strom J, Sonnenblick EH, Le-Jemtel TH. Noninvasive quantification of mitral regurgitation in dilated cardiomyopathy: Correlation of two Doppler echocardiographic methods. *Am Heart J* 1988;116:758-764.
26. Helmcke F, Nanda NC, Hsiun MC, Soto B, Adey CK, Goyal RG, Gatewood RP Jr. Color Doppler assessment of mitral regurgitation with orthogonal planes. *Circulation* 1987;75:175-183.
27. Shiota T, Jones M, Teien D, Yamada I, Passafini A, Knudson O, Sahn DJ. Color Doppler regurgitant jet area for evaluating eccentric mitral regurgitation: and animal study with quantified mitral regurgitation. *J Am Coll Cardiol* 1994;24:813-819.
28. Xie GY, Berk MR, Hixson CS, Smith AC, DeMaria AN, Smith MD. Quantification of mitral regurgitant volume by the color Doppler proximal isovelocity surface area method: a clinical study. *J Am Soc Echocardiogr* 1995;8:48-54.
29. Shiota T, Sinclair B, Ishii M, Zhou X, Ge S, Teien DE, Gharib M, Sahn DJ. Three-dimensional reconstruction of color Doppler flow convergence regions and regurgitant jets: an in vitro quantitative study. *J Am Coll Cardiol* 1996;27:1511-8.

SUMMARY AND FUTURE DIRECTIONS

Summary and Future Directions

This thesis recognizes various applications of three-dimensional echocardiography (3DE) in coronary artery disease (CAD) and associated complications.

Following the introduction and overview of the thesis, the second chapter is an overview of 3DE and its application in various cardiac abnormalities including CAD and complications. It pointed out the potential, as well as the existing problems and future directions of 3DE.

The third chapter explored the appropriate rotational 3DE data acquisition interval for measurement of left ventricular (LV) volumes in subject with various LV shapes and function. It concluded that 12° might be the proper rotational interval for 3DE data acquisition, which resulted in accurate LV volume measurement and saved about 80% of time compared with data obtained at 2° intervals.

Chapter 4 described the quantitative methods of 3DE in the measurement of LV dysfunctional mass in the settings of acute experimental myocardial infarction produced by coronary artery occlusion. The sum of akinetic and dyskinetic myocardial mass from 3DE correlated well with the anatomically determined infarct mass.

Chapter 5 compared the LV dysfunctional mass measured by 3DE and that measured by magnetic resonance imaging in patients with acute myocardial infarction with no interventional revascularization procedures. Good correlation between the results from these two techniques pointed out a new direction of 3DE in evaluation of patients with acute myocardial infarction.

Although dysfunctional mass may indicate infarct myocardium in the setting of single acute infarction, in patients with chronic ischemic disease, multiple infarctions or reperfusion therapy following infarction, there could be dysfunctional mass that is viable. Chapter 6 explored the potential of 3DE in quantifying the myocardial mass at risk during ischemia and residual infarct mass following reperfusion using an intravenous ultrasound contrast agent. It demonstrated that 3DE could be an accurate method in the evaluation of the efficacy of reperfusion.

The methodology and feasibility of coronary artery imaging by 3DE and the diagnostic accuracy of semi-quantitative assessment of coronary stenosis is shown in chapter 7.

Carotid artery disease has been shown to be co-existent with CAD. Chapter 8 studied the potential of 3-dimensional ultrasound in accurately quantifying plaque volumes and in studying the impact of endarterectomy on the regional anatomy of the vessel.

Chapter 9 and 10 are reports of two studies demonstrating qualitative and quantitative application of 3DE in CAD related abnormalities, such as mitral valve regurgitation and intracardiac mass lesions.

Future Directions

The clinical and experimental applications of 3DE has been well recognized in chamber volume measurements, congenital heart diseases and valvular diseases. Its role in studying CAD has not been fully explored previously. The studies included in this thesis point out a new direction of 3DE in the diagnosis and evaluation of CAD and its incremental value to 2DE. In the future, along with technical developments in 3DE such as real-time 3DE and digital 3DE of tissue Doppler, color Doppler, power Dop-

pler and so on will enable us to study other physiologies of the heart in multi-dimensions. Automatic border detection might be able to facilitate analysis of three-dimensional shape or local curvature of the cardiac chambers and regional wall motion. Quantitative gray-scale analysis and color encoding technique might help in graded analysis of myocardial perfusion and intra-myocardial blood volume. 3DE information of multiple functional and physiological indices of the heart including multiple two-dimensional image reconstruction or bulls-eye presentation, three-dimensional image reconstruction, regional extraction and three-dimensional display, virtual reality interactive 3DE workshop, stereolithography and holography and so on. The 3DE in the future could be able to provide more comprehensive information with multiple parameters in one package for accurate evaluation of the heart in patients with CAD.

SAMENVATTING

Samenvatting

Dit proefschrift handelt over verschillende applicaties van drie-dimensionele echocardiografie (3DE) bij patiënten met coronaire arterie afwijkingen en aanverwante ziekten.

Na de introductie en overzicht van dit proefschrift, laat het tweede hoofdstuk een overzicht zien van het gebruik van 3DE technieken bij verschillende cardiale afwijkingen, inclusief coronaire arterie afwijkingen, en complicaties. Het potentieel van 3DE werd beschreven als wel de huidige problematiek en de toekomstige ontwikkelingen.

Het derde hoofdstuk doet onderzoek naar de accuratesse van het gebruik van verschillende rotationele intervallen, wanneer een rotatie acquisitietechniek wordt gebruikt, voor volume metingen aan linker ventrikels (LV) met verschillende geometrie. De conclusie was dat stappen van 12^0 het juiste interval voor 3DE acquisitie zou kunnen zijn. Dit resulteerde in nauwkeurige LV volume metingen en bespaarde 80% tijd in vergelijking met 3DE data, welke met een interval van 2^0 was verkregen.

Hoofdstuk 4 beschrijft kwantitatieve methoden van 3DE voor het meten van LV disfunctionerende massa's in het geval van experimentele acute infarcten veroorzaakt door het afsluiten van een coronair arterie. De som van akinetische en diskinetische myocard massa, berekend met 3DE, correleerde goed met het anatomische bepaalde infarct massa.

Hoofdstuk 5 vergeleek de LV disfunctionerende massa gemeten met 3DE met dat gemeten m.b.v magnetische kernspinresonantie technieken (MRI) bij patiënten met een acuut myocard infarct en welke geen interventionele revascularisatie procedure hadden ondergaan. De goede correlatie tussen beide technieken wijst op een nieuw terrein voor 3DE in evaluatie van patiënten met een acuut myocard infarct.

Hoewel een disfunctionerende massa in het geval van een enkel acuut infarct een geïnfarcteerd myocardium aangeeft, bij patiënten met chronische ischemie, meerdere infarcten of een reperfusie therapie na een infarct, zou er disfunctionerende massa kunnen zijn dat levensvatbaar is. Hoofdstuk 6 onderzocht het potentieel van 3DE voor kwantificatie van de myocard massa in gevaar gedurende ischemie en de resterende infarct massa na reperfusie met gebruikmaking van een intraveneuze echo contrast vloeistof. Er werd aangetoond dat 3DE een nauwkeurige methodiek is voor evaluatie van de doeltreffendheid van reperfusie na revascularisatie.

De methodologie en bruikbaarheid van het visualiseren van de coronaire arteriën m.b.v. 3DE en de diagnostische nauwkeurigheid van semi-kwantitatieve bepalingen van coronaire stensoses, is beschreven in hoofdstuk 7.

Atherosclerotische afwijkingen in de arteria carotis komen meestal voor tezamen met coronaire arterie afwijkingen. Hoofdstuk 8 bestudeerde het potentieel van 3DE voor het accuraat kwantificeren van atherosclerotische plaque volumes en het bepalen van de invloed van endarteriëctomie op de regionale anatomie van het vat.

Hoofdstuk 9 en 10 zijn rapporten van twee studies die over kwalitatieve als wel kwantitatieve applicaties van 3DE in coronaire arterie gerelateerde afwijkingen zoals mitraal klep regurgitatie en intracardiale massa's.

Toekomstige ontwikkelingen

De klinische en experimentele applicaties

van 3DE voor het meten van volumina van de rechter- en linkerventrikel, bij congenitale afwijkingen en klepgebreken, is erkend. Zijn rol voor het bestuderen van coronaire afwijkingen was nog niet eerder bestudeerd. De studies beschreven in dit proefschrift wijzen op nieuwe toepassingen van 3DE voor diagnose en evaluatie van coronaire afwijkingen en zijn toegevoegde waarde t.o.v. 2DE. In de toekomst, tezamen met technische ontwikkelingen in 3DE zoals real-time 3DE en digitale 3DE van weefsel Doppler en kleuren Doppler e.a., zal ons in staat stellen om andere pathofysiologische aspecten van het hart in meerdere modaliteiten te bestuderen. Automatische contour detectie zou de mogelijkheid kunnen bieden om 3D vormen van locale krommingen van de cardiale kamers en regionale wandbewegingen te analyseren. Kwantitatieve grijs-waarde analyse en kleur gecodeerde technieken kunnen helpen in een graduele analyse van myocard perfusie en het bepalen van intra-cardiale volumina. 3DE informatie van meerdere functionele grootheden van het hart zou kunnen worden gerealiseerd met reconstructies van meerdere twee-dimensionele beelden, drie-dimensionele reconstructies, extractie van regionale functies en drie-dimensionale weergave, virtual reality, stereolithografie en holografie. 3DE zal in de toekomst in staat zijn uitgebreide informatie van meerdere parameters voor de nauwkeurige evaluatie van patiënten met coronaire afwijkingen te verschaffen in één pakket te laten zien.

ACKNOWLEDGEMENT

Acknowledgement

Grew up in the period of "Cultural Revolution" in red China, the first book I learned to read from my grandfather was the "red book" of Chairman Mao. The first sentence I could recite was "To serve the people whole-heartedly". I also learnt from the book that, for the sake of "China's liberation", a Canadian doctor - Dr. Berthune - came to China from thousands of miles away and dedicated his life to the Chinese people. At that time, I never dreamed I would one day get my highest medical degree in a beautiful land far away from my hometown. I am deeply indebted to Prof. Roelandt for his support and the opportunity he provided me with to work in the Thoraxcenter and to obtain a Ph.D. degree. He expanded my vision in clinical research with his profound knowledge and sharp insights. I was very impressed by his great enthusiasm in the emerging techniques in cardiology, that inspired and encouraged me in my studies. With his travelling stories filled with affection for the nature, art and culture, Prof. Roelandt also refined my understanding of the true value of life.

During my study in Thoraxcenter, I got tremendous help and support from many people of different departments. I wish I could mention everybody's name here. I would like to give my special thanks to Mr. Wim Vletter, René Frowijn and all sonographers in the echo lab for their support of my projects, to Dr. Folkert Ten Cate, Dr. Pim de Feijter and Dr. Don Poldermans of cardiology, Dr. Taams and Dr. Lex van Herwerden of surgical department and Dr. van Sambeek of vascular surgery for their instruction, support and help in carrying out my projects. I also had the pleasure to work with the most talented and hard-working fellows from various parts of the world, including Dr. Jaroslaw Kasprzak (Poland), Dr. Anita Dall'Agata (Italy), Dr. Youssef Nosir (Egypt), Dr. Riccardo Rambaldi (Italy) Dr. Abdou Elhandy (Egypt), Dr. lubov koroleva (Russia) and so on.

Talking of the thesis, there was an equally important experience in my research life. Before coming to Thoraxcenter, I received a grant from the World Health Organization to study "adavanced echocardiography" in the United States. I chose Tufts-New England Medical Center for its well known reputation in echocardiography and Dr. Pandian became my mentor and sponsor. He has a special talent and enthusiasm in teaching. He always catches the new wave in echocardiography and has been in the frontier of various new developments. Among many options, he recommended Thoraxcenter and introduced me to Prof. Roelandt with very good reasons when I left the States in 1996.

In my whole life, I have been very lucky to have a lot of great mentors guiding my way. Besides my grandparents, my mother, a high school teacher, and my father, a doctor, were the first teachers in and through my life. My first official teacher, Mr. Qiao, was the teacher of all my classes in the first 3 years of my school. According to an old Chinese tradition from the time of Confucius, I still owe him a swine head. A sentence, which always helps me in difficult times, was from my high school math teacher. He told us: "There is no cure for regret, so don't even try it". I always remember it. Many of my high school teachers taught me the Chinese culture, morality and science under the risk of being removed from their positions and being sent away to the most torturing farms. When I was in the medical school, I attended 1st experimental

"English medical class" in China. Many professors spent numerous hours of their spare time to prepare the lectures in a language most of them never had a chance to speak. Prof. Jing-chun Ruan, a renowned cardiologist, who later became my mentor in the postgraduate school, inspired my interest in cardiology when I was in the 4th year of medical school. He impressed me with the greatest personality, the deepest insight, the most classic charisma, and a great sense of humor. With the help of Dr. Yun Zhang, co-mentor of my postgraduate study, and the help of many colleagues in the Cardiology division of Shandong Medical University hospital, I did my 1st research project in echocardiography. As I was preparing my postgraduate thesis (Computer-aided left ventricular regional wall motion analysis in normal subjects and in patients with acute myocardial infarction) in 1988, an American professor, went to Shanghai to give lectures on the same topic. While I was confused by his Indian accent, I got enough inspiration to finish my thesis. I never realized until I came to Boston almost 7 years later that I would ever meet him again. Who is the aforementioned Dr. Pandian. When I got two grants to go to Japan for further training in cardiology, I didn't hesitate to choose the National Cardiovascular Center in Osaka. Dr. Miyatake (my mentor), and Drs. Beppu, Ishikura, Yamaguchi and so on brought me to the front of echocardiography in a world-class echo lab.

After all, all my achievement is because I have a caring, supporting and understanding family.

CURRICULUM VITAE

Curriculum Vitae

Jiefen Yao, born in P.R.China on 10.27.63

Education:

1979-1985	Medical School, Shandong Medical University Jinan, China
1985-1988	Post-graduate school, Shandong medical University Jinan, China

Professional Experience:

1988 - 1991	Resident Cardiology Division Department of Medicine Hospital of Shandong Medical University Jinan, China
1991 -	Physician-in-Chief & Faculty Cardiologist Cardiology Division Department of Medicine Hospital of Shandong Medical University Jinan, China
1991.8-12	Visiting Cardiologist Cardiology Division National Cardiovascular Center Osaka, Japan

Research Experience:

1995 - 1996	Research fellow Cardiovascular Imaging and Hemodynamic Lab. Division of Cardiology New England Medical Center Tufts University School of Medicine
1997.1-1998.1	Research fellow Division of Cardiology Thoraxcenter Erasmus University Rotterdam, the Netherlands
1998.2 -	Research fellow Cardiovascular Imaging and Hemodynamic Lab. Division of Cardiology New England Medical Center Tufts University School of Medicine Boston, MA

PUBLICATIONS

Publications

1. Li CY, **Yao J**, Cui XY, Zhu WP. Preliminary study of the diagnosic value of high frequency electrocardiogram in cardiac neurosis. *Shandong Biomedical Engineering* 1992;10:122-123
2. Li CY, **Yao J**, Pu PL, Wang SC. Specific characteristics of high frequency electrocardiogram in patients with virus myocarditis. *J Chin Med* 1994;11:143-145
3. Liu TT, **Yao J**, Zhou RH, Gao HQ, Zhang AX, Wang SC. Effect of Captopril on the level of lipid peroxidation and nitric oxide in patients with coronary heart disease. *ACTA Academiae Medicinae Shandong* 1995;33(4):320-322
4. **Yao J**, Cao QL, Marx G, Pandian NG. Three-dimensional echocardiography: Current development and future directions [review]. *J Med Ultrasound* 1996; 4(1): 11-19
5. Stefano De Castro, **Jiefen Yao**, Giuseppina Magni and Natesa G. Pandian (Eds). *Echocardiografia Tridimensionale: Dalla ricerca all'applicazione clinica* (Three-Dimensional Echocardiography), A Monograph, 1996, Il Pensiero Scientifico Editore, Rome, Italy.
6. **Yao J**, Cao QL, Masani N, Delabays A, Magni G, Acar P, Laskari C, Pandian NG. Three-dimensional echocardiographic estimation of infarct mass based on quantification of dysfunctional left ventricular mass. *Circulation* 1997; 96(5):1660-6
7. **Jiefen Yao**, Navroz D. Masani, Natesa G. Pandian. Three-dimensional echocardiographic assessment of myocardial perfusion abnormalities. A chapter in "*Advances in echo imaging using contrast enhancement*" (2nd edition, 1997); Navin C. Nanda, Reinhard Schlief and Barry B. Goldberg (eds). Kluwer Academic Publishers, Boston, USA. 1997; Page 465-477.
8. **Yao J**, Roelandt JRTC. Three-dimensional echocardiography: a new era of cardiac imaging. [review] *Current Med Literature: Cardiac Imaging* 1997;Pilot Issue:2-10
9. **Yao J**, Cao QL, Pandian NG, Sugeng L, Marx G, Masani N, Yeung H. Multiplane transthoracic echocardiography: Image orientation, anatomic correlation, and clinical experience with a prototype phased array multilane surface probe. *Echocardiography* 1997;14: 559-88
10. Breburda CSM, **Yao J**, van der Linden M, Beelen DPW, Roelandt JRTC. Quantitative transthoracic three-dimensional echocardiography guides management of acute hemopericardium. *Thoraxcenter J* 1997;9: 19-22
11. De Castro S, **Yao J**, Magni G, Cacciootti L, Trambaiolo P, De Sanctis M, Fedele F. Three-dimensional echocardiographic assessment of the extension of dysfunctional mass in patients with coronary artery disease. *Am J Cardiol* 1998;81(12A): 103G-106G
12. De Castro S, **Yao J**, Pandian NG. Three-dimensional echocardiography: clinical relevance and application. *Am J Cardiol* 1998;81(12A): 96G-102G
13. **Yao J**, Masani N, Cao QL, Nikuta P, Pandian NG. Clinical application of transthoracic Volume-rendered three-dimensional echocardiography in the assessment of mitral regurgitation. *Am J Cardiol* 1998;82:189-196
14. Nosir YFM, Lequin MH, Kasprzak JD, van Domburg RT, Vletter WB, **Yao J**, Stoker J, Ten Cate FJ, Roelandt JRTC.

Measurements and day-to-day variabilities of left ventricular volumes and ejection fraction by three-dimensional echocardiography and comparison with magnetic resonance imaging. *Am J Cardiol* 1998;82:209-214

15. **Yao J**, van Sambeek MRHM., Dall'Agata A, van Dijk LC, Kozakova M, Koudstaal PJ, Roelandt JRTC. Three-dimensional ultrasound study of carotid arteries before and after endarterectomy: analysis of stenotic lesions and surgical impact on the vessel. *Stroke 1998;29:2026-2031*
16. Roelandt JRTC, **Yao J**, Kasprzak JD. Three-Dimensional Echocardiography. [review] *Current Opinion in Cardiology* 1998,13:386-396
17. De Castro S, **Yao J**, Fedele F, Pandian NG. Three-dimensional echocardiography in ischemic heart disease. *Coronary Artery Disease* 1998;9(7):427-434
18. Tsui-Lieh Hsu, **Jiefen Yao,** Stefano De Castro, Natesa G. Pandian. Three-dimensional echocardiography. A chapter in *Atlas of Cardiac Imaging*, by Richard T. Lee and Eugene Braunwald (eds). Current Medicine, Inc., Philadelphia, PA, USA. 1998; Page 11.1-11.11.
19. Arsenault M, Masani N, Magni G, **Yao J,** Deras L, Pandian N. Variation of anatomic valve area during ejection in patients with valvular aortic stenosis evaluated by two-dimensional echocardiographic planimetry: comparison with traditional Doppler data. *J Am Coll Cardiol* 1998;32:1931-1937
20. **Jiefen Yao**, Lissa Sugeng, Gerald Marx, Natesa G. Pandian. Three-dimensional echocardiography: methodology and applications. Chapter 9 in "*Diagnostic Medical Sonography, Volume II: Echocardiography*", (2nd edition) by Mark Allen, et al. Lippincott-Raven Publishers, Philadelphia, PA, USA. 1998; Page 167-178
21. **Jiefen Yao**, Natesa G. Pandian. Visión tridimensional (Three-dimensional echocardiography: methodology and application). A chapter in "*Cardiologia 2000*", by Gianciulli (ed), Argentine. 1997; page 838-850
22. **Yao J**, Taams MA, Kasprzak JD, de Feijter PJ, ten Cate FJ, van Herwerden LA, Roelandt JRTC. Usefulness of three-dimensional transesophageal echocardiographic imaging for evaluating narrowing in the coronary arteries. *Am J Cardiol 1999;84: in press*

ACKNOWLEDGEMENT FOR FINANCIAL SUPPORT

The following companies are gratefully acknowledged for their technical support in my research and financial support in printing this thesis:

Acusphere Inc, Cambridge, MA, USA

Bayer B.V., the Netherlands

Bracco Diagnostics Inc., Princeton, NJ, USA

Esaote S.P.A., Florence, Italy

GE Ultrasound, Milwaukee, WI, USA

Hewlett-Packard, Andover, MA, USA

Mallinckrodt inc., Lexington, MA, USA

Nycomed Amersham, Oslo, Norway

Rhonê-Poulenc Rorer B.V., the Netherlands

Roche Netherland B.V., the Netherlands

Schering AG, Berlin, Germany

TomTec Imaging Systems GmβH, Munich, Germany